INSTITUTO TECNOLÓGICO DE COSTA RICA

VICERRECTORÍA DE INVESTIGACIÓN Y EXTENSIÓN

DIRECCIÓN DE PROYECTOS

ESCUELA DE INGENIERÍA FORESTAL

CENTRO DE INVESTIGACIÓN EN INTREGRACIÓN BOSQUE INDUSTRIA

INFORME FINAL DE PROYECTO DE INVESTIGACIÓN

APLICACIONES DE NANOTECNOLOGÍA EN EL REFORZAMIENTO DE MADERAS COMERCIALES DE COSTA RICA

Código: 5401-1401-1019

(DOCUMENTO I)

INVESTIGADORES:

Ing. Roger Moya R. Ph.D.
Ing. Carolina Tenorio Monge M Sc.
Ing. Ana Rodíguez Zúñiga Lic.

Junio, 2015

ÍNDICE GENERAL

Pág.

1. Artículo 1. Effect of silver nanoparticles on white-rot wood decay and some physical properties of three tropical wood species

EFFECT OF SILVER NANOPARTICLES ON WHITE-ROT WOOD DECAY AND SOME PHYSICAL PROPERTIES OF THREE TROPICAL WOOD SPECIES

*Róger Moya**†
Professor
E-mail: rmoya@itcr.ac.cr

Alexander Berrocal
Professor
E-mail: aberrocal@itcr.ac.cr

Ana Rodriguez-Zuñiga
Research Scientist
Escuela de Ingeniería Forestal
Instituto Tecnológico de Costa Rica
Apartado 159-7050, Cartago, Costa Rica
E-mail: ana.rodriguez@itcr.ac.cr

José Vega-Baudrit
Research Scientist
Laboratório Nacional Nanotecnologia (LANOTEC)
Centro Nacional de Alta Tecnologia-CENAT
San Jose, Costa Rica
E-mail: jvegab@gmail.com

Sindy Chaves Noguera
Research Scientist
Laboratório Institucional de Nanotecnología
Instituto Tecnológico de Costa Rica
Apartado 159-7050, Cartago, Costa Rica
E-mail: schaves@itcr.ac.cr

(Received February 2014)

Abstract. Wood is one of the most widely used materials and is used in many applications. However, decay resistance of wood is limited in tropical conditions. Nanotechnology applications have potential for improving materials. In this study, a solution with a concentration of 50 ppm silver nanoparticles was incorporated by pressure into three commercial species (*Acacia mangium*, *Cedrela odorata*, and *Vochysia guatemalensis*) of Costa Rica. The white-rot fungus (*Trametes versicolor*) was tested, and some physical properties were also measured. According to the results, synthetized silver nanoparticles (10-25 nm) presented little agglomeration and were adequately distributed. The retention achieved was 25-102 silver mg/kg^{-1} of wood, varying among species and with presence of sapwood and heartwood. Mass loss was less than 5% in wood treated with silver nanoparticles; thus, the wood was classified as highly resistant or class A. Meanwhile, untreated wood presented losses greater than 20% with white-rot fungi. Also, water absorption capacity decreased for wood treated with silver nanoparticles in the three species tested, and dimensional stability increased for *Cedrela odorata* and *Vochysia guatemalensis* treated with silver nanoparticles.

Keywords: Wood preservatives, nanotechnology, tropical species, boric acid, sodium borate.

* Corresponding author
† SWST member

Wood and Fiber Science, 46(4), 2014, pp. 527-538

INTRODUCTION

Nanotechnology is being intensively developed for a wide variety of applications, from material behavior improvement to medical uses (Scott and Chen 2013). Nanotechnology development has improved the properties of wood and the products derived from it (Tarmian et al 2012). Studies on wood nanotechnology applications focus on the following areas: 1) changes in physical and mechanical properties; 2) dimensional stability of wood; 3) changes in wood appearance (color) and resistance to outdoor conditions; and 4) resistance to the attack of micro-organisms. The interest in silver nanoparticles for different types of applications, among them medical applications because of their antibacterial activity, has grown worldwide (Mahapatra et al 2013). This type of nanoparticle has also gained popularity in plant biology (Anjum et al 2013), material reinforcement (Reidy et al 2013), and wood property improvement. The use in wood has the objective to enhance the physical and mechanical properties of wood and its durability and behavior before chemical substances or radiation (Mie et al 2013). Nanotechnology applications improve material properties and use only small quantities.

Silver nanoparticles have improved wood protection (Liu et al 2002a, 2002b, 2002c), behavior against fire (Taghiyari 2012), physical properties (Taghiyari 2012; Taghiyari and Bibalan 2013), thermal treatment (Taghiyari et al 2012), densification (Rassam et al 2012), particleboard production (Taghiyari et al 2011), and drying (Tarmian et al 2012).

There are different methods for synthetizing silver nanoparticles (Tan and Cheong 2013). The most important are reduction methods (Mavani and Shah 2013) using sodium borohydride ($NaBH_4$) as a silver reduction agent for synthesizing nanoparticles (Mavani and Shah 2013). The studies of effects of silver nanoparticles on wood fungi resistance properties (Liu et al 2002a, 2002b, 2002c; Akhtari et al 2013) do not offer a description of silver nanoparticle synthetizing methodologies. In addition, little is known about the effects on tropical woods. We believe that the synthesis of silver nanoparticles with $NaBH_4$ as a silver reduction agent has potential, because boron particles, an active wood preservative component (Lloyd 1998), are added in silver nanoparticle solution. Applications for bacterial growth control (Mavani and Shah 2013), wood protection (Schultz et al 2008), and human medicine (Crabtree et al 2003) have been studied.

This study reports on the synthetizing of silver nanoparticles by reduction with $NaBH_4$ and how silver nanoparticles effect wood absorption capacity, retention, resistance to the attack of *Trametes versicolor* (white-rot), density and specific gravity and dimensional stability (swelling).

MATERIALS AND METHODS

Materials

For nanoparticle synthetizing, three components were used: silver nitrate ($AgNO_3$) as a source of the reduced metal, supplied by Merck (White House Station, NJ) (99.9% purity), $NaBH_4$ as a reduction agent, supplied by Merck (99% purity), and polyvinylpyrrolidone (PVP) as a stabilizing agent, supplied by Magnacol Ltd. (Newtown, Wales, UK) The reaction was performed in an aqueous medium. Samples of three tropical wood species in Costa Rica were used: sapwood and heartwood of *Acacia mangium*, sapwood and heartwood of *Cedrela odorata*, and sapwood of *Vochysia guatemalensis*. The fungi tests were performed with the white-rot fungus *Trametes versicolor*.

Synthetizing Silver Nanoparticles

Silver nanoparticles were synthesized using the method described by Mavani and Shah (2013). It is based on a reduction reaction in which an excess of $NaBH_4$ as a reducing agent, PVP as a stabilizing agent, and $AgNO_3$ as the silver source are used. The reaction is carried out in an aqueous medium in an ice bath. This reaction involves taking 0.93 L of a solution of 0.015 M $NaBH_4$, which is stirred constantly within an ice

bath. Then, the 0.015-M $NaBH_4$ solution is added to 0.90 mL of 3% PVP. After these two solutions ($NaBH_4$ and PVP) were homogenized, 62.8 mL of 0.0073-M $AgNO_3$ solution is added slowly (1 drop per second) until it presents a gold to brown coloration. More detail on the process of the reaction can be obtained from Mavani and Shah (2013), and the reaction of silver nitrate with sodium borohydride may be written as Eq 1. The reaction efficiency was not evaluated and was therefore considered to be a 100% conversion of silver nitrate to reduced silver. The concentration of silver nanoparticles in this solution was 50 ppm. PVP was used to protect the silver nanoparticles from agglomeration. This product was added to the solution without any treatment.

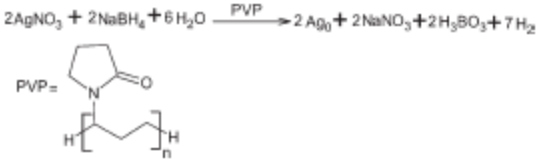

(1)

UV Observation and Transmission Electron Microscope Images

To perform the UV measurements, a sample was taken from the nanoparticle solution, which was then poured on the UV sample holder. The characterization was based on UV-visible spectroscopy (T18 manufactured by PG Instruments, Leicestershire, UK). The measurement was performed with respect to a blank of distilled water. A small sample was again taken to obtain the transmission electron microscope (TEM) images, which was then placed in the microscope using 100-kV acceleration and 10,000× (B and C) and 30,0000× (D) amplification. The images of the silver nanoparticles were observed with a JEOL (Akishima-Shi, Tokyo, Japan) TEM, JEM-2100 model. In the case of observation with atomic force microscopy (AFM), a 5-mL sample of the nanoparticle solution was taken, dissolved in 5 mL of ethanol, and then centrifuged for 5 min. Then, a small drop of this solution was observed in AFM on a ceramic surface and ethanol needed to evaporate to make the measurement. The asylum research model MFP 3D was used to take images of the AFM.

Preservation of Wood Samples with Silver Nanoparticles

Five 25-mm thick × 20-cm wide boards for each species were bought locally. The boards were dried to 12% MC in a room chamber at 22°C and 65% in RH. Afterward, 25-mm × 25-mm cross-section billets were cut from each board and separated in sapwood and heartwood. Then they were planed to 20 mm × 20 mm in cross-section and samples measuring 20 × 20 × 20 mm were prepared. Sixty heartwood samples and 60 sapwood samples each for *A. mangium* and *C. odorata* and 60 samples of sapwood for *V. guatemalensis* were randomly selected for testing. For the latter species, heartwood was not tested because it is not discernable in this species. All samples were placed into a 1-m^3 experimental pressure vessel commonly used for wood preservation. The preservation process consisted of 30 min of vacuum at –78 kPa (gauge), 2 h of pressure at 690 kPa, and 15 min of vacuum at –78 kPa (gauge). The samples were weighed before and after the preservation process. Absorption capacity for each sample was calculated as the absorption of solution in liters/timber volume. Nanosilver retention was determined by weight gain of the nanosilver solution.

Decay Resistance

The species tested were *Acacia magnium* (acacia), *Cedrela odorata* (cedro amargo), and *Vochysia guatemalensis* (cebo). The effectiveness of silver nanoparticles in these species was measured by the degradation of wood against fungal attack, specifically resistance to white decay (*Trametes versicolor*). A total of 30 samples of 20 × 20 × 20 mm of each species was injected with the nanoparticle solution by vacuum pressure (15 min of vacuum and 4 h of pressure). For each sample, the concentration of nanoparticles was calculated based on weight gain. These samples

were oven-dried to 0% moisture and then placed into a desiccator with water for 2 wk. Thirty samples (20 × 20 × 20 mm) without any treatment were also conditioned and used as controls. This conditioning allowed the wood samples to reach 30% MC. Subsequently, the samples were sterilized and placed in a soil-block medium into bottles previously inoculated with the fungus, according to the ASTM D2017 Standard (ASTM 2003) and exposed for 4 months. The sample was then cleaned, oven-dried to determine the final weight, and weight loss calculated.

Specific Gravity, Density, and Moisture Content

Thirty samples (20 × 20 × 20 mm) each of untreated wood and nanosilver-treated wood per species were tested. The samples were placed in a conditioning chamber maintained at 12% equilibrium MC (22°C and 60% RH). Then, the treated and the untreated samples were weighed and their volume measured, and the samples were placed into an oven at 103°C for 24 h to reach the moisture-free mass. The following properties were determined: specific gravity based on sample volume and 12% MC (oven-dry weight/volume at 12%), density (weight at 12%/volume at 12%), and moisture content (water weight at 12% /oven-dry volume) were determined.

Swelling and Water Absorption

The remaining 30 samples (treated and untreated) were used to measure swelling and water absorption. Thirty 50-mm-wide × 50-mm-long × 12-mm-thick samples were obtained from the wood treated with silver nanoparticles, and their radial and tangential positions were adequately oriented. Likewise, 30 samples were extracted from the untreated wood with the same dimensions and also adequately oriented. The samples were immersed in water for 24 h at room temperature. Each sample was weighed, and their tangential and radial dimensions before and after immersion were measured. Lastly, the samples were placed in an oven at 103°C to determine their oven-dry weight. With this information, moisture content, radial and tangential swelling before and after drying, and percentage of absorbed water by the wood after the 24-h immersion were determined.

Statistical Analysis

A descriptive analysis was developed (mean and standard deviation) for absorption parameters (density of the wood and solution absorption and retention), properties of wood (weight loss, specific weight, and moisture content), and dimensional stability parameters (radial and tangential swelling, moisture content before and after immersion in water, and water absorption percentage). In addition, it was verified if the variables met the assumptions of normal distribution, homogeneity of variances, and the presence of extreme data. Subsequently, an analysis of variance was applied to verify the effect of treatment (two levels: treated and untreated) with the silver nanoparticles on the previously indicated properties of the wood of each species studied. Tukey's test was set at a 99% confidence level to determine the statistical difference between the means.

RESULTS AND DISCUSSION

Characterization of Nanoparticles

The silver nanoparticle synthesis method used in the investigation showed that the solution was unclear and had a light greenish yellow color. Nanoparticle size ranged from 10 to 25 nm (Fig 1a-b). AFM analysis shows the presence of nanoparticles in a solution and also gives evidence that the irregularity can reach 15 nm (Fig 1a). These measurements were confirmed by TEM, which allows the observation of nanoparticles with diameters up to 25 nm (Fig 1b). Particles were spherical in shape, and the largest ones were prismatic (Fig 1c). An important aspect is that although PVP was added to prevent agglomeration of particles, clustered areas (Fig 1d) occurred. Also, the UV-Vis spectrum of the nanoparticles showed a distinct band centered around 400 nm (Fig 1e).

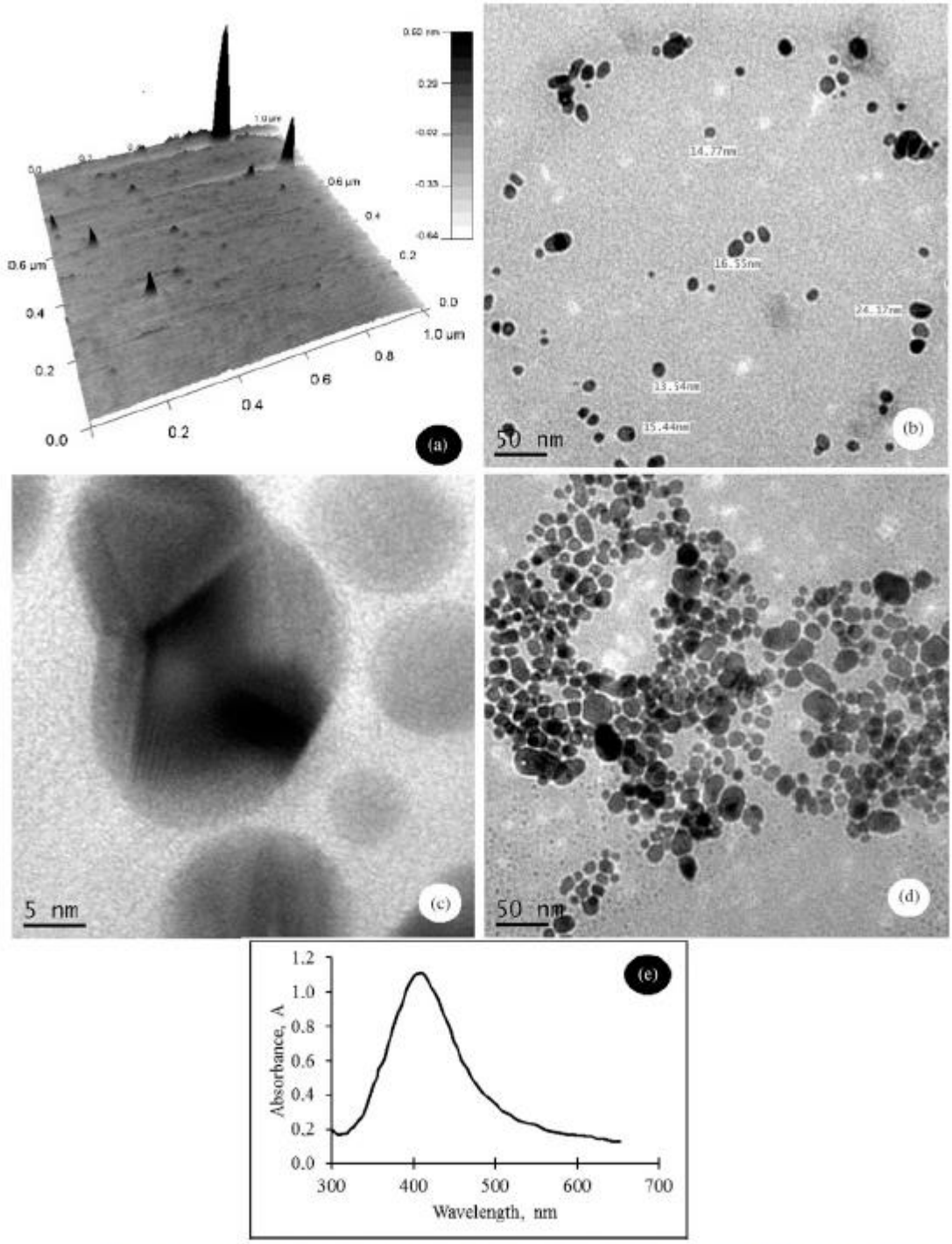

Figure 1. Silver nanoparticles used in wood and observed by (a) atomic force microscopy, (b) transmission electron microscopy, (c) shape of silver nanoparticles, (d) region of agglomerated silver nanoparticles, and (e) UV-vis spectrum of silver nanoparticles.

There are different synthetizing methods for silver nanoparticles. Among the most popular are those based on chemical reduction, photoreduction, and thermal decomposition (Mavani and Shah 2013). The method applied in this study, considered one of the simplest and most efficient (Mavani and Shah 2013), resulted in silver nanoparticles of adequate size and slight agglomeration (Fig 1), as demonstrated by the observations from the AFM (Fig 1a) and TEM (Fig 1b-d) and the measurements carried out with the UV-Vis spectrum. This last technique proves that most of the particles with sizes less than 50 nm are on the band above 400 nm, which was also demonstrated by Sileikaite et al (2006) and Prema and Raju (2009).

Absorption and Retention of Silver Nanoparticles

V. guatemalensis was the species with the highest capacity to absorb the solution, therefore the one to retain the most silver nanoparticles per volume of wood (g_{Ag}/m^3_{wood}) followed by *A. mangium*. Neither of these two species showed any difference between sapwood and heartwood absorption. The sapwood of *C. odorata* was the wood with the lowest capacity to absorb the solution and with the lowest retention of nanoparticles (Table 1). However, when absorption by wood mass was projected, the behavior was slightly different. *V. guatemalensis* showed greater retention followed by heartwood of *A. mangium* and sapwood of *C. odorata*, and then by sapwood of *A. mangium*, with a statistically lower retention than previous types of wood. Lastly, the heartwood of *C. odorata* had the statistically lowest value (Table 1).

The silver nanoparticle absorption values obtained, from 267 to 653 L/m^3_{wood}, were evidence that it is possible to use the vacuum-pressure method commonly used in the preservation of wood (Schultz et al 2007; Barnes 2008) with the solution of silver nanoparticles. However, further research is needed to evaluate the effect of the nanoparticle solution on the metallic and plastic components that are part of these preservation systems (Glover et al 2011).

The absorption obtained in the heartwood of *A. mangium* and *C. odorata* should be analyzed in detail, because the heartwood of most species is refractory (Lebow 2010). However, the absorptions of *A. mangium* and *C. odorata* were 514 and 267 L/m^3_{wood}, respectively, which are high compared with other tropical woods such as *Tectona grandis*, *Swietenia macrophylla*, *Cupressus lusitanica*, and *Gmelina arborea*. Those species are generally considered to be refractory to penetration of substances (Moya and Muñoz 2010). The high absorption may be explained first by the fact that wood of 20-mm maximum length was used, allowing a degree of longitudinal penetration in the wood (Islam et al 2008). Second, the heartwood of some species from tropical climates shows some degree of penetration with this method (Keenan and Tejada 1988; Stan 2010). This capability of absorbing a liquid or not is related to the anatomical structure and abundance and number of wood extractives (Stan 2010).

The value of absorption of silver nanoparticles solution in sapwood (Table 1) is considered rather high, similar to the absorption values presented by other tropical species, between 121 and 417 L/m^3_{wood} (Moya and Muñoz 2010). The difference between these species was caused

Table 1. Absorption and retention of silver nanoparticles in treated and untreated wood of the species *Acacia mangium*, *Vochysia guatemalensis*, and *Cedrela odorata*.[a]

Species	Type of wood	Absorption (L/m^3_{wood})	Retention of nanosilver (g_{Ag}/m^3_{wood})	Retention of nanosilver (mg_{Ag}/kg_{wood})	Wood density before impregnation (g/cm^3)
Acacia mangium	Sapwood	497^{A} (12.41)	24.89^{A} (12.41)	45.75^{A} (15.31)	0.55^{A} (7.52)
	Heartwood	514^{A} (28.76)	25.75^{A} (28.76)	58.48^{B} (43.41)	0.48^{B} (20.96)
Cedrela odorata	Sapwood	510^{A} (8.03)	25.50^{A} (8.03)	54.35^{B} (11.94)	0.47^{B} (5.17)
	Heartwood	267^{B} (20.93)	13.36^{B} (20.93)	25.27^{C} (36.68)	0.55^{A} (11.19)
Vochysia guatemalensis	Sapwood	653^{C} (7.06)	32.66^{C} (7.06)	101.96^{D} (14.40)	0.33^{C} (12.67)

[a] Values in parentheses are coefficients of variation. Average values identified with A and B are statistically different at $\alpha = 99\%$.

by their differences in weight (Keenan and Tejada 1988). Woods with low specific weight, such as *V. guatemalensis*, have high absorption, whereas woods with higher specific weight such as *A. mangium* absorb less (Table 1).

Tropical woods with high absorption have the advantage of absorbing a larger amount of silver nanoparticles when treated with that solution. Such is the case of *V. guatemalensis*, with the highest retention values, either by wood volume (g_{Ag}/m^3_{wood}) or by wood weight (mg_{Ag}/kg_{wood}) (Table 1). The absorption values found were similar to those reported by Taghiyari (2012) for *Fagus orientalis*, *Populus nigra*, *Platanus orientalis*, *Alnus* spp., and *Abies alba* but lower than the values given by Liu et al (2002a, 2002b, 2002c).

Decay Resistance

Adding silver nanoparticles had an effect on the protection of wood against biodeterioration by the action of *Trametes versicolor*. In untreated wood, weight losses were about 50, 35, and 25% for *A. mangium*, *V. guatemalensis*, and *C. odorata*, respectively. However, when silver nanoparticles were added, weight loss was less than 5% for both heartwood and sapwood of the three species. These results confirm that the effect was caused by the application of silver nanoparticles as a wood preservative.

Several studies have demonstrated the potential of silver nanoparticles for wood protection (Liu et al 2002a, 2002b, 2002c), behavior in fire (Taghiyari 2012), improvement of wood properties (Taghiyari 2012; Taghiyari and Bibalan 2013), or for already known wood treatments such as thermal treatment (Taghiyari et al 2012), wood densification (Rassam et al 2012), or particleboard manufacturing (Taghiyari et al 2011). However, the advantage of using a silver nanoparticle solution compared with a boron salts treatment (BAE) is not well quantified. A saturated solution of boric acid (H_3BO_3) and sodium borate ($Na_2B_4O_7$) at 22°C contains 94.75 g/L of H_3BO_3, whereas the system used for the synthesis of nanoparticles produces 28 mg of H_3BO_3 (Eq 1), about 1670 less times per liter than the boric acid generated for the combination of H_3BO_3 and $Na_2B_4O_7$. Similarly, the effectiveness of boric acid in terms of the BAE varies from 0.7 to 3.0 kg/m^3_{wood} (Lloyd 1998), whereas concentration of nanoparticles varies from 13.36 to 32.66 g_{Ag}/m^3_{wood}, which is equivalent to a decrease of about 100 times of active element.

One advantage compared with traditional wood preservatives is that the silver nanoparticles at low concentrations, apart from protecting wood, can also be added in wood preservatives allowing the nondecay micro-organisms to degrade the organic preservatives (Schultz et al 2008). Likewise, the low levels of metal used may have some advantages when depositing or discarding the treated wood. However, the authors note that this type of preservative is still unprofitable.

According to ASTM D-2017 (ASTM 2003), sapwood and heartwood of the three species treated with silver nanoparticles (Fig 2) were classified as highly resistant (Class A) to attack by *T. versicolor*. Wood affected by the action of white-rot fungus, the main rot type that affects broadleaf woods, showed differences associated with treatment, type of wood, and species (Moya et al 2009; Moya and Berrocal 2010). The sapwood and heartwood of *A. mangium* without

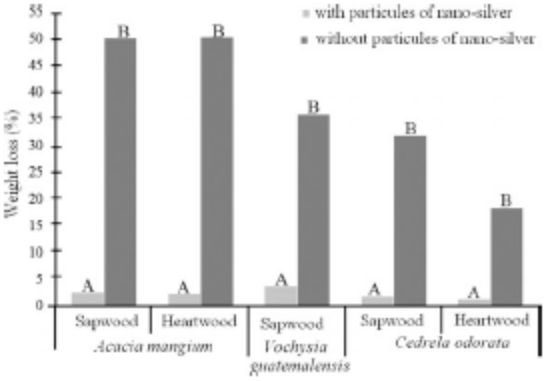

Figure 2. Weight loss caused by *Trametes versicolor* (b) on *Acacia mangium*, *Vochysia guatemalensis*, and *Cedrela odorata* wood untreated and treated with nanosilver in Costa Rica (average values identified with A and B are statistically different at $\alpha = 99\%$).

treatment was classified as resistant (Class D), whereas the sapwood of *V. guatemalensis* and *C. odorata* was classified as moderately resistant (Class C). Heartwood of *C. odorata* was considered, according to the norm, as resistant (Class B). Instead, wood treated with silver nanoparticles, regardless of the type of wood and species, was classified as highly resistant (Class A) to this type of decay.

The effect of silver nanoparticles on fungi associated with tropical species agrees with other studies. For example, Velmurugan et al (2009) found that mycelial growth of stain fungi *Ophiostoma flexuosum*, *O. tetropii*, *O. polonicum*, and *O. ips* decreased on media amended with different concentrations of silver nanoparticles synthesized from silver nitrate and sodium borohydride. They found that mycelial growth decreased with nanosilver concentration. Mycelial growth was at the highest with a concentration of 1 ppm, and the lowest growth was found with a concentration of 100 ppm. Conversely, Liu et al (2001, 2002a, 2002b, 2002c) also found a decrease of wood decay with different stabilizing agents and with addition of different fungicides to silver nanoparticle solution.

According to Dorau et al (2004), wood decay fungi have been shown to be susceptible to silver nanoparticles because the silver ions, in solution, inhibit the activity of their cellulose enzymes (Highley 1975). Wood decay fungi feeding on a block treated with silver halide would probably release more silver as a result of oxidative Fenton reactions during the breakdown of cellulose (Xu and Goodell 2001). Besides, silver nanoparticles constitute a reservoir for the antimicrobial effect. In the presence of moisture, metallic silver oxidizes, which results in the release of the silver ions. Silver ions are the species that are responsible for microbial inhibition. Because silver oxidation is a slow reaction, the size of silver particles is critical to achieve micro-organism growth inhibition. The smaller the particle size, the higher the surface area and the greater the area available for oxidation. Particles with diameters less than 100 nm are required to have the surface area necessary to allow a continuous release of silver ions. The main advantages of silver nanoparticles compared with organic biocides are that they are nonvolatile and nondegradable with time, are odorless, and have long-term efficacy (Clausen 2007).

Likewise, heat-transferring properties of silver nanoparticles are able to intensify the effect on heat treatment of wood at all temperatures. Nanosilver impregnation (400 ppm) had an intensifying effect on the results of the heat treatment against *T. versicolor* (Moradi et al 2013). Similar results were found by Reza et al (2013). They concluded that nanosilver impregnation aggravates the effects of heat treatment; however, heat treatment on nanosilver-impregnated specimens may have a greater impact on mechanical properties than physical properties. The decreasing or increasing effects of heat treatment at higher or lower temperatures on properties are also dependent on the density of the wood species.

Specific Gravity, Density, Moisture Content, Swelling and Moisture Absorption

Evaluation of wood physical properties showed that the specific gravity at 12% was only higher in the heartwood of *C. odorata* treated with silver nanoparticles (Fig 3a; Table 1). Regarding wood density, none of the species or wood types (sapwood or heartwood) were found to be significantly affected by the treatment with silver nanoparticles (Fig 3b; Table 2).

Evaluation of dimensional stability revealed a statistical decrease in swelling in the radial direction in *V. guatemalensis* and *C. odorata* (Table 2), and swelling in tangential direction also diminished in *C. odorata* (Table 2). Conversely, neither radial swelling nor tangential swelling in *A. mangium* nor tangential swelling in *V. guatemalensis* was affected statistically by the application of silver nanoparticles to the wood (Table 2). After the wood was impregnated (treated) with the nanoparticles, water absorption diminished in all three species (Table 2). Also, moisture content before the absorption test was statistically equivalent in the three species, but after the absorption test,

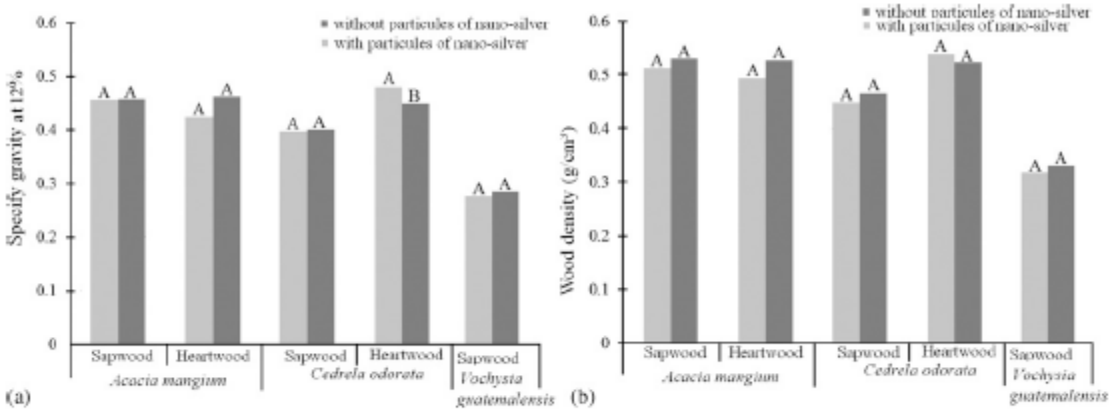

Figure 3. Comparison of specific gravity (left) and wood density (right) in wood untreated and treated with silver nanoparticles from *Acacia mangium*, *Vochysia guatemalensis*, and *Cedrela odorata* (average values identified with A and B are statistically different at $\alpha = 99\%$).

the wood treated with silver nanoparticles presented statistically lower moisture content than the untreated wood in all three species (Table 2).

The increase in specific gravity in *Cedrela odorata* can be attributed either to the amount of nanoparticles added, which in this type of wood (Table 1) was significant compared with untreated wood, or to samples of higher specific gravity being collected as specific gravity increases from pith to bark (Wiemann and Williamson 1989). For wood density of 12%, this parameter was not significantly affected by adding the nanoparticles (Fig 3b). For wood density, amount of nanoparticles added to the wood (Table 1) produced no significant increase.

The wood property most significantly affected by impregnation with nanoparticles was swelling (Tables 1 and 2). However, there appears to be no relation between absorption and swelling in radial and tangential directions because the percentage of absorption was significantly affected for all the species and for the two types of wood, whereas the swelling values were affected only for *V. guatemalensis* and *C. odorata* in the radial direction and for *C. odorata* in the tangential direction (Table 2). These results show that treatment with silver

Table 2. Swelling parameters of *Acacia mangium*, *Vochysia guatemalensis*, and *Cedrela odorata* wood untreated and treated with silver nanoparticles.[a]

Wood properties	Treatment	*Acacia mangium*	*Vochysia guatemalensis*	*Cedrela odorata*	Average
Radial swelling (%)	With nanosilver	2.92^{A} (20)	3.68^{A} (11)	1.42^{A} (22)	3.13 (29)
	Without nanosilver	3.08^{A} (23)	4.12^{B} (18)	2.36^{B} (20)	2.73 (41)
Tangential swelling (%)	With nanosilver	1.00^{A} (32)	1.38^{A} (43)	0.98^{A} (16)	1.43 (40)
	Without nanosilver	1.02^{A} (37)	1.27^{A} (50)	1.92^{B} (17)	1.09 (41)
Moisture content before nanosilver treated (%)	With nanosilver	12.95^{A} (6)	14.95^{A} (7)	14.11^{A} (3)	14.00 (8)
	Without nanosilver	12.47^{A} (9)	14.45^{A} (7)	15.11^{A} (2)	15.34 (15)
Moisture content after nanosilver treated (%)	With nanosilver	74.63^{A} (9)	148.17^{A} (8)	45.65^{A} (6)	89.48 (49)
	Without nanosilver	67.28^{B} (10)	125.15^{B} (10)	40.34^{B} (7)	77.59 (47)
Water absorption	With nanosilver	54.60^{A} (10)	115.92^{A} (9)	27.65^{A} (9)	66.06 (57)
	Without nanosilver	48.71^{B} (12)	93.30^{B} (10)	19.84^{B} (12)	53.95 (58)

[a] Values in parentheses show coefficient of variation. Average values identified with A and B are statistically different at $\alpha = 99\%$.

nanoparticles decreased the absorption of water in the various tropical species but that water absorbed to some species such as *A. mangium* had no effect in increasing the dimensional stability. The cell wall of the timber reveals porosity on a molecular level because of the partial arrangement of the cellulose microfibrils and because of the partial filling of these spaces by lignin, hemicellulose, and extractives (Wegner and Jones 2006). Very small-sized nanoparticles can penetrate the pores, preventing moisture from entering and thus decreasing water absorption (Mantanis and Papadopoulos 2010a), as occurred in all the species studied (Table 2). Nevertheless, dimensional stability was different for each species, probably because of the nature of the extractives in *A. mangium*, which does not allow nanoparticles to join the OH cellulose and hemicellulose groups (Mantanis and Papadopoulos 2010b). Hygroscopicity decreased in the treated wood because the adsorbed water was separated into hydrate water relating to monomolecular sorption and dissolved water relating to polymolecular sorption (Mantanis and Papadopoulos 2010b).

CONCLUSIONS

Dimensions of the synthetized silver nanoparticles ranged from 10 to 25 nm with few clusters and a good distribution in the solution. Retentions of 25-102 silver mg were achieved, depending on the species and the presence of sapwood and heartwood. This level of nanoparticle retention is approximately 1670 times less than the retention of the wood when preserved with a combination of boric acid and sodium borate.

Silver nanoparticles applied to the tropical species studied here improved durability of the wood of those species. For all cases, the nanoparticle-treated woods were classified as highly resistant or Class A for white (*Trametes versicolor*) decay fungi, as opposed to untreated wood, whose weight losses were more than 20%. Also, in addition to improved resistance to fungal attack, water absorption capacity of wood from the three species tested decreased with silver nanoparticles and dimensional stability increased in *Cedrela odorata* and *Vochysia guatemalensis*.

ACKNOWLEDGMENTS

We thank the Vicerrectoría de Investigación y Extensión at the Instituto Tecnológico de Costa Rica (ITCR), Maderas Cultivadas de Costa Rica, and Escuela de Agricultura de Trópico Húmedo (EARTH) for providing raw material and other help with this study.

REFERENCES

Akhtari M, Taghiyari HR, Kokandeh MG (2013) Effect of some metal nanoparticles on the spectroscopy analysis of Paulownia wood exposed to white-rot fungus. Eur J Wood Prod 71(2):283-285.

Anjum NA, Gill SS, Duarte AC, Pereira E, Ahmad I (2013) Silver nanoparticles in soil–plant systems. J Nanopart Res 15(9):1-26.

ASTM (2003) D-2017 Standard method of accelerated laboratory test of natural decay resistance of woods. American Society for Testing and Materials, West Conshohocken, PA.

Barnes HM (2008) Wood preservation trends in North America. Pages 583-597 *in* TP Schultz, H Militz, MH Freeman, B Goodell, and DD Nicholas, eds. Development of commercial wood preservatives, efficacy, environmental, and health issues. ACS Symposium Series 982, American Chemical Society, Washington, DC.

Clausen CA (2007) Nanotechnology: Implications for the wood preservation industry. Document No. IRG/WP 07-3041. International Research Group on Wood Protection, Stockholm, Sweden. 5 pp.

Crabtree JH, Burchette RJ, Siddiqi RA, Huen IT, Handott LL, Fishman A (2003) The efficacy of silver-ion implanted catheters in reducing peritoneal dialysis-related infections. Perit Dial Int 23:368-374.

Dorau B, Arango R, Green F III (2004) An investigation into the potential of ionic silver as a wood preservative. *In* Woodframe housing durability and disaster issues, 4-6 October 2004, Las Vegas, NV. Forest Prod Soc, Madison, WI. 15 pp.

Glover RD, Miller JM, Hutchison JE (2011) Generation of metal nanoparticles from silver and copper objects: Nanoparticle dynamics on surfaces and potential sources of nanoparticles in the environment. ACS Nano 5(11):8950-8957.

Highley TL (1975) Inhibition of celluloses of wood-decay fungi. Res Pap FPL-247. USDA For Serv Forest Prod Lab, Madison, WI. 9 pp.

Islam MN, Ando K, Yamauchi H, Kobayashi Y, Hattori N (2008) Comparative study between full cell and passive impregnation method of wood preservation for laser incised Douglas fir lumber. Wood Sci Technol 42(4):343-350.

Keenan FJ, Tejada M (1988) Maderas tropicales como material de construcción en los países del grupo andino de América del Sur (Tropical timber as a building material in the countries of the Andean Group of South America). ITDS-49S, International Development Research Centre, Ottawa, Canadá. 147 pp.

Lebow S (2010) Chapter 15: Wood Preservation Publication Pages 15-1-15-28 in Wood handbook, Gen Tech Rep FPL-GTR-190. USDA For Serv, Forest Prod Lab, Madison, WI.

Liu Y, Laks P, Heiden P (2001) Use of nanoparticles for controlled release of biocides in solid wood. J Appl Polym Sci 79(3):458-465.

Liu Y, Laks P, Heiden P (2002a) Controlled release of biocides in solid wood: I. Efficacy against brown rot wood decay fungus (*Gloeophyllum trabeum*). J Appl Polym Sci 86(3):596-607.

Liu Y, Laks P, Heiden P (2002b) Controlled release of biocides in solid wood: II. Efficacy against *Trametes versicolor* and *Gloeophyllum trabeum* wood decay fungi. J Appl Polym Sci 86(3):608-614.

Liu Y, Laks P, Heiden P (2002c) Controlled release of biocides in solid wood: III. Preparation and characterization of surfactant-free nanoparticles. J Appl Polym Sci 86(3):615-621.

Lloyd JD (1998) Borates and their biological applications. Document No. IRG/WP 98-30178. International Research Group on Wood Preservation, Stockholm, Sweden. 17 pp.

Mahapatra I, Clark J, Dobson PJ, Owen R, Lead JR (2013) Potential environmental implications of nano-enabled medical applications: Critical review. Environmental Science: Processes & Impacts 15(1):123-144.

Mantanis G, Papadopoulos NN (2010a) Reducing the thickness swelling of wood based panels by applying a nanotechnology compound. Eur J Wood Prod 68(2):237-239.

Mantanis G, Papadopoulos NN (2010b) The sorption of water vapour of wood treated with a nanotechnology compound. Wood Sci Technol 44(3):515-522.

Mavani K, Shah M (2013) Synthesis of silver nanoparticles by using sodium borohydride as a reducing agent. International Journal of Engineering Research and Technology 2(3):1-5.

Mie R, Samsudin MW, Din LB (2013) A review on biosynthesis of nanoparticles using plant extract: An emerging green nanotechnology. Adv Mat Res 667(Suppl 1):251-254.

Moradi BM, Ghorban MK, Taghiyari HR, Mirshokraie SA (2013) Effects of silver nanoparticles and fungal degradation on density and chemical composition of heat-treated poplar wood (*Populus euroamerica*). Eur J Wood Prod 71(4):491-495.

Moya R, Berrocal A (2010) Wood colour variation in sapwood and heartwood of young trees of *Tectona grandis* and its relationship with plantation characteristics, site, and decay resistance. Ann Sci 67(1):109-128.

Moya R, Leandro L, Murillo O (2009) Wood characteristics of *Terminalia amazonia*, *Vochysia guatemalensis* and *Hyeronima alchorneoides* planted in Costa Rica. Bosques 30(2):78-87.

Moya R, Muñoz F (2010) Physical and mechanical properties of eight fast-growing plantation species in Costa Rica. J Trop For Sci 22(3):317-328.

Prema P, Raju R (2009) Fabrication and characterization of silver nanoparticle and its potential antibacterial activity. Biotechnol Bioproc E 14(6):842-847.

Rassam G, Ghofrani M, Taghiyari HR, Jamnani B, Khajeh MA (2012) Mechanical performance and dimensional stability of nano-silver impregnated densified spruce wood. Eur J Wood Prod 70(5):595-600.

Reidy B, Haase A, Luch A, Dawson KA, Lynch I (2013) Mechanisms of silver nanoparticle release, transformation and toxicity: A critical review of current knowledge and recommendations for future studies and applications. Materials (Basel) 6(6):2295-2350.

Reza HT, Enayati A, Gholamiyan H (2013) Effects of nano-silver impregnation on brittleness, physical and mechanical properties of heat-treated hardwoods. Wood Sci Technol 47(3):467-480.

Schultz TP, Nicholas DD, McIntyre CR (2008) Recent patents and developments in biocidal wood protection systems for exterior applications. Recent Patents on Material Sci 1(2):128-134.

Schultz TP, Nicholas DD, Preston AF (2007) A brief review of the past, present and future of wood preservation. Pest Manag Sci 63(8):784-788.

Scott N, Chen H (2013) Nanoscale science and engineering for agriculture and food systems. Ind Biotechnol (New Rochelle NY) 8(6):340-343.

Sileikaite A, Prosycevas I, Puiso J, Juraitis A, Guobiene A (2006) Analysis of silver nanoparticles produced by chemical reduction of silver salt solution. Mater Sci 12(4):287-291.

Taghiyari HR (2012) Fire-retarding properties of nano-silver in solid woods. Wood Sci Technol 46(5):939-952.

Taghiyari HR, Bibalan OF (2013) Effect of copper nanoparticles on permeability, physical, and mechanical properties of particleboard. Eur J Wood Prod 71(1):69-77.

Taghiyari HR, Enayati A, Gholamiyan H (2012) Effects of nano-silver impregnation on brittleness, physical and mechanical properties of heat-treated hardwoods. Wood Sci Technol 47(3):1-14.

Taghiyari HR, Rangavar H, Bibalan OF (2011) Effect of nano-silver on reduction of hot-pressing time and improvement in physical and mechanical properties of particleboard. Bioresources 6(4):4067-4075.

Tan KS, Cheong KY (2013) Advances of Ag, Cu, and Ag–Cu alloy nanoparticles synthesized via chemical reduction route. J Nanopart Res 15(4):1-29.

Tarmian A, Sepehr A, Gholamiyan H (2012) The use of nano-silver particles to determine the role of reverse temperature gradient in moisture flow in wood during low-intensity convective drying. Special Topics & Reviews in Porous Media Int J 3(2):149-156.

Velmurugan N, Kumar GG, Han SS, Nahm KS, Lee YS (2009) Synthesis and characterization of potential fungicidal silver nano-sized particles and chitosan membrane containing silver particles. Iran Polym J 18(5):383-392.

Wegner TH, Jones P (2006) Advancing cellulose-based nanotechnology. Cellulose 13(2):115-118.

Wiemann MC, Williamson GB (1989) Radial gradients in the specific gravity of wood in some tropical and temperate trees. Forest Sci 35(1):197-210.

Xu G, Goodell B (2001) Mechanisms of wood degradation by brown-rot fungi: Chelator-mediated cellulose degradation and binding of iron by cellulose. J Biotechnol 87(1):43-57.

2. Artículo 2. Effect of silver nanoparticles synthetized with $AgNO_3$- ethylene glycol ($C_2H_6O_2$) on brown decay and white decay fungi of ten tropical woods

Journal of Wood Science

Effect of silver nanoparticles synthetized with NPsAg- ethylene glycol (C2H6O2) on brown decay and white decay fungi of ten tropical woods

--Manuscript Draft--

Manuscript Number:	
Full Title:	Effect of silver nanoparticles synthetized with NPsAg- ethylene glycol (C2H6O2) on brown decay and white decay fungi of ten tropical woods
Article Type:	Original article
Keywords:	Wood preservatives, nanotechnology, tropical species, weight loss, fugal attack.
Corresponding Author:	Roger Moya, Ph.D. Instituto Tecnológico de Costa Rica Cartago, Cartago COSTA RICA
Corresponding Author Secondary Information:	
Corresponding Author's Institution:	Instituto Tecnológico de Costa Rica
Corresponding Author's Secondary Institution:	
First Author:	Roger Moya, Ph.D.
First Author Secondary Information:	
Order of Authors:	Roger Moya, Ph.D.
	Ana Rodriguez-Zuñiga, Bs.
	Alexander Berrocal, Dr
	José Vega-Baudrit, Dr.
Order of Authors Secondary Information:	
Abstract:	Nanotechnology applications have potential for improving decay resistance of wood under tropical conditions. In this work, nine commercial timbers from Costa Rica were treated with silver nanoparticles synthetized with NPsAg- ethylene glycol through pressure. White-rot (Trametes versicolor) and brown-rot (Lenzites acuta) fungi were tested. According to the results, the sizes of the synthetized silver nanoparticles were 40 to 100 nm. The retention achieved was of 16 to 112 mg of silver per kilogram of wood or 7.7 to 25.1 mg of silver per cubic meter of wood. Specific gravity affected the retention in Cordia alliodora, Gmelina arborea, Goethalsia meiantha, Tectona grandis and Vochysia guatemalensis. Loss of weight was less in wood treated with silver nanoparticles, its values ranging from 8% to 35% in L. acuta and 7% to 11% in T. versicolor. As for durability, the wood of the species treated with silver nanoparticles is classified as highly resistant to T. versicolor and moderately to moderately resistant to L. acuta. Moreover, the effect of retention of the nanoparticles was not significant for weight in all of the species. This parameter was positively affected in C. odorata, E. cyclocarpum, G. arborea, T. grandis and V. ferruginea, although unaffected for other species.
Suggested Reviewers:	Mario Tomazello Filho, Dr Sao Paoblo Univerisity mtomazel@usp.br he know about tropical species
	Antonios N. Papadopoulos Department of Forestry and Management of Natural Environment, Lab of Wood and Wood Products, Technological Education Institute of Kavala, 66100 Drama, Greece antonios1974@hotmail.com He knows about nanotechnology
	Majid Kiaei

Powered by Editorial Manager® and ProduXion Manager® from Aries Systems Corporation

	Department of Wood and Paper Science and Technology, Chaloos Branch, Islamic Azad University, Chaloos, Mazandaran, Iran. mjd_kia59@yahoo.com he kwons about nanotechnology
Opposed Reviewers:	

Effect of silver nanoparticles synthetized with NPsAg- ethylene glycol ($C_2H_6O_2$) on brown decay and white decay fungi of ten tropical woods.

*Róger Moya**
Escuela de Ingeniería Forestal
Instituto Tecnológico de Costa Rica
Apartado 159-7050, Cartago, Costa Rica
email: rmoya@itcr.ac.cr

Ana Rodriguez-Zuñiga
Escuela de Ingeniería Forestal
Instituto Tecnológico de Costa Rica
Apartado 159-7050, Cartago, Costa Rica
email: ana.rodriguez@itcr.ac.cr

Alexander Berrocal
Escuela de Ingeniería Forestal
Instituto Tecnológico de Costa Rica
Apartado 159-7050, Cartago, Costa Rica
email: aberrocal@itcr.ac.cr

José Vega-Baudrit
Laboratório Nacional Nanotecnologia (LANOTEC)
Centro Nacional de Alta Tecnologia-CENAT, San Jose, Costa Rica
email: jvegab@gmail.com

List of submit materials

Title: 1 page
Abstract: 1 page.
Text: 19 pages.
Acknowledgement: 1 page
Reference: 5 pages
Figure legend: 1 pages
Figure: 3 pages
Tables: 2 pages

Key words: Wood preservatives, nanotechnology, tropical species, fugal attack.

*Authors correspondence, Email: rmoya@itcr.ac.cr

Effect of silver nanoparticles synthetized with NPsAg- ethylene glycol ($C_2H_6O_2$) on brown decay and white decay fungi of ten tropical woods.

Summary

Nanotechnology applications have potential for improving decay resistance of wood under tropical conditions. In this work, nine commercial timbers from Costa Rica were treated with silver nanoparticles synthetized with NPsAg- ethylene glycol through pressure. White-rot (*Trametes versicolor)* and brown-rot (*Lenzites acuta*) fungi were tested. According to the results, the sizes of the synthetized silver nanoparticles were 40 to 100 nm. The retention achieved was of 16 to 112 mg of silver per kilogram of wood or 7.7 to 25.1 mg of silver per cubic meter of wood. Specific gravity affected the retention in *Cordia alliodora*, *Gmelina arborea*, *Goethalsia meiantha*, *Tectona grandis* and *Vochysia guatemalensis*. Loss of weight was less in wood treated with silver nanoparticles, its values ranging from 8% to 35% in *L. acuta* and 7% to 11% in *T. versicolor*. As for durability, the wood of the species treated with silver nanoparticles is classified as highly resistant to *T. versicolor* and moderately to moderately resistant to *L. acuta*. Moreover, the effect of retention of the nanoparticles was not significant for weight in all of the species. This parameter was positively affected in *C. odorata*, *E. cyclocarpum*, *G. arborea*, *T. grandis* and *V. ferruginea*, although unaffected for other species.

Key words: Wood preservatives, nanotechnology, tropical species, weight loss, fugal attack.

65 **INTRODUCTION**

66 In recent years, approach to wood preservation has focused on developing
67 environmentally friendly preservatives through improved formulations [1]. The aim is to
68 develop preservatives that contain the least amount of active component, in order to reduce
69 or avoid the health problems and chemical contamination associated with them while the
70 wood product is being used and one it has fulfilled its useful life [2].

71 Worldwide there is an intensive development of nanotechnology applications in
72 many areas, from improving the behavior of materials to medical purposes [3]. As for
73 materials, the aim of the application of nanotechnology is to increase their mechanical and
74 physical properties and durability and improve the material's response to chemicals [4].
75 The aim of nanotechnology applications is using small quantities to increase the properties
76 of the materials [5].

77 Silver nanoparticles have gained much attention worldwide for various types of
78 applications, including medical applications, because of its antibacterial activity [6]. Silver
79 nanoparticles have also gained popularity in other areas, such as in plant biology and
80 reinforcement of materials [7,8]. Wood has also been researched to improve its properties.
81 Silver nanoparticles have been applied to improve the protection of the wood [9-12], its
82 behavior against fire, improved physical properties, heat treatment, densification of wood,
83 particleboard manufacturing and wood drying [5,13-17].

84 Various methods for silver nanoparticle synthetizing are available [18]; of those,
85 reduction methods are among the most important [19-20].For synthetizing, an excess of
86 ethylene glycol ($C_2H_6O_2$) is used as reducing agent, polyvinylpyrrolidone (PVP) as a

87 stabilizer to prevent agglomeration of the nanoparticles, and silver nitrate ($AgNO_3$) as silver
88 source [19].

89 The studies conducted on wood regarding fungal resistance [9-10,21]; give few
90 details on the synthesis of silver nanoparticles; in addition, little is known about the effects
91 of silver nanoparticles on tropical woods, which generally exhibit long durability. One of
92 the first studies on tropical woods is the one conducted by Moya et al. [12], who
93 synthetized silver nanoparticles by means of reduction with sodium borohydride and also
94 tested its effectiveness in three commercial species (*Acacia mangium*, *Cedrela odorata* and
95 *Vochysia guatemalensis*) from Costa Rica. However, the mentioned authors believe that
96 boron particles (an active wood preservative component) [22], are added into the silver
97 nanoparticle solution, which leads to confusion as to the real potential of the silver
98 nanoparticles.

99 This study reports on the synthetizing of silver nanoparticles (by reduction with an
100 excess of ethylene glycol ($C_2H_6O_2$), as reducing agent, polyvinylpyrrolidone (PVP) as
101 stabilizing and silver nitrate ($AgNO_3$) as silver source and their effects on the wood's
102 absorption capacity, retention, and resistance to the attack of two types of fungi (brown-rot
103 *L. acuta* and white-rot *T. versicolor*) in nine tropical species (*A. mangium*, *C. odorata*, *C.*
104 *alliodora*, *E. cyclocarpum*, *G. arborea*, *G. meiantha*, *O. pyramidale*, *T. grandis* and *V.*
105 *ferruginea*).
106
107

MATERIALS AND METHODS

Materials

Three components were utilized for synthesizing the silver nanoparticles: silver nitrate ($AgNO_3$) as a source of the reduced metal, supplied by MERCK (pureness 99,9+%), ethylene glycol ($C_2H_6O_2$) as reducing agent, supplied by J.T. Baker (pureness 99.9%) and polyvinylpyrrolidone (PVP) as stabilizing agent supplied by Magnacol Ldt. Wood samples from 9 tropical species in Costa Rica were used: *A. mangium*, *C. odorata, C. alliodora, E. cyclocarpum*, *G. arborea*, *G. meiantha*, *O. pyramidale*, *T. grandis* and *V. ferruginea*. These are woods traditionally employed in Costa Rica to manufacture doors, wood-based products and products used in engineering, which requires intensive use of adhesives. *A. mangium*, *G. arborea* and *T. grandis* are grown in forest plantations, while *G. meiantha*, *O. pyramidale* and *V. ferruginea* come from secondary forests and *C. odorata*, *C. alliodora* and *E. cyclocarpum* are found in agroforestry systems. The wood was obtained in various sites of commercialization of lumber. The fungal test was performed with two types of fungi: *T. versicolor* (white-rot fungus) and *L. acuta* (brown-rot fungus).

Synthesis of the silver nanoparticles and determination of the concentration

The silver nanoparticles were synthesized using the one step procedure proposed by Kheybari et al. [19], which is based on a reduction reaction, where an excess of ethylene glycol ($C_2H_6O_2$ as a reducing agent, polyvinylpyrrolidone (PVP) as stabilizing agent to prevent agglomeration of the nanoparticles and silver nitrate ($AgNO_3$) as a source of silver, were used. The synthesis is carried out by reflux at a temperature between 50 °C and 65 °C

for 15 minutes. This reaction consists in dissolving 0.32 g of $AgNO_3$ in 5 mL of ethylene glycol. Then, 5 g of PVP (PVP, MagnacolLdt.) are dissolved in 30 mL of ethylene glycol. Then, these two solutions were mixed together and homogenized in the flask of the reflux system and left stirring and heating until reaching a coloration ranging from gold to brown(Equation 1). More details on the process of the reaction can be consulted at Kheybari et al [19].

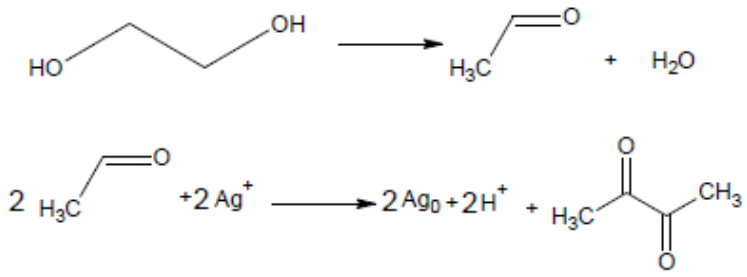

(1)

The concentration of synthesized silver nanoparticles was determined indirectly; for this, a UV-absorption calibration-curve is constructed. A sample was taken from a standardized solution of silver nanoparticles at a concentration of 50 ppm, prepared by the reduction of silver nitrate with sodium hydroborane [20]. Then, 5 different concentrations (40, 30, 20 and 10 ppm) were prepared by diluting the above sample with distilled water. A small sample was taken from each sample of each concentration to measure its absorbance in the UV-vis spectrum, which gave equation 2 as a result. Lastly, absorbance and concentration of the solution of synthetized silver nanoparticles were determined employing the polyol method. Ultraviolet-visible spectroscopy (T18 manufactured by PG Instruments) was used for nanoparticle characterization.

$$Concentration\ (ppm) = \frac{Abs + 0{,}025}{0{,}056} \qquad (2)$$

148

149 **Characterization of the nanoparticles**

150 The size of the silver nanoparticles was determined by means of 3 different
151 techniques: UV observation and TEM and AFM images. To perform the UV
152 measurements, a sample was taken from the nanoparticle solution and then poured into the
153 UV sample holder. The characterization was based on UV-visible spectroscopy (T18
154 manufactured by PG Instruments, Leicestershire, UK). The measurement was performed
155 with respect to a blank of distilled water. A small sample was again taken to obtain the
156 TEM images, which was then placed in the microscope using 100-kV acceleration and
157 10,000X (B and C) and 30,0000X (D) amplification. The images of the silver nanoparticles
158 were observed with a JEOL (Akishima-Shi, Tokyo, Japan) TEM, JEM-2100 model. In the
159 case of observation with AFM images, a 5-mL sample of the nanoparticle solution was
160 taken, dissolved in 5 mL of ethanol, and then centrifuged for 5 min. Then, a small drop of
161 this solution was observed with the AFM on a ceramic surface and ethanol was needed to
162 evaporate in order to make the measurement. The asylum research model MFP 3D was
163 used to take images of the AFM.

164

165 **Preservation of wood samples with silver nanoparticles**

166 Five 25 mm thick and 20 cm width boards of each one of the species were bought in
167 various sites of commercialization of lumber. The boards were dried to 12% moisture
168 content (MC) in a chamber at 22 °C and 65% relative humidity. Then, 25 mm x 25 mm

169 cross-sections were extracted from each board. Then they were planned in 20 mm x 20 mm
170 and samples measuring 20- × 20- × 20-mm were prepared. 60 samples from each species
171 were randomly selected. Heartwood was not tested in wood species with tissue because it is
172 un-treated with preservant. All samples were placed into a 1 m^3 experimental pressure
173 vessel commonly used for wood preservation. The preservation process consisted of 30 min
174 at -78 kPa vacuum, 2 h at 690 kPa pressure, and 15 min at -78 kPa vacuum. The samples
175 were weighed before and after the preservation process. Absorption capacity for each
176 sample was calculated as the absorption of solution in liters/wood volume. Nano-silver
177 retention was determined by weight gain of the wood sample due to the nano-silver
178 absorption.
179

180 **Decay resistance**

181 The effectiveness of silver nanoparticles in the 30 wood samples treated (*A.*
182 *mangium*, *C. odorata*, *C. alliodora*, *E. cyclocarpum*, *G. arborea*, *G. meiantha*, *O.*
183 *pyramidale*, *T. grandis* and *V. ferruginea*) was measured by the performance of wood
184 against fungal attack, specifically as regards to resistance to brown decay and white decay
185 (*L. acuta* and *T. versicolor*, respectivamente). These samples were oven-dried to 0% MC
186 and then placed into a desiccator with water for 2 wk. Thirty samples (20 × 20 × 20 mm)
187 without any treatment were also conditioned and used as control. This conditioning allowed
188 the wood samples to reach 30% MC. Subsequently, the samples were sterilized and placed
189 in a soil-block medium into glasses previously inoculated with the fungi, according to
190 ASTM D-2017 Standard and exposed for four months [23]. The sample was then cleaned,
191 oven-dried to determine the final weight, and weight loss percentage was calculated. For

192 fungal exposition in glasses in the accelerated degradation test, an environmental control
193 chamber was used (Darwin Chambers Company SA, St. Louis, MO).

194

195 **Statistical Analysis**

196 A descriptive analysis was developed (mean and standard deviation) for absorption
197 parameters (density of the wood and solution absorption and retention) and weight loss
198 percentage. In addition, it was verified if the variables met the assumptions of normal
199 distribution, homogeneity of variances, and the presence of extreme data. Subsequently, an
200 ANOVA was applied to verify the effect of treatment (two levels: treated and untreated)
201 with the silver nanoparticles, on the previously indicated properties of the wood of each
202 species studied. Tukey's test was set at 99% confidence level to determine the statistical
203 difference between the means.

204 Additionally, a regression analysis was established between the retention (measured
205 in mg_{Ag}/m^3_{wood} and mg_{Ag}/kg_{wood}) and density of the wood for each one of the species, in
206 order to establish the correlation between the two parameters. Also, the correlation between
207 retention and weight loss was established for each one of the species in the two tested fungi
208 (*L. acuta* and *T. versicolor*). In both cases the significance level was 99%.

209

210

211 **RESULTS AND DISCUSSION**

212 **Characterization of nanoparticles**

213 The polyol synthetizing method (Ag-polyol NPs) of silver nanoparticles with ethylene
214 glycol produced dark yellow to brown colloidal dispersions. The size of the nanoparticles
215 ranges from 40 to 100 nm (Fig. 1a and 1b). The AFM analysis shows irregularities on the
216 surface in a solution of nanoparticles which evidently can reach 11.7 nm (Fig. 1c). These
217 measurements were verified with the TEM, which shows that the diameter of the
218 nanoparticles may range between 40 to 100 nm (Fig. 1a and 1b). The particles used were
219 spherical (Fig. 1a) and prismatic (Fig. 1b). Also, the UV-Vis spectrum of the nanoparticles
220 showed a distinct band centered around 410 nm (Fig. 1d), which is the measurement for
221 particle sizes of 40 nm.

222 Various methods are available for synthetizing silver nanoparticles, of which those
223 based on chemical reduction, photoreduction and thermal decomposition are among the
224 most popular [20]. These methods have been developed to control growth of bacteria, for
225 wood protection and in human medicine [2,24]. The method applied in this work,
226 considered one of the most simple and effective [20], enabled production of silver
227 nanoparticles of adequate size (Fig. 1). This is demonstrated by the TEM (Fig. 1a-1b),
228 AFM (Fig. 1c) observations and UV-Vis spectrum measurements (Fig. 1c). In the latter
229 technique the band of absorbance at 400 nm shows that most particles are less than 50 nm
230 (Fig. 1e), which is consistent with Prema and Raju and Sileikaite et al [25,26].

231

232 **Absorption and retention of silver nanoparticles**

233 The statistical analysis of the absorption and retention of the solution expressed in
234 mg_{Ag}/m^3_{wood} showed different groups: a first group of greater absorption comprising *G.*
235 *meiantha*, followed by *C. alliodora* and *V. ferruginea* with significantly different
236 absorption (Table 1). Then comes a group consisting of *A. mangium*, *C. odorata* and *O.*
237 *pyramidale*, which showed no differences in absorption (Table 1). *T. grandis* forms a
238 solitary group with values statistically different from other species. Lastly, *E. cyclocarpum*
239 and *G. arborea* form the group of species with the lowest absorption and retention values in
240 mg/m^3 (Table 1).

241 As for retention in treated wood measured in mg_{Ag}/kg_{wood} the behavior was different: the
242 highest statistical retention was obtained with *O. pyramidale*, followed by *C. alliodora* and
243 *G. meiantha* with statistically similar values; then, a group consisting of *C. odorata* and *V.*
244 *ferruginea* again with statistically similar values (Table 1). The species *A. mangium* and *E.*
245 *cyclocarpum* show statistically equivalent values, and lower retention than the previous
246 species, although statistically greater than *T. grandis* and *G. arborea*, which are the species
247 with statistically lower retention (Table 1).

248 As for the air dry density before impregnation with silver nanoparticles, results
249 showed that the species showing statistically higher density was *T. grandis*, followed by *V.*
250 *ferruginea* and *A. mangium* and then by *G. arborea*, with a density of 495 kg m^{-3}. The
251 following group consists of *C. odorata* and *G. meiantha* with no statistical difference
252 between them. Then, *C. alliodora* and *E.cyclocarpum* form a group with no statistical
253 differences and low retentions, whereas *O. pyramidale* was the species with the lowest
254 statistical density (Table 1).

255 As regards to the coefficient of variation (CV) of absorption and retention expressed in
256 mg_{Ag}/m^3_{wood}, *G. arborea* showed a CV above 73%; *A. mangium*, *O. pyramidale* y *T.*
257 *grandis* presented CV close to 20%, while for the rest of the species the CV was lower than
258 10% in these two parameters. As for retention expressed in mg_{Ag}/kg_{Wood}, *T. grandis* and *V.*
259 *ferruginea* showed a CV over 20%; for *A. mangium*, *C. odorata*, *C. alliodora* and *T.*
260 *grandis*, the CV ranged between 12 and 19%, while in *E. cyclocarpum* and *G. meiantha* the
261 variation was lower than 10% (Table 1). Regarding the parameter of wood density, the CV
262 was generally lower than 10%, except for *O. pyramidale* and *V. ferruginea* presenting
263 26.1% and 14.7%, respectively.

264 With regard to the absorptions of the solution of silver nanoparticles obtained —
265 from 194 to 640 liters/m^3_{wood}— it appears that it is possible to use the pressure-vacuum
266 method, commonly used in wood preservation [27,28], with the dissolution of silver
267 nanoparticles. However, it will be necessary to evaluate the effect of nano-particle solutions
268 in metal and plastic components that are part of these preservation systems [29].

269 The differences between the absorption values in the different species (Table 1)
270 must be analyzed in detail. Although the absorption is associated with the specific gravity
271 of wood [30], this did not occur in the present study. O. *pyramidale*, with very low specific
272 gravity (Table 1), showed intermediate absorption values among the species, similar to *A.*
273 *mangium* and *C. odorata*, which have much higher specific gravity values. *A. mangium* did
274 not show the lowest absorption values, although it is a species with high density. *G.*
275 *arborea* and *E. cyclocarpum,* with intermediate values of specific gravity, show low
276 absorption values. The only case that seems to match is *G. meiantha*, which has low density

277 and presents the highest absorption values. This lack of relationship between specific
278 gravity and absorption is associated with other characteristics of wood, such as the presence
279 of heartwood and anatomical structure [30]. As for the heartwood of most species, liquid
280 impregnation by the vacuum-pressure method is refractory [30], and for *A. mangium*, *C.*
281 *odorata*, *G. arborea*, *E. cyclocarpum* and *T. grandis*, although efforts were made to
282 consider sapwood alone, these species show a region of transition in which the heartwood
283 cannot be distinguished from the sapwood [31], where liquid penetration into the wood is
284 affected. With regard to the anatomical structure, the ability to absorb or not a liquid is
285 related to the abundance and size of points of communication between the different wood
286 cells, as well as the abundance and quantity of wood extractives, which in many cases
287 block the passage of fluids [30].[30]

288 The absorption of the solution of silver nanoparticles obtained with these species
289 (Table 1) is similar in other tropical species. For example, Moya et al. [12] also found
290 variability in the values of absorption in a study on silver nanoparticle absorption in *A.*
291 *magium*, *C. odorata* and *V. guatemalensis*. Furthermore, absorptions of wood preservative
292 between 121 and 417 liters/m^3_{wood} were found in a group of 8 species [31], similar values to
293 those found in the present work (Table 1).

294 Because of the high absorption found in tropical woods (except for *G. arborea* and
295 *E. cyclocarpum*, which have low levels of absorption) high amounts of silver nanoparticles
296 can be found in wood treated with a solution of such particles. High absorption of *G.*
297 *meiantha*, for example, result in the highest values of retention, either by wood volume
298 (g_{Ag}/m^3_{wood}) or by wood weight (mg_{Ag}/kg_{wood}) (Table 1). The absorption values found are
299 similar to those reported by Taghiyari [13] for *Fagus orientalis*, *Populus nigra*, *Platanus*

300 *orientalis*, *Alnus spp.* and *Abies alba*, but lower than the values obtained by Liu et al. [9-
301 11].
302

303 **Effect of the density on the retention**

304 The effect of the density on the retention measured in mg_{Ag}/m^3_{wood} and mg_{Ag}/kg_{wood}
305 showed variation among the species. In the species *C. alliodora*, *G. arborea*, *G. meiantha*,
306 *T. grandis* and *V. guatemalensis*, the retention measured in mg_{Ag}/m^3_{wood} decreased
307 statistically as the density increased (Fig. 2a), while in *C. odorata* and *E. cyclocarpum* the
308 retention in mg_{Ag}/m^3_{wood} is not affected by the variation of the density (Fig. 2b). On the
309 other hand, in *A. mangium* and *O. pyramidale*, an increasing retention (mg_{Ag}/m^3_{wood}) with
310 increasing density occurs, although with low correlation coefficients (Fig. 2b).
311 The correlation analysis of the retention (mg_{Ag}/kg_{Wood}) of the various species showed
312 again that the retention decreases with the density in *C. alliodora*, *G. arborea*, *G. meiantha*,
313 *T. grandis* and *V. guatemalensis* (Fig. 2c). Furthermore, the species *O. pyramidale* and *C.*
314 *odorata* present this same decrease, whereas in *A. mangium* and *E. cyclocarpum* the
315 retention measured in mg_{Ag}/kg_{Wood} was statistically unaffected by the density (Fig. 2d).

316 The internal variation of wood density has a negative effect in the values of the
317 retention of nanoparticles for *C. alliodora*, *G. arborea*, *G. meiantha*, *T. grandis* and *V.*
318 *ferruginea*, since the higher the density, the lower the retention of the nanoparticles (Fig. 2a
319 and 2c). Low concentrations of the chemical element to protect the wood makes it more
320 susceptible to microorganisms [9]. As regards to *A. mangium* and *O. pyramidale*, there is
321 an increment in the retention of the nanoparticles measured in mg_{Ag}/m^3_{wood} (Fig. 2b), since

322 the durability of the species is influenced by the increment in the density. No effects have
323 been observed in *C. odorata* and *E. cyclocarpum* regarding variation of the density as a
324 result of nanoparticle retention (Fig. 2b).

325

326 **Decay resistance**

327 Weight loss due to the attack of brown-rot fungus and white-rot fungus (*L. acuta* and
328 *T. versicolor*) is shown in Fig. 3. In the nanoparticle-untreated wood, weight loss
329 percentage ranged from 15% to 75% in *L. acuta* and from 8% to 55% in *T. versicolor*,
330 while in wood treated with silver nanoparticles weight loss percentage ranged from 8% to
331 35% in *L. acuta* and 7% to 11% in *T. versicolor*. In both types of fungi, treatment with the
332 nanoparticles statistically decreased weight loss in most species except in *T. grandis* with
333 *L. acuta* (Fig. 3a) and *C. odorata* with *T. versicolor* (Fig. 3b). As for the species *V.*
334 *ferruginea,* treatment with nanoparticles increased weight loss in *T. versicolor* (Fig. 3b).
335 Another important aspect to highlight is that the biggest differences between nanoparticle-
336 treated and -untreated wood were observed in greater magnitude in *T. versicolor* (Fig. 3b)
337 compared to *L. acuta* (Fig. 3a).

338 The evaluation of the effect of the retention measured in mg_{Ag}/m^3_{wood} or mg_{Ag}/kg_{Wood}
339 on weight loss showed that the variation of the retention does not affect statistically the
340 weight loss percentage in *A. mangium* nor in *O. pyramidale*, with any of the two fungi
341 tested. Regarding *L. acuta*, weight loss percentage was not affected statistically by the
342 retention in *C. odorata*, *C. alliodora*, *G. meiantha*, *T. grandis* and *V. ferruginea* (Table 2).
343 On the other hand, in *E. cyclocarpum* and *G. arborea*, retention is statistically related with

344 weight loss percentage in both types of fungi. With *T. versicolor* a positive relationship was
345 found in *C. odorata*, *E. cyclocarpum*, *G. arborea*, *T. grandis* and *V. ferruginea* (Table 2).
346 Lastly, a significant correlation was observed in *T. versicolor* between the retention
347 expressed in mg_{Ag}/kg_{wood} in *C. alliodora* and *G. meiantha*; however, this correlation was
348 not significant when retention was expressed in mg_{Ag}/m^3_{wood}.

349 Several works have shown the potential of the use of silver nanoparticles in wood
350 protection[9-11], behavior in case of the fire, improvement of the properties of the wood or
351 already known wood treatments such as heat treatment, densification of wood or
352 particleboard manufacturing [13-17].

353 The advantage of using a solution of nanoparticles, compared to a treatment with
354 boron salts, is hardly quantified. A saturated solution of boric acid (H_3BO_3) and sodium
355 borate ($Na_2B_4O_7$) at 22°C contains 94.75 grams of H_3BO_3 L^{-1}, while the system used with
356 nanoparticles is 7.7 to 25.1 mg_{Ag}/ m^3_{wood}, an amount of active ingredient much smaller than
357 that used in the combination of H_3BO_3 and $Na_2B_4O_7$. Also, the effectiveness of boric acid
358 varies from 0.7 to 3.0 kg/m^3_{wood} [22], while the concentration of the nanoparticles ranges
359 from 7.7 to 25.1 g_{Ag}/m^3_{wood}, equivalent to a decrease of about 100 times less active element.
360 One advantage noted by Schultz et al. [28], is that silver nanoparticles in low
361 concentrations, in conjunction with traditional wood preservatives, in addition to protect the
362 wood, can also be added to wood preservatives in order to promote non-decay
363 microorganisms degrading organic preservatives. Moreover, the low levels of metal
364 employed could bring some advantages at the moment of depositing or discarding the
365 treated wood [28]. However, the same authors point out that even this type of preservatives
366 are uneconomical [28].

In relation with weight loss percentage with different fungi and according to the ASTM D2017-05 standard [23], most of the protection obtained is against the white-rot fungus *T. versicolor* (Fig. 3b); less effective is the protection against the brown-rot fungus *L. acuta* (Fig. 3a). Impregnation with nanoparticles does not achieve protection against *L. acuta* in *T. grandis* (Fig. 3a), but it does for the rest of the species; however, this protection is classified as moderate or resistant according to the ASTM D2017-05 standard [23], since weight losses percentage between 10 and 40% occur. High resistance in the wood by means of protection with nanoparticles is only achieved for *G. arborea*.

Regarding behavior of the nanoparticles against *T. versicolor*, the 10 species were classified as highly resistant (A) to *T. versicolor* (Fig. 3b), except for *C. cyclocarpum* because of low levels of retention (Table 1). Contrastingly, untreated wood of most species was classified as non-resistant (D), as weight loss percentages were close to 50% (Fig. 3b).

The reduction of decay in nine tropical species agrees with other studies with nano-silver particles [12]. For example, Velmururan et al. [32] with mycelial growth of the stain fungi *Ophiostoma flexuosum*, *O. tetropii*, *O. polonicum* and *O. ips* were reduced on media amended with different concentrations of silver nano-sized particles synthesized from silver nitrate and sodium borohydride. They found that mycelial growth decrees with nano-silver concentration. The mycelial growth was the highest with a concentration of 1 ppm and the lowest growth was found with a concentration of 100 ppm. On the other hand, Liu et al. [1, 9-11] found also a reduction of wood decay with different stabilizing agents or adding different fungicides to the nano-silver particles solution.

388 According to Dorau et al. [33] wood decay fungi have been shown to be susceptible
389 to silver nanoparticles because silver ions, in solution, inhibited the activity of their
390 cellulase enzymes [34]. Wood decay fungi feeding on a block treated with silver halide
391 would likely release more silver as a result of oxidative Fenton reactions during the
392 breakdown of cellulose [35]. Besides, silver nanoparticles constitute a reservoir for the
393 antimicrobial effect; in the presence of moisture, metallic silver oxidizes, which results in
394 the release of the silver ions. Silver ions are the species that are responsible for microbial
395 inhibition. Because silver oxidation is a slow reaction, the size of silver particles is critical
396 to achieve microorganism growth inhibition. The smaller the particle size, the higher the
397 surface area, and the greater the area available for oxidation. Particles with diameter less
398 than 100 nm are required to have the surface area necessary to allow a continuous release of
399 silver ions. The main advantages of nano-silver particles over organic biocides are: 1) non-
400 volatile and non-degradable over time, 2) odorless and 3) long term efficacy.

401 Lastly, nanoparticle concentration is one more aspect influencing the values of weight
402 loss percentage due to fungal attack [2]; moreover, a correlation between retention and
403 weight loss percentage was found in most of the species (Table 2). Although in the present
404 work greater effectivity was observed against the attack of *T. versicolor* with a
405 concentration of silver nanoparticles of 50 ppm (Fig. 3b), no values of weight loss were
406 observed for *L. acuta* as to enable classifying the species as highly resistant (Fig. 3a). One
407 of the results confirming that the concentration is probably not suitable is the correlation
408 between retention and weight loss (Table 2), because the resistance to fungal attack is
409 related to the concentration of the active element in the wood preservative [30]. Therefore,
410 in order to achieve better performance against fungal attack it is desirable to further

411 increase the concentration of nanoparticles. For example, Velmururan et al [32]. and Liu et
412 al. [2,9-11] worked in their studies with concentrations between 100 and 200 ppm, much
413 higher values than the 50 ppm used in this study.

CONCLUSIONS

Synthesized silver nanoparticles have dimensions from 40 to 100 nm. When applied to wood, retentions of 16 to 112 mg of silver per kilogram of wood or 7.7 to 25.1 mg of silver per cubic meter of wood are achieved, varying with the species. It was also observed that the effect of density on retention varies between species. In *C. alliodora*, *G. arborea*, *G. meiantha*, *T. grandis* and *V. guatemalensis* the retention decreased statistically with increasing specific gravity. While in *C. odorata* and *E. cyclocarpum* the retention in mg_{Ag}/m^3_{wood} is not affected by the variation of the density. Furthermore, in *O. pyramidale* and *A. mangium* increasing retention occurs as the density increases, but with low correlation coefficients.

Applying silver nanoparticles to the tropical species studied, improves their durability and classifies them as Class A or highly resistant to white-rot fungus *T. versicolor*. However, resistance of the species to the brown-rot fungus *L. acuta* is lower; this can be attributed to low particle concentration. Also, it was observed that the effect of nanoparticle retention was not significant in all species. In *A. mangium* and *O. pyramidale* the variation of the retention with these two methods did not affect statistically the weight loss in the two types of fungus, whereas in *E. cyclocarpum* and *G. arborea,* the retention is statistically related with weight loss percentage in both types of fungi. In the rest of the species this relation varies with the type of fungus.

Acknowledgement

The authors wish to thank the Vicerrectoría de Investigación y Extensión at the Instituto Tecnológico de Costa Rica (ITCR) for financial support for the study.

436 **REFERENCES**

437 1. Liu Y, Laks P, Heiden P (2001) Use of nanoparticles for controlled release of biocides
438 in solid wood. J Appl Poly Sci 79: 458-465.
439 2. Schultz TP, Nicholas DD, Preston AF (2007) A brief review of the past, present and
440 future of wood preservation. Pest Manag Sci 63(8): 784-788.
441 3. Scott N, Chen H (2013) Nanoscale science and engineering for agriculture and food
442 systems. Ind Biotech 9: 17-18.
443 4. Mie R, Samsudin MW, Din LB (2013) A review on biosynthesis of nanoparticles using
444 plant extract: An emerging green nanotechnology. Adv Mat Res 667: 251-254.
445 5. Tarmian A, Sepehr A, Gholamiyan H (2012) The use of nano-silver particles to
446 determine the role of reverse temperature gradient in moisture flow in wood during
447 low-intensity convective drying. Special Top Rev Porous Media Int J 3: 149-156
448 6. Mahapatra I, Clark J, Dobson PJ, Owen R, Lead JR (2013) Potential environmental
449 implications of nano-enabled medical applications: critical review. Env Sci Proc
450 Impacts 15: 123-144.
451 7. Anjum NA, Gill SS, Duarte AC, Pereira E, Ahmad I (2013) Silver nanoparticles in
452 soil–plant systems. J nanoparticle Res 15(9): 1-26.
453 8. Reidy B, Haase A, Luch A, Dawson KA, Lynch I (2013). Mechanisms of silver
454 nanoparticle release, transformation and toxicity: A critical review of current
455 knowledge and recommendations for future studies and applications. Materials 6:
456 2295-2350.

457 9. Liu Y, Laks P, Heiden P (2002a) Controlled release of biocides in solid wood: I.
458 Efficacy against brown rot wood decay fungus (*Gloeophyllum trabeum*). J Appl Poly
459 Sci 86: 596-607.
460 10. Liu Y, Laks P, Heiden P (2002b) Controlled release of biocides in solid wood: II.
461 Efficacy against Trametes versicolor and *Gloeophyllum trabeum* wood decay fungi. J
462 Appl Poly Sci 86: 608-614.
463 11. Liu Y, Laks P, Heiden P (2002c) Controlled release of biocides in solid wood: III.
464 Preparation and Characterization of surfactant-free nanoparticles. J Appl Poly Sci 86:
465 615-621.
466 12. Moya R., Berrocal A, Rodriguez-Zuñiga A, Vega-Baudrit J, Chaves-Noguera S
467 (2014). Effect of silver nanoparticles on white-rot wood decay and some physical
468 properties of three tropical wood species. Wood Fiber Sci 46(4): 527-538.
469 13. Taghiyari HR (2012) Fire-retarding properties of nano-silver in solid woods. Wood Sci
470 Tech 46: 939-952.
471 14. Taghiyari HR., & Bibalan OF (2013) Effect of copper nanoparticles on permeability,
472 physical, and mechanical properties of particleboard. Eur J Wood and Wood
473 Prod, 71(1): 69-77.
474 15. Taghiyari HR, Enayati A, & Gholamiyan H (2013) Effects of nano-silver impregnation
475 on brittleness, physical and mechanical properties of heat-treated hardwoods. Wood
476 Sci Tech, 47 (3): 467-480.
477 16. Taghiyari HR., Rangavar H, & Bibalan OF (2011) Effect of nano-silver on reduction of
478 hot-pressing time and improvement in physical and mechanical properties of
479 particleboard. BioResources, 6(4), 4067-4075.

480 17. Rassam G, Ghofrani M, Taghiyari HR, Jamnani B, Khajeh MA (2012). Mechanical
481 performance and dimensional stability of nano-silver impregnated densified spruce
482 wood. Eur J Wood Prod 70(5): 595-600.
483 18. Tan KS, & Cheong KY (2013) Advances of Ag, Cu, and Ag–Cu alloy nanoparticles
484 synthesized via chemical reduction route. J Nanoparticle Res, 15(4): 1-29.
485 19. Kheybari S, Samadi NASRIN, Hosseini SV, Fazeli A., & Fazeli MR (2010) Synthesis
486 and antimicrobial effects of silver nanoparticles produced by chemical reduction
487 method. Daru: Journal of Faculty of Pharmacy, Tehran Univ. Medical Sci, 18(3), 168-
488 172.
489 20. Mavani K, Shah M (2013) Synthesis of silver nanoparticles by using sodium
490 borohydride as a reducing agent. Int J Eng Res Tech 2(3): 1-5
491 21. Akhtari M, Taghiyari HR, Kokandeh MG (2013) Effect of some metal nanoparticles on
492 the spectroscopy analysis of Paulownia wood exposed to white-rot fungus. Eur J Wood
493 Prod 71:283-285.
494 22. Lloyd JD (1998) Borates and their biological applications. Inteernational Research
495 Group on Wood Preservation. IRG/WP 98-30178. IRG Secretariat, Stockholm
496 Sweden. 17 p.
497 23. ASTM (2003) D-2017. Standard method of accelerated laboratory test of natural decay
498 resistance of woods. American Society for Testing and Materials, West Conshohocken,
499 PA.
500 24. Crabtree JH, Burchette RJ, Siddiqi RA, Huen IT, Han dott LL, Fishman A (2003) The
501 efficacy of silver-ion implanted catheters in reducing peritoneal dialysis-related
502 infections. Perit Dial Int 23:368-74.

503 25. Prema P, Raju R (2009) Fabrication and characterization of silver nanoparticle and its
504 potential antibacterial activity. Biotech Bioprocess Eng 14: 842-847
505 26. Sileikaite A, Prosycevas I, Puiso J, Juraitis A, Guobiene A (2006) Analysis of silver
506 nanoparticles produced by chemical reduction of silver salt solution. Mat Sci 12: 287-
507 291.
508 27. Barnes HM (2008) Wood Preservation Trends in North America. In ACS symposium
509 series (Vol. 982, pp. 583-597). Oxford University Press.
510 28. Schultz TP, Nicholas DD, McIntyre CR (2008) Recent patents and developments in
511 biocidal wood protection systems for exterior applications. Recent Pat Mat Sci 1: 128-
512 134
513 29. Glover RD, Miller JM, Hutchison JE (2011) Generation of metal nanoparticles from
514 silver and copper objects: nanoparticle dynamics on surfaces and potential sources of
515 nanoparticles in the environment. Acs Nano 5: 8950-8957.
516 30. Stan L (2010) Wood Handbook, Chapter 15: Wood Preservation Publication: General
517 Technical Report FPL-GTR-190. Madison, WI: U.S. Department of Agriculture, Forest
518 Service, Forest Products Laboratory: 15-1 - 15-28.
519 31. Moya R, Muñoz F (2010) Physical and mechanical properties of eight fast-growing
520 plantation species in Costa Rica. J Trop For Sci 22: 317-328.
521 32. Velmurugan N, Kumar GG, Han SS, Nahm KS and Lee YS (2009) Synthesis and
522 Characterization of Potential Fungicidal Silver Nano-sized Particles and Chitosan
523 Membrane Containing Silver Particles. Iranian Polym J. 18 (5): 383-392.
524 33. Dorau B, Arango R, Green F III (2004) An Investigation into the Potential of Ionic
525 Silver as a Wood Preservative. Woodframe Housing Durability and Disaster Issues

526 October 4-6, 2004 Aladdin Resort & Casino Las Vegas, Nevada, USA. Forest Products
527 Society Madison, WI 15 p
528 34. Highley TL (1975) Inhibition of celluloses of wood-decay fungi. Res. Pap. FPL-247.
529 U.S. Department of Agriculture, Forest Service, Forest Prod. Lab., Madisson, WI. 9 p.
530 35. Xu G and Godell B (2001) Mechanisms of wood degradation by brown-rot fungi:
531 Chelator-mediated cellulose degradation and binding of iron by cellulose. J.
532 Biotechnology. 87: 43-57

533 **Fig. 1.** Silver nanoparticles utilized in wood and observed by means of a Transmission Electron
534 Microscope-TEM (a and b), an Atomic Force Microscope-AFM (c) and the UV-Vis spectrum
535 of silver nanoparticles (d).

536

537 **Fig. 2.** Relationship between retention measured in cubic meters of timber (a and b) and weight in
538 kilograms (c and d) in nine commercial species of Costa Rica.

539

540 **Fig. 3.** Weight loss percentage caused by *L. acuta* (a) and *T. versicolor* (b) in nine tropical species
541 treated and untreated with nano-silver particles in Costa Rica.
542 Note: The bars represent the confidence intervals at $\alpha = 99\%$.
543
544

545

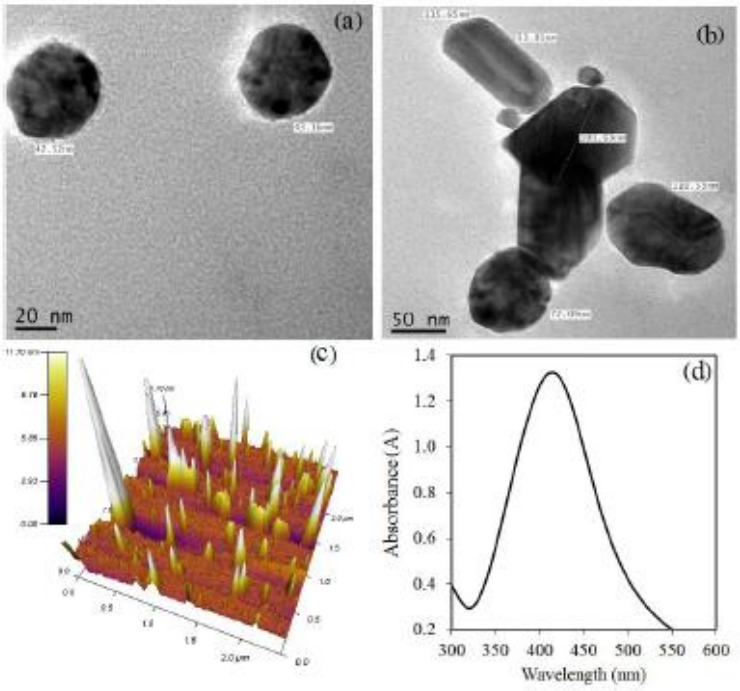
(a)
20 nm
(b)
50 nm
(c)
(d)
Absorbance (A)
Wavelength (nm)
1.4
1.2
1.0
0.8
0.6
0.4
0.2
300 350 400 450 500 550 600

546

547 Fig. 1.

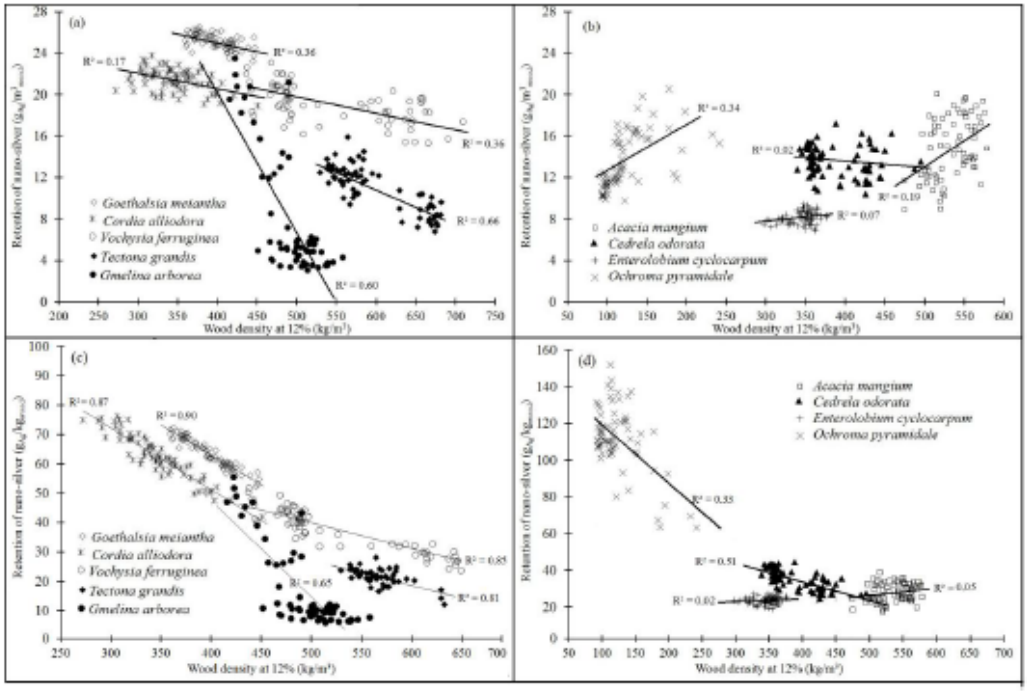
(a)
(b)
(c)
(d)
Retention of nano-silver (g/m³)
Wood density at 12% (kg/m³)
Goethalsia meiantha
Cordia alliodora
Vochysia ferruginea
Tectona grandis
Gmelina arborea
Acacia mangium
Cedrela odorata
Enterolobium cyclocarpum
Ochroma pyramidale

548

549 Fig. 2.

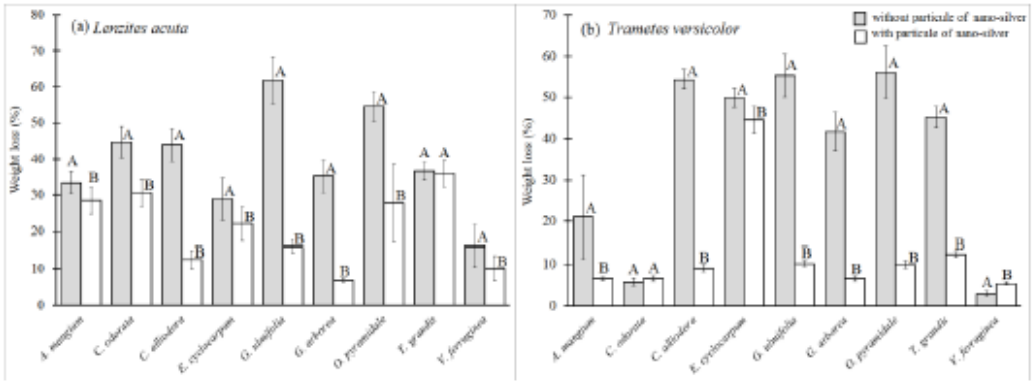
(a) Lonzites acuta
(b) Trametes versicolor
without particule of nano-silver
with particule of nano-silver
Weight loss (%)
A. marginata
C. odorata
C. alliodora
E. cyclocarpum
G. ulmifolia
G. arborea
O. pyramidale
T. grandis
V. ferruginea

Fig. 3.

552 Table 1. Absorption and retention of silver nanoparticles in treated and untreated wood of nine
553 tropical species from Costa Rica.
554

Type of wood	Absorption (liters/m^3_{wood})	Retention of nano-silver (mg_{Ag}/ m^3_{wood})	Retention of nano-silver (mg_{Ag}/ kg_{wood})	Wood density before impregnation (g/cm^3)
Acacia mangium	377^{A} (20.0)	14.6^{A} (20.0)	27.2^{A} (18.7)	533^{A} (5.6)
Cedrela odorata	345^{A} (10.9)	13.5^{A} (10.9)	34.9^{B} (15.4)	391^{B} (9.8)
Cordia alliodora	546^{B} (5.2)	21.4^{B} (5.2)	62.5^{C} (12.4)	346^{C} (10.0)
Enterolobium cyclocarpum	207^{C} (7.3)	8.1^{C} (7.6)	23.5^{AD} (7.5)	346^{C} (4.9)
Gmelina arborea	194^{C} (73.1)	7.7^{C} (73.1)	15.9^{E} (82.0)	495^{D} (6.6)
Goethalsia meiantha	640^{D} (2.9)	25.1^{D} (2.9)	63.3^{C} (8.0)	399^{B} (6.0)
Ochroma pyramidale	346^{A} (19.8)	13.6^{A} (19.8)	112.0^{F} (16.1)	124^{E} (26.1)
Tectona grandis	283^{E} (19.2)	11.1^{E} (19.2)	19.0^{DE} (25.1)	596^{A} (8.4)
Vochysia ferruginea	487^{F} (9.5)	19.1^{F} (9.5)	36.1^{B} (21.1)	544^{A} (14.7)

555 Note: the values in parenthesis represent the coefficient of variation. Average values
556 identified with the letters A and B are statistically different at $\alpha = 99\%$.

557 Table 2. Correlation between weight loss caused by *L. acuta* and *T. versicolor* and retention of
558 nano-silver particles in wood treated with nano-silver in nine tropical species in Costa Rica.

Type of wood	Fungal species	Retention of nano-silver (mg_{Ag}/m^3_{wood})	Retention of nano-silver (mg_{Ag}/kg_{wood})
Acacia mangium	*L. acuta*	0.20 ^{NS}	0.13 ^{NS}
	T. versicolor	0.16 ^{NS}	0.23 ^{NS}
Cedrela odorata	*L. acuta*	0.21 ^{NS}	0.25 ^{NS}
	T. versicolor	0.60**	0.66**
Cordia alliodora	*L. acuta*	0.30 ^{NS}	0.15 ^{NS}
	T. versicolor	0.25 ^{NS}	0.36*
Enterolobium cyclocarpum	*L. acuta*	0.69**	0.71**
	T. versicolor	0.77**	0.79**
Gmelina arborea	*L. acuta*	0.40*	0.56**
	T. versicolor	0.82**	0.72**
Goethalsia meiantha	*L. acuta*	0.30 ^{NS}	0.05 ^{NS}
	T. versicolor	0.12 ^{NS}	0.60**
Ochroma pyramidale	*L. acuta*	0.14 ^{NS}	0.09 ^{NS}
	T. versicolor	0.18 ^{NS}	0.19 ^{NS}
Tectona grandis	*L. acuta*	0.15 ^{NS}	0.19 ^{NS}
	T. versicolor	0.49**	0.47**
Vochysia ferruginea	*L. acuta*	0.05 ^{NS}	0.09 ^{NS}
	T. versicolor	0.56*	0.41*

559 Note: the values in parenthesis show the coefficient of variation. Average values
560 identified with the letters A and B are statistically different at $\alpha = 99\%$.

3. Artículo 3. Effects of adding nano-clay (montmorillonite) on performance of polyvinil acetate (PVAc) and urea-formaldehyde (UF) adhesives in Carapa guianensis, a tropical species

International Journal of Adhesion & Adhesives 59 (2015) 62–70

Contents lists available at ScienceDirect

International Journal of Adhesion & Adhesives

journal homepage: www.elsevier.com/locate/ijadhadh

Effects of adding nano-clay (montmorillonite) on performance of polyvinyl acetate (PVAc) and urea-formaldehyde (UF) adhesives in *Carapa guianensis*, a tropical species

Róger Moya [a,*], Ana Rodríguez-Zúñiga [a], José Vega-Baudrit [b], Vera Álvarez [c]

[a] Escuela de Ingeniería Forestal, Instituto Tecnológico de Costa Rica, Apartado, 159-7050 Cartago, Costa Rica
[b] Laboratório Nacional Nanotecnologia (LANOTEC), Centro Nacional de Alta Tecnologia-CENAT, San Jose, Costa Rica
[c] Grupo de Materiales Compuestos de Matriz Polimérica (CoMP) – Instituto de Investigaciones en Ciencia Y Tecnología de Materiales (INTEMA), Mar del Plata, Argentina

ARTICLE INFO

Article history:
Accepted 9 February 2015
Available online 17 February 2015

Keywords:
Wood adhesives
Nanotechnology
Tropical species
Nano-clay
Thermal analysis

ABSTRACT

The aim of this study was to improve the bond strength resistance of polyvinyl acetate (PVAc) and urea-formaldehyde (UF) adhesives modified with nano-clay (montmorillonite) with a tropical species of wood known to exhibit adhesion related problems. These adhesives were evaluated with 1.0 and 1.5 wt% nano-clay concentrations with lap shear strength (SS), and the percentage of wood failure (PWF) in dry and wet conditions being evaluated. An additional aim of this study was to observe the presence of nano-clay within both adhesive types using Atomic Force Microscopy (AFM) and the Transmission Electron Microscopy (TEM). Color, viscosity and the thermostability of these adhesives with nano-clay were also evaluated. First, AFM and TEM studies showed adequate dispersion and impregnation of nano-clay. The viscosity of PVAc adhesive was not affected by the incorporation of nano-clay, whereas the UF adhesive was. With both PVAc and UF adhesives, the presence of nano-clay increased the L^* and b^* color parameters, especially when 1.5 wt% nano-clay was used. The incorporation of the nano-clay improved thermostability, as determined by thermogravimetric analysis (TGA). Finally, it was shown that the nano-clay incorporation improved SS and PWF. The highest values of SS were obtained when nano-clay was added at 1.5 wt% concentration in the PVAc adhesive under dry conditions. SS was not affected by nano-clay addition in the UF adhesive under dry conditions. However, under wet conditions, both 1.0 and 1.5 wt% loadings of nano-clay increased SS with both adhesive types. The addition of nano-clay in both proportions increased PWF by approximately 15% and between 20–30% in dry and wet conditions, respectively, for the PVAc adhesive. For the UF adhesive, PWF increased by approximately 10% under dry conditions and 25–50% in wet conditions.

1. Introduction

Wood adhesives and wood products are important to the manufacturing of products for construction and for furniture production [1]. Adhesives are also used to produce wood composed products, such as plywood, fiberboard and oriented strand board (OSB) and also for wood re-use [2]. It is estimated that 70% of currently marketed products use adhesives [3]. Adhesives also improve the usefulness of wood, allowing the use of low-quality wood and of small-sized pieces so that wood waste can be more effectively used [3].

In addition, many adhesives are manufactured with synthetic products, which are easy to use, present a wide variety of applications, are low-cost and are designed using high technology [3]. In this regard, the development of nanotechnology, specifically nano-particles, has helped to produce a new generation of high performance adhesives [4]. Various nano-particles, layered silicates, aluminum oxide and nanocellulose among them, have been used to improve the performance of several wood adhesives [5].

Organo-clays derived from natural montmorillonite and modified with quaternary ammonium salt (dimethyl benzyl hydrogenated tallow ammonium) have been shown to improve the properties of polyvinyl acetate [2,7–9] and urea-formaldehyde adhesives [10–13]. However, the effect of nanoparticle incorporation on the performance of adhesives used with tropical wood is still unknown. While the behavior of adhesives with nano-particles is relatively well understood in temperate countries, in regions of high temperature and high humidity, such as in tropical countries, it can create many problems [14]. Furthermore, tropical species have high specific gravity and high contraction coefficients

* Corresponding author.
E-mail addresses: rmoya@itcr.ac.cr (R. Moya), ana.rodriguez@itcr.ac.cr (A. Rodríguez-Zúñiga), jvegab@gmail.com (J. Vega-Baudrit), alvarezvera@fi.mdp.edu.ar (V. Álvarez).

http://dx.doi.org/10.1016/j.ijadhadh.2015.02.004
0143-7496/

which, together with the presence of naturally occurring resinous material, could influence joint integrity characteristics [15].

The purpose of this work was to study the performance in bond strength of the PVAc and UF adhesives modified with nano-clay (montmorillonite) with a tropical species (*Carapa guianensis*) having a high content of extractives and some adhesion problems [16,17]. It also showed the changes that occurred in the nano-clay due to modification with benzalkonium chloride and the change in color of the adhesive, thermal stability, entropy factor and activation energy in the decomposition kinetics of the PVAc and UF adhesives modified with nano-clay.

2. Materials and methods

2.1. Materials

The commercial clay Closite® Na^+, which is an unmodified montmorillonite supplied by Rocwood Clay based additives, was used as a nanofiller. According to the description of the supplier, the moisture content of the product ranges between 4–9%, its density is 2.86 g cm^{-3} and the distribution of the size of the particles is as follows: 10% less than 2 μm, 50% less than 6 μm and 90% of the particles are less than 13 μm in size. Benzalkonium chloride ($C_6H_5CH_2N^+(CH_3)_2RCl^-$) was used to improve the miscibility of the layered silicates with the adhesive matrices (PVAc and UF) and the nanoclay, and it was chosen by several methods proposed by Ray and Okamoto [16].

Two types of wood adhesive were used. The first type was a water-based polyvinyl acetate (PVAc), Resistol[M.R.] 850® trademark, produced by Henkel Capital S.A. (http://www.resistol.com.mx/es.html). The technical description of the product indicates that the resin is polyvinyl acetate and water, with 54.5–55.5% solid content and a viscosity of 1600–2200 cPs. The second type of adhesive used was a water-based urea-formaldehyde (UF), CR-560 UF Resin trademark, produced by Central Chemistry Quibor SA (http://www.agroquibor.com). The technical description of the product indicates that the liquid resin is urea-formaldehyde (UF), with 64–65% solids content and 650–900 cPs viscosity.

The species used for the adhesion tests was *C. guianensis*, which is a species traditionally used in Costa Rica for manufacturing doors and other wood-based products [17]. This species has presented problems with gluing [18] and is considered to demonstrate a behavior similar to the species *Acer Saccharum* or *Acer nigrum*, recommended by the ASTM D-905-08 standard for measuring the strength of the glue line [19]. This wood was obtained from three different sawn-wood marketing sites.

2.2. Preparation of adhesives with nanoclays

With both types of adhesive the nano-clay was added in three different concentrations: 0% (or control), 1% and 1.5% (wt%). According to studies carried out by Kaboorani and Riedl in temperate species [7], these proportions achieved the best performance. First, the commercial nano-clay was modified in order to improve chemical compatibility with both adhesive types. In order to improve affinity, a treatment of cation exchange with benzalkonium chloride was applied, based on the proposal of Ollier et al. [20,21]. The proposal was to treat the unmodified montmorillonite with the aqueous solution at 7% of benzalkonium chloride. For this, the nano-clay was mixed in a solution of ethanol–water (volume rate at 20:80%) at 60 °C for 1 h under stirring (solution A). Simultaneously a solution of 7% benzalkonium chloride (solution B) was prepared at room temperature, also stirring for 1 h. After that time solution A was mixed with solution B. Both were mixed at a temperature of 60 °C with constant stirring for 12 h. The mixture was then filtered until the chlorides test indicated no presence of chlorine, for which purpose a solution of saturated silver nitrate, as proposed by Ollier et al. [20], was used. Finally, the treated nano-clay was left to dry at 105 °C, and once dry, it was pulverized in a mortar to achieve the finely ground nano-clay.

The various mixtures of adhesives modified with nano-clay were prepared as follows: (i) PVAc adhesive was stirred at 1600 rpm for 15 min with the aid of four 45°-inclined d-blade impellers at room temperature, during which time the nano-clay was slowly added into the PVAc resin; and (ii) with UF adhesive, because it is a 3-component adhesive (resin, wheat flour, and catalyst of sulfates), the resin and flour were prepared and then mixed with the unmodified nano-clay. As in the previous case, the resin was stirred at 1600 rpm for 15 min with the aid of an inclined blade (45°), while the nano-clay and flour were slowly added until dispersed in the resin.

2.3. Adhesive characterization

The extent to which the nano-clay was dispersed within the adhesive was assessed using Atomic Force Microscopy (AFM) and Transmission Electron Microscopy (TEM). With both techniques, an appropriate volume of adhesive with either 1% concentration of modified nano-clay (wt%) or unmodified nano-clay at the same concentration was prepared. For TEM observations (trademark Jeol and JEM-2100 model), small samples of modified and unmodified clay were placed in the microscope, where a 100-kV acceleration and 10,000× (B and C) and 300,000× (D) amplifications were used. Because AFM observations were performed in adhesive, they were carried out using a NanoScope V, an atomic force microscope (model Asylum Research model MFP 3D) fitted with a Hybrid XYZ scanner. Atomic force microscope measurements were done under ambient air conditions in tapping mode. The sensitivity of the tip deviation and the scanner resolution was 0.3 nm. The resolution was set to 250 lines by 256 pixels for all observations.

To measure viscosity, a 0.5-liter sample of the two adhesives in the three concentrations of nano-clay was made and placed in the viscometer, Brokfield-11+Pro LV. 2.4.4.

In the case of color assessment, a sample 3 cm wide, 10 cm long and approximately 2 mm thick was prepared with each adhesive. A neoprene rectangle 4 mm thick was formed on a glass and filled with the various adhesives prepared. When the solvent had completely separated (approximately 72 h later) the adhesive sample was removed and its color was measured. A Hunter Lab Scan XE Plus mini model spectrophotometer was used to obtain the L^*, a^* and b^* parameters. The measurement was set to within the visible range of 400–700 nm at intervals of 10 nm with a measuring aperture of 11 mm. For the reflection reading, the observer component was set at an angle of 10° to the sample's normal surface. According to HUNTERLAB [22], the CIE L^*, a^* and b^*'s color system estimates the color in three coordinates: L^* for lightness that represents the position on the black–white axis ($L=0$ for black, $L=100$ for white), a^* for chroma value that defines the position on the red–green axis (+100 values for red, −100 values for green), and b^* for chroma value that defines the position of the yellow–blue axis (+100 values for yellow, −100 values for blues). Three measurements were taken at each point to obtain the average values for the L^*, a^* and b^* coordinates. The color difference index ΔE^* of the adhesives, according to the ASTM D 2244 standard [23], was used to compare adhesive color parameters between adhesives with different concentrations of nano-clay. This index defines the wood color difference in magnitude between two adhesives using CIE L^*, a^* and b^*'s color coordinates, according to Eq. 1. This index was calculated using the average color values for all heartwood and sapwood samples from each adhesive.

$$\Delta E^* = \sqrt{(\Delta L^*)^2 + (\Delta a^*)^2 + (\Delta b^*)^2} \quad (1)$$

where $\Delta L^* = L^{*M} - L^{*P}$, $\Delta a^* = a^{*M} - a^{*P}$, $\Delta b^* = b^{*M} - b^{*P}$, M=Average

value for adhesive without nano-clay and P=Average value for adhesive with nano-clay.

The thermal stability was analyzed for the two types of adhesives at the 3 concentrations of nano-clay. Measurements of TGA were carried out using 30–35 mg of each adhesive in each concentration, at a heating rate of 50 °C/min in a nitrogen atmosphere reaching a temperature of 1000 °C in approximately 20 min. A thermal gravimetric analysis model TGA 5000, Instrument NBr brand, was used. To analyze the information obtained, the reactions were identified with the aid of DTG. Two reactions were identified in the case of PVAc; only the second reaction was analyzed in UF, corresponding to polymer decomposition. The first corresponds to water elimination. For each reaction, the temperature and the mass remnant at the start of the reaction, at the maximum reaction point and at the end of the reaction, were identified. Next, the kinetics was calculated for each reaction (Eq. 1) by means of lineation (Eq. 2), according to Vyazovkin and Sbirrazzuoli [24], where the differential isoconversional method of Friedman is utilized.

$$K = K_0 * e^{\left(\frac{-E}{RT}\right)} \tag{2}$$

$$\ln\left(\frac{d\alpha}{dt}\right) = \ln K_0 + \left(\frac{-E}{RT}\right) + n\ln(1-\alpha) \tag{3}$$

where: α: degraded mass, $d\alpha/dt$: percentage of the degraded sample in unit time, K_0: entropy factor, E: energy of activation, and T: temperature.

2.4. Bond strength

Assessments of bond strength for the two types of resin with added nano-clay were evaluated by a compressive shear technique (SS), according to ASTM D-905-98 [19]. After preparing the two types of adhesives with nano-clay, the wood of *C. guianensis* was prepared and bonded. A total of 90 shear tests were carried out (30 samples per concentrations × 3 concentrations). The wood was stabilized at a condition of 12% moisture for one week. The adhesive was applied in accordance with the manufacturer's specifications, which recommend an amount of 100 g^{-2} for both adhesives. After applying adhesive to the wood surface, the samples were pressed in a hydraulic machine at a pressure of 0.20 Nmm^{-2} for 24 h. Before pressurizing, bonded samples were conditioned to 20 °C and 60% relative humidity for two weeks. Next, 30 samples were extracted and tested for each set of formulation. The SS was measured in dry and wet states under ambient air conditions. A Tinus Olsen hydraulic test machine with 10 kN capacity was used for load application and the data were acquired by means of a computer. Wood failure and maximum load were recorded for each test. The block shear tests were carried out according to ASTM D905-98 [19]. The sizes of samples for "wet state" tests were the same as for "dry state" tests. For "wet state" tests, the samples were taken directly out of the water after being immersed for 24 h. Before the tests, excess water was wiped from the samples. During the water immersion period, the temperature of the water was maintained at 20 °C. After each sample was tested in the compression test, the percentage of wood failure (PWF) was evaluated according to ASTM D-5266-13 standard [25].

2.5. Analysis of the information

Verification was made of compliance of the variables determined with the assumptions of normal distribution and variance homogeneity, as well as the presence of extreme data. Later, a variance analysis was performed to verify the effect of the adhesion of the nano-clay (three levels: 0%, 1% and 1.5% nano-clay) on viscosity, values of entropy factor, energy activation, decomposition function, and temperature and mass remnant in different reactions of the kinetics of decomposition. The Tukey test at a 99% confidence level was established to determine whether there was a statistically significant difference between the means.

3. Results

3.1. Adhesive characterization

3.1.1. AFM and TEM observations

With respect to the AFM analysis of the nano-clay modified adhesives, the adhesive surfaces with nano-clay were found to be irregular, with the presence of peaks. Fig. 1(a) and (b) shows AFM spectra for formulations having nano-clay concentrations of 1.0 wt% and 1.5 wt% for the UF adhesive. According to Fig. 1a, with the concentration of 1.5 wt%, the number of peaks is higher than of

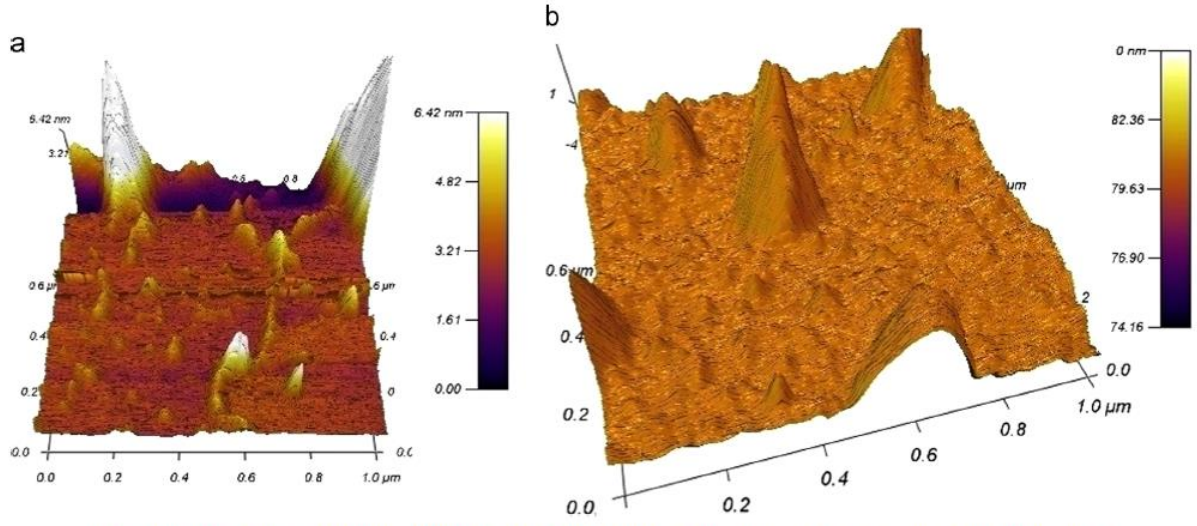

Fig. 1. Atomic force microscope-AFM spectra of nano-clay particles utilized in PVAc wood adhesive: (A) 1.5% with nano-clay and (B) 1.0 nano-clay.

those occurring in the UF adhesive with a concentration of 1% (Fig. 1b). The dispersion of peaks on the surface is uniform at both concentrations.

Fig. 2 shows TEM images obtained for the systems studied. First, it was observed that nano-clay particles appear short and tubular in some areas of the PVAc matrix (Fig. 2a–b). They are short and their diameter is almost 50 nm (Fig. 2a). In addition, it was observed that typical montmorillonite particles mixed in the PVAc matrix were of length approximately 1 μm (Fig. 2c) and some montmorillonite particles had little separation between their clay layers (Fig. 2d).

3.1.2. Viscosity and color

Nano-clay statistically increases the viscosity of the adhesive in comparison with the adhesive without the nano-clay. In the case of the PVAc-type adhesive, no significant difference between the adhesive with 1.0 wt% and 1.5 wt% nano-clay contents was found regarding viscosity (Fig. 3a), whereas for the UF adhesive, the 3 types of nano-clay content were significantly different (Fig. 3b) and increased as a function of nano-clay content.

In relation to color of the various adhesives prepared (Table 1), luminosity (L^* parameter) was found to increase statistically in PVAc with the increment of the proportion of clay, while the a^* parameter (redness) shows reduction only in the proportion 1.5 wt%. Meanwhile, yellowness (the b^* parameter) in the same type of adhesive statistically increases in the two proportions in relation to the adhesive without nano-clay. However, the greatest increment is observed in the 1% nano-clay samples (Table 1). Regarding the effects of the nano-clay in UF, it was found that both proportions of nano-clay affect the 3 color parameters, except for the L^* parameter in the adhesive with 1% nano-clay (Table 2). Color change evaluation, determined by the ΔE^*, shows that in PVAc adhesive the value is approximately 6, while in UF the highest values, above 8.87, are obtained when the proportion of nano-clay is 1.5 wt% (Table 1).

3.1.3. Thermal stability of the adhesives

The TGA spectrum of samples, unmodified or modified with the two concentrations of nano-clay (1.0 and 1.5 wt%) and benzalkonium chloride, are presented in Fig. 4(a) and (b). The analysis of both PVAc and UF adhesives prepared with two concentrations of nano-clay (1.0 and 1.5 wt%) showed two important inflexions in the mass loss of PVAc adhesive (Fig. 4a), whereas in the case of UF adhesive only one inflexion was observed (Fig. 4b). The first inflexion with the PAVc-adhesive occurs at approximately 315 °C and the second at 425 °C (Fig. 4a), while with the UF adhesive the highest inflexion was observed at 260 °C (Fig. 4b). On the other hand, samples modified with nano-clay demonstrated different behavior to their un-modified counter parts (Fig. 4a–b) with benzalkonium chloride decomposition being much greater with adhesives containing nano-clay.

The analysis of the mass derivative as a function of the temperature (DTG) of the data obtained from the TGA experiments confirmed the various inflexions or reactions in the decomposition of the adhesives with different proportions of the nano-clay (Fig. 4(d) and (e)). DTG, however, first shows a stable mass loss as a function of temperature, augmenting the decomposition (starting point) until reaching a peak (highest point), then the decomposition drops until becoming stable once again (final point). With the PVAc, the first reaction of the adhesive without nano-clay occurs between 310 °C and 327 °C, whereas in both types of PVAc with nano-clay the temperature range diminishes slightly to between 303 °C and 318 °C. The second reaction, however, occurs within a similar range for all 3 types of nano-clay, between 325 °C and

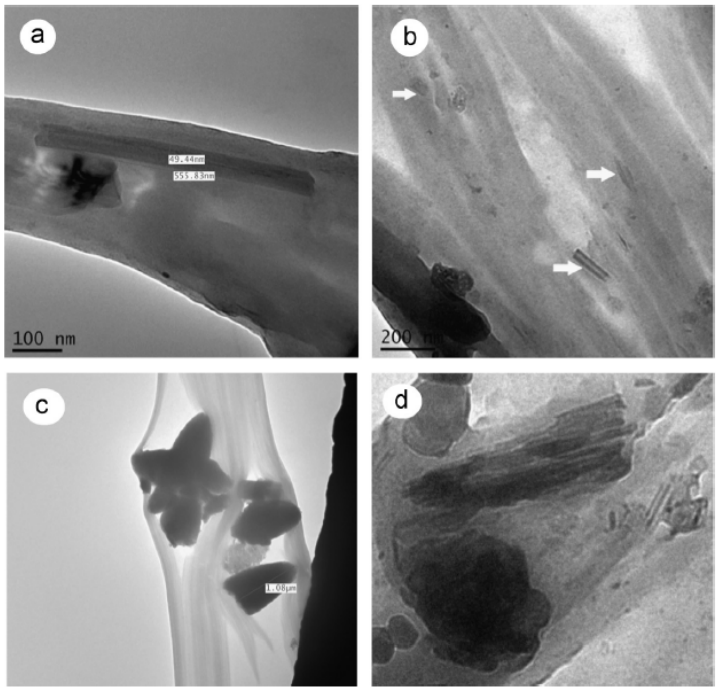

Fig. 2. Transmission Electron Microscopy (TEM) images of PVA/nano-clay composites: (a–b) short-tubular of nano-clay mixed into PVAc polymers, (c) typical montmorillonite particles inside of two PVAc chain and (d) nano-clay in layers and particles mixed into PVAc adhesive.

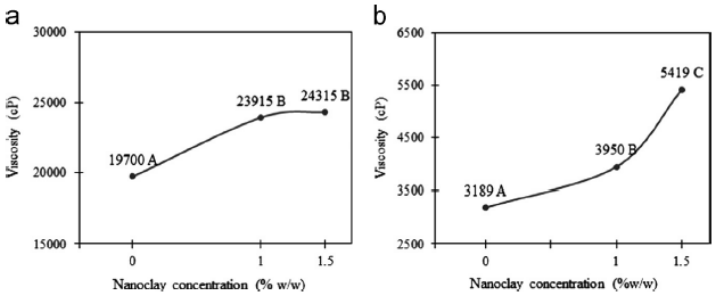

Fig. 3. Viscosity values of PVAc and UF wood adhesive, adding different concentrations (wt%) of nano-clay.

Table 1
Adhesive color parameter of PVAc and UF adhesive with different nano-clay concentrations.

Adhesive	Concentration (wt%)	L^* color parameter	a^* color parameter	b^* color parameter	ΔE^*
PVAc	0	47.67A	−1.32A	−2.05A	–
	1	49.61B	−1.5A	0.06B	5.88
	1.5	53.86C	−2.52B	−1.50C	6.33
UF	0	39.89A	7.75A	14.46A	–
	1	41.33AB	9.21B	19.14B	8.87
	1.5	42.35B	8.93B	19.08B	12.06

Table 2
Temperature and mass remaining after different reactions of decomposition kinetics of PVAc and UF wood adhesive, adding different concentrations (weight/weight) of nano-clay.

Adhesive	Nano-clay concentration (wt%)	Reaction 1						Reaction 2						Ash content (%)
		Initial point		Maximum peak		Final point		Initial point		Maximum peak		Final point		
		Temp (°C)	MR (%)	Temp (°C)	MR (%)	Temp (°C)	MR (%)	Temp (°C)	MR (%)	Temp (°C)	MR (%)	Temp (°C)	MR (%)	
PVAc	0	294^{A}	93.74^{A}	316^{A}	67.35^{A}	324^{A}	38.70^{A}	425^{A}	27.36^{A}	436^{A}	22.03^{A}	446^{A}	15.80^{A}	11.24^{A}
	1.0	292^{A}	91.17^{A}	312^{A}	67.98^{A}	324^{A}	39.63^{A}	425^{A}	26.04^{A}	433^{A}	21.60^{A}	448^{A}	13.86^{A}	10.01^{A}
	1.5	303^{A}	87.78^{B}	312^{A}	68.67^{A}	319^{B}	42.00^{B}	418^{A}	27.54^{A}	434^{A}	21.39^{A}	447^{A}	14.81^{A}	12.01^{A}
UF	0	–	–	–	–	–	–	237^{A}	81.34^{A}	248^{A}	66.83^{A}	246^{A}	53.80^{A}	13.30^{A}
	1.0	–	–	–	–	–	–	244^{B}	80.87^{A}	254^{B}	69.70^{B}	264^{B}	57.30^{B}	14.33^{A}
	1.5	–	–	–	–	–	–	243^{B}	80.93^{A}	254^{B}	69.87^{B}	264^{B}	58.23^{B}	15.00^{A}

Temp: temperature, MR: mass remnant.

345 °C (Fig. 4d). The adhesives prepared with UF show similarity between the adhesives with and without nano-clay (Fig. 4e). Similarly, the 2 proportions of nano-clay (1.0 and 1.5%) show important mass loss under 100 °C, although the greatest loss is observed between 200 °C and 400 °C (Fig. 4e).

Temperatures and mass remnants involved in each reaction of the different adhesives are detailed in Table 2. No significant difference was observed in the initial, final and maximum peak temperatures and mass remnant in the first and second reactions of the PVAc adhesive, between 1 wt% of nano-clay and the adhesive without nano-clay. The 1.5 wt% nano-clay adhesive, however, shows differences in the initial temperature of the mass remnant in the initial and final points and the final temperature of the first reaction (Table 2). Nano-clay adhesion to the UF adhesive, regardless of the percentage loading, produces a significant alteration in the temperature and mass remnant of the analyzed reaction 2, with the exception of the mass remnant at the start of the reaction, where no difference is observed in the proportions and the adhesive is without nano-clay. No significant differences were found in the adhesives with 1.0 wt% and 1.5 wt% between the various parameters evaluated (Table 2).

Another aspect evaluated regarding TGA behavior was the amount of ash remnant. Neither of the two adhesive types showed a difference between the adhesives without nano-clay and the adhesives with nano-clay in either of the concentrations studied (Table 2).

Combustion kinetics of the different types of adhesives with the distinct nano-clay proportions was determined based on the first order of the reactions present during the decomposition of the adhesives (Table 3). The activation energy of the adhesive without the nano-clay is statistically lower than the energy that occurs in the adhesive with 1.0 wt% and 1.5 wt% nano-clay, and increased as a function of nano-clay content (Table 3). Likewise, differences were found between the entropy factor and the function of composition of the combustion kinetics in the adhesive reactions. In the PVAc, the adhesive entropy factor was statistically superior to that of the adhesive with nano-clay in the first and second reactions and the degree of decomposition function is again statistically higher than for nano-clay adhesives in the two reactions. While in the UF resin, 1 wt% nano-clay added to the adhesive presents no significant difference from the adhesive without nano-clay, whereas adding 1.5 wt% produces a significant

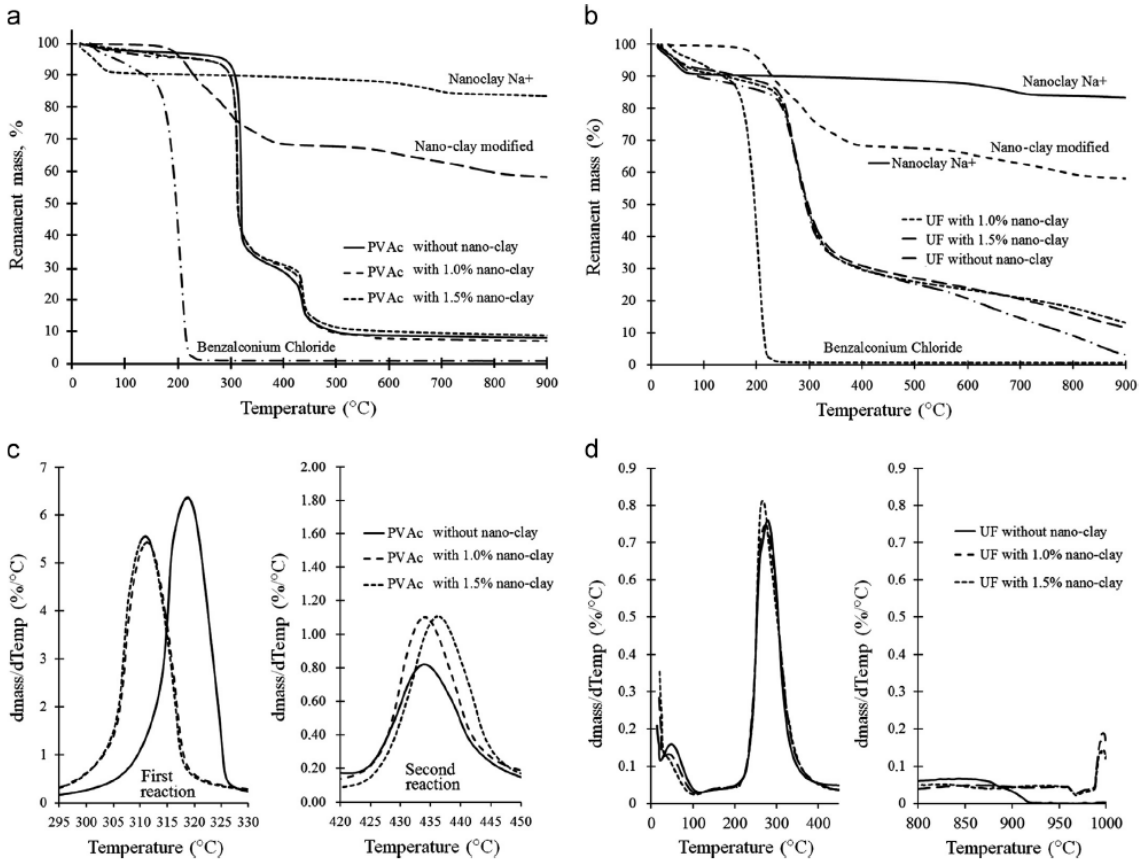

Fig. 4. TGA (a, b) and DTG of different reaction (c, d) curves of PVAc and UF wood adhesive, adding different concentrations of nano-clay.

Table 3
Values of entropy factor, energy activation, function of decomposition degree and correlation coefficient of decomposition kinetics of PVAc and UF wood adhesive adding different concentrations (weight/ weight) of nano-clay.

Adhesive	Reaction	Nano-clay concentration (wt%)	Entropy factor (K_0 in s^{-1})	Energy activation (E in kJ mol^{-1})	Function of decomposition degree (n)	Correlation coefficient (R)
PVAc	First	0	$^{A}3.87 \times 10^{25}$	$^{A}3.8$	$^{A}1.95$	0.72
		1.0	$^{B}7.04 \times 10^{2}$	$^{B}8.1$	$^{B}0.45$	0.58
		1.5	$^{C}2.03 \times 10^{1}$	$^{C}13.7$	$^{B}0.63$	0.70
	Second	0	$^{A}3.58 \times 10^{21}$	$^{A}242.9$	$^{A}18.61$	0.83
		1.0	$^{B}6.88 \times 10^{0}$	$^{B}259.9$	$^{B}9.49$	0.91
		1.5	$^{C}2.38 \times 10^{12}$	$^{C}281.2$	$^{C}13.07$	0.88
UF		0	$^{A}7.02 \times 10^{28}$	$^{A}240.6$	$^{A}8.55$	0.98
		1.0	$^{A}2.11 \times 10^{27}$	$^{B}268.7$	$^{A}8.56$	0.98
		1.5	$^{B}2.03 \times 10^{23}$	$^{C}287.6$	$^{B}6.83$	0.98

difference from the adhesive without nano-clay and with 1.0 wt% of nano-clay (Table 3).

3.1.4. Bond strength

The results showed that adding nano-clay to PVA improves the shear strength of glue line (SS) in dry and wet conditions (Fig. 5a). However, the best results were obtained when nano-clay is added at 1.5 wt% and under wet conditions in both nano-clay proportions (Fig. 5b). In the UF type resin, although the nano-clay in both proportions increased SS, this increase was not significant in the dry condition (Fig. 5c). Meanwhile, the best result in SS of the nano-clays was obtained under wet conditions because the highest statistical SS was observed with 1.0 or 1.5 wt% nano-clay content in the adhesive (Fig. 5d).

Although the SS was not as effective, an evaluation of PWF found that the addition of nano-clay in the two proportions decreased PWF (Table 4). Under dry conditions, in the PVAc adhesive, the wood failure rate decreased by 15%, while under wet conditions, the percentage reduction was greater, between 20–30%. In the UF adhesive, the failure rate also decreased by 10% under dry conditions, 25% in the proportion of 1.0% and 50% under

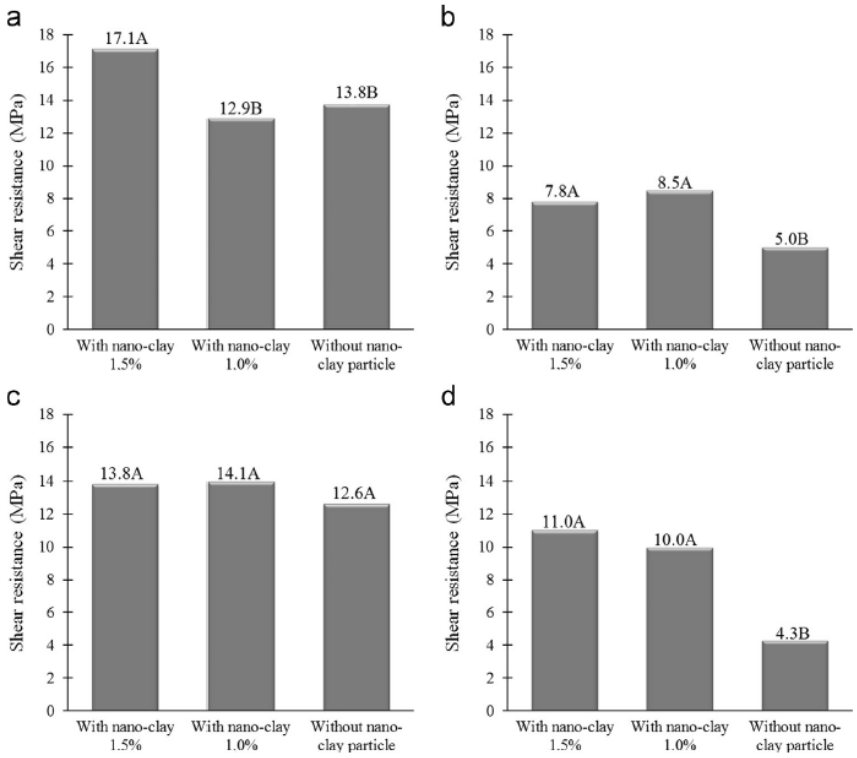

Fig. 5. Resistance of shear strength for dry and wet condition of *C. guianensis* glued with PVA and UF adhesive with and without nano-clay.

Table 4
Moisture content and failure area percentage in shear test of PVAc and UF wood adhesives using different concentrations (weight/weight) of nano-clay.

Parameter	Nano-clay concentration (wt%)	PVAc wood adhesive		UF wood adhesive	
		Dry	Wet	Dry	Wet
Moisture content (%)	0.0	12.20^{A}	39.93^{A}	11.05^{A}	36.84^{A}
	1.0	11.95^{A}	36.97^{B}	11.74^{A}	38.14^{A}
	1.5	11.95^{A}	37.93^{B}	11.69^{A}	37.41^{A}
Failure area (%) in shear test	0.0	44.50^{A}	89.33^{A}	31.33^{A}	87.75^{A}
	1.0	31.00^{B}	62.00^{B}	21.17^{B}	63.42^{B}
	1.5	28.67^{B}	69.33^{B}	23.33^{B}	38.84^{C}

wet conditions (Table 4). It is important to note that the samples with nano-clay showed lower water absorption because the moisture content decreased statistically under wet conditions (Table 4).

4. Discussion

4.1. Adhesive characterization

4.1.1. Viscosity and color

Nano-clay addition causes irregularity of the surface (Fig. 2 (b) and (c)). The regularity, or lack thereof, is associated with rugosity values. The rugosity values (Ra and Rq) are given in Table 1 and they are in agreement with values presented by Kaboorani et al. [2], whose data indicate that low values are attributed to wood adhesives not having nano-clay, the addition of which causes increase of Ra and Rq and the higher the amount of added nano-clay, the higher the values of Ra and Rq. Therefore, the absence of peaks indicated low values of rugosity, and high values of rugosity indicate nano-clay presence. Another relevant aspect, shown by the AFM images, is that peak distribution is slightly uniform, showing no agglomerations of the added nano-clay in the adhesive but adequate dispersion instead [2,8].

4.1.2. Viscosity and color

The increase in the viscosity of the adhesive is explained by the fact that exfoliation or even intercalation of clay leads to a strong viscosity increase [26]. Viscosity is highly related to the degree of exfoliation of the clay. Gopakumar et al. [27] have shown that compounds of polypropylene with various types of clay will increase the viscosity of the liquid relative to the increase in exfoliation of the clay. Exfoliation allows for increased adhesion area of the exfoliated clay [26]. It is important to note that, an increase in viscosity was observed from 1 wt% to 1.5 wt% concentration in UF adhesive (Fig. 3a), which does not occur with the PVAc adhesive (Fig. 3b). Although the effect of the initial viscosity of pure resin on the final viscosity of resin nano-clay adhesive was not tested in this study, most likely the changes in the viscosity for nano-clay adhesion in modified resin are associated with the initial viscosity of the resin. For example, Zhul and Xanthos [28] found that in resin with higher viscosity, the effect of nano-clay adhesion was greater than resin with lower viscosity. Therefore, the increased amount of nano-clay in PVAc has no effect on viscosity, as occurs with the UF resin.

According to the results for adhesive color (Table 1), nano-clay addition, especially in the proportion 1.5 wt%, is likely to change

color in PVAc and increase luminosity and yellowness. With the UF-adhesive, meanwhile, although a change of tonality occurs (a slightly higher index of yellowness), no color change appears in the adhesives with 1.5 wt% and 1.0 wt% nano-clay. The same behavior regarding color change was found by Chaochanchaikul et al. [29] and Awad et al. [30] for PVAc with the different concentrations of nano-clay. They attributed these color changes to high clay concentrations and excellent nano-clay dispersion.

4.1.3. Thermal stability of the adhesives

First, adhesives modified with nano-clay demonstrated a different behavior from un-modified adhesives (Fig. 4a–b), most likely influenced by benzalkonium chloride decomposition. The thermogravimetric analysis (TGA) of both types of adhesives prepared with two concentrations of nano-clay (1.0 and 1.5 wt%) showed two important inflexions in the mass loss in PVAc adhesive (Fig. 4a), whereas in the case of UF adhesive, only one inflexion was observed (Fig. 4b). These inflexions are related to chemical reactions that occur in each adhesive [7]. However, in the case of the UF adhesive at less than 100 °C, although an inflexion occurred (Fig. 4b), there will be no reaction as this temperature and inflexion correspond to water loss in the urea-formaldehyde resin [31].

The addition of nano-clay in PVAc adhesive produced no significant effects on the decomposition of PVAc as the two common reactions in this polymer are maintained [32–33], which is shown by inflexions in the curves of mass loss (Fig. 4a). Although the decomposition of PVAc is very complex [32–33], note that in the first reaction (at approximately 315 °C), the decomposition of acetic acid occurs and in the second reaction (at approximately 425 °C), the decomposition of unsaturated polymers is observed.

However, rises in the temperature and the mass remnant in the first reaction (Table 2), together with the higher activation energy (Table 3) observed in PVAc adhesive, indicate that nano-clay increases the thermostability of the PVAc adhesive. These results agree with those found by Peruzzo et al. [6] for PVAc and by Lee and Jang [34], Ollier et al. [21] and Ahamad and Alshehri [35] working on methyl methacrylate, styrene, epoxy precursors, polystyrene, who reported an increase in thermal stability as a result of adding nano-clay to the matrix polymer. Improved thermal stability of nanocomposites is attributed to hindered outdiffusion of the volatile decomposition products (mainly cyclic silicates), as a direct result of the decrease in permeability, usually observed in exfoliated nanocomposite [36]. Valera-Zaragoza et al. [37], working on PPeEP/EVA/organoclay nanocomposites, stated that the retarding process was assigned to the exfoliation and dispersion of the silicate layers that impeded heat diffusion to the macromolecules. In addition, nano-clay maintains greater thermal stability than adhesives (Fig. 4a–b) and therefore this nano-clay produced more thermal stability.

Urea–formaldehyde (UF) resins are thermosetting polymers, prepared by the reaction of two monomers, urea, formaldehyde and water [31]. In the case of nano-clay addition to UF adhesive, normal behavior is observed in this type of resin, a first inflexion at a temperature less than 100 °C, which corresponds to water elimination [31], and a second reaction within a temperature range of 240–265 °C, which corresponds to the degradation of the polymer. In the latter reaction, a series of components is freed, of which the major components are methylene, methylols, dimethylene ethers, methylene methyl ethers, methylene glycols (formaldehyde) and components with carbonyl and triazine groups, among others [38].

As occurred with the PVAc adhesive, adding nano-clay significantly improved the thermal stability of UF adhesive, the initial temperature of the reaction, the temperature of the maximum peak, the mass remnant on the different periods of temperature studied (Fig. 4e and Table 1) and increased the entropy factor and activation energy in the kinetics of decomposition of the resin (Table 3). These results are consistent with the results obtained by Samaržija-Jovanović et al. [31], Roumeli et al. [39], Hazarika et al. [40], Cai et al. [41] and Doğar et al. [42], which also include studies with the UF adhesive modification with SiO_2 nanoparticles or nano-clay. Once again, the increase in thermal stability of the resin was attributed to the dispersion of the silicate layers, which impeded heat diffusion to the macromolecules [42]. However, no significant differences were found in the adhesives with 1.0 wt% and 1.5 wt% between the various parameters evaluated in the UF adhesive (Table 2) that can be attributed to saturation or agglomeration of nano-clay [7].

The activation energy of the adhesive without the nano-clay is statistically lower than the energy that occurs in the adhesive with 1.0 wt% and 1.5 wt% nano-clay, and increased as a function of nanoclay content (Table 3). This behavior is important because adhesive modified with nano-clay helps to improve the performance of the glue-line in different products fabricated with *C. guianensis* wood, especially in end-uses with high temperature and humidity.

Finally, the results found that no difference in ash content between the adhesive without nano-clay and the adhesives with nano-clay in either of the concentrations can be attributed to lower concentrations of nano-clay utilized, from 1.0% to 1.5% (Table 2).

4.1.4. Bond shear strength

The results showed that adding nano-clay to PVAc adhesives improves SS both under dry and wet conditions, such as a tropical climate, which tends to cause adhesion problems (Fig. 5a). This result is in agreement with other studies on PVAc-based adhesives [2,7,9] but disagrees in the case of UF adhesives modified with nano-clay [10–13]. The improvement of SS can be explained based on the study conducted by Kaboorani and Riedl [7]. They mentioned that nano-clay can modify the response of a polymer to a load through several mechanisms. Nano-clay particles have an inherently high surface area to volume ratio, leading to a large interfacial area between fillers and matrix. This in turn leads to a suggestion that there is an interaction zone surrounding each filler particle that substantially alters the physical properties relative to the neat polymer matrix, such as higher or lower polymer mobility, entanglement density and altered modulus. In addition, the polymer–clay nanocomposites exhibit extremely strong interfaces with polymers due to the confinement of polymer chains within the galleries of clay platelets. It is possible that the confinement of polymer–clay interactions could affect the local chain dynamics to a certain extent.

Another important aspect regarding the results of humid conditions is that the addition of nano-clay improves the behavior of the percentage of wood failure, particularly with the UF-based resin, but not with the PVAc one (Table 4). Lei et al. [10] presented a hypothesis that first, all montmorillonite nano-clay itself is water repellent and second, the observed reinforcement effect induced by the presence of filler may also be attributed to a percolation phenomenon between the nano-clay particles. Montmorillonite nano-clay particles may be modeled as thin disks. When dispersed inside a continuous medium such as a UF resin matrix, the particles are expected to touch each other, thus forming a connected and infinite cluster even at low concentrations. Thus, the water resistance increased in the UF resin, but most likely the affinity of PVAc resin with water did not permit adequate resistance.

5. Conclusion

The montmorillonite type nano-clay modified with benzalkonium chloride ($C_6H_5CH_2N(CH_3)$ 2RCl) and added to polyvinyl

acetate (PVAc) and urea-formaldehyde (UF) improved the thermogravimetric properties of these adhesives, increased starting temperature, increased maximum peak temperature, increased mass remnant in the different temperature periods studied of the reactions present in the adhesives and increased entropy factor and activation energy of the kinetics of decomposition of the resin. In addition, PVAc and UF adhesives with the modified nano-clay affected other physical features, slightly increasing the viscosity of the resin and the brightness and the yellowness of the adhesives, especially in the proportion of 1.5%.

Nano-clay added in PVAc and UF adhesives improved shear strength of the glue line (SS) and the percentage of wood failure (PWF). The highest values of SS were obtained when nano-clay was added in 1.5 wt% in PVAc adhesive under dry conditions. SS was not affected by nano-clay addition in UF adhesive under dry conditions. However, under wet conditions, both 1.0 and 1.5 wt% of nano-clay into adhesive increased SS in the two adhesives. The addition of nano-clay in the two proportions increased PWF at 15% and between 20% and30% under both dry and wet conditions, respectively for PVAc adhesive. In the UF adhesive, PWF increased 10% under dry conditions and 25–50% under wet conditions.

Acknowledgments

The authors wish to thank the Vicerrectoría de Investigación y Extensión at the Instituto Tecnológico de Costa Rica (ITCR) for financial support for the study.

References

[1] Stoeckel F, Johannes K, Wolfgang G. Mechanical properties of adhesives for bonding wood—a review. Int J Adhes Adhes 2013;45:32–41.
[2] Kaboorani A, Riedl B, Blanchet P. Ultrasonication technique: a method for dispersing nano-clay in wood adhesives. J Nanomater 2013;3:1–9.
[3] Zhao LF, Liu Y, Xu ZD, Zhang YZ, Zhao F, Zhang SB. State of research and trends in development of wood adhesives. For Stud China 2011;13:321–6.
[4] Roussak OV, Gesser HD. Adhesives and adhesion. Applied Chemistry. US: Springer; 2013. p. 219–32.
[5] Mohan P. A critical review: the modification, properties, and applications of epoxy resins. Polym-Plast Technol Eng 2013;52.2:107–25.
[6] Peruzzo PJ, Bonnefond A, Reyes Y, Fernández M, Fare J, Ronne E, et al. Beneficial in-situ incorporation of nano-clay to waterborne PVAc/PVOH dispersion adhesives for wood applications. Int J Adhes Adhes 2014;48:295–302.
[7] Kaboorani A, Riedl B. Effects of adding nano-clay on performance of polyvinyl acetate (PVA) as a wood adhesive. Compos Part A: Appl Sci Manuf 2011;42(8):1031–9.
[8] Kaboorani A, Riedl B, Blanchet P, Fellin M, Hosseinaei O, Wang S. Nanocrystalline cellulose (NCC): a renewable nano-material for polyvinyl acetate (PVA) adhesive. Eur Polym J 2012;48:1829–37.
[9] Pique TM, Pérez CJ, Alvarez VA, Vázquez A. Water soluble nanocomposite films based on poly (vinyl alcohol) and chemically modified montmorillonites. J Compos Mater 2014;48:545–53.
[10] Lei H, Du G, Pizzi A, Celzard A. Influence of nano-clay on urea-formaldehyde resins for wood adhesives and its model. J Appl Polym Sci 2008;109(4):2442–51.
[11] Pirayesh H, Khanjanzadeh H, Salari A. Effect of using walnut/almond shells on the physical, mechanical properties and formaldehyde emission of particleboard. Compos Part B: Eng 2013;45(1):858–63.
[12] Xian D, Semple KE, Haghdan S, Smith GD. Properties and wood bonding capacity of nano-clay-modified urea and melamine formaldehyde resins. Wood Fiber Sci 2013;45(4):383–95.
[13] Ates E, Uyanik N, Kizilcan N. Preparation of urea formaldehyde resin/layered silicate nanocomposites. Pigment Resin Technol 2013;42:283–7.
[14] Bourreau D, Aimene Y, Beauchêne J, Thibaut B. Feasibility of glued laminated timber beams with tropical hardwoods. Eur J Wood Prod 2013;71(5):653–62.
[15] Gérard J. Specific features of tropical hardwoods bondability: adding values to secondary wood species and multi-species gluing (In French). Ann Génie Civil Bois Collage Struct 1999;1:15–30.
[16] Sinha Ray S, Okamoto M. Polymer/layered silicate nanocomposites: a review from preparation to processing. Prog Polym Sci 2003;28(11):1539–641.
[17] Diener BJ, Saklad H. Portico SA. J Bus Res 1997;38(1):89–96.
[18] Chahud E, Rocco FA, Rosi RR. O uso de espécies nativas comercializadas em Belo Horizonte na composição de madeira laminada colada. Construindo 2009;1:42–9.
[19] ASTM. (2013). D905-08.Standard test method for strength properties of adhesive bonds in shear by compression loading. Annual book of ASTM standards, 2013, vol.11 (06), 5 p.
[20] Ollier R, Vázquez A, Alvarez V. Biodegradable nanocomposites based on modified bentonite and polycaprolactone. Adv Nanotech 2011;1:1–10.
[21] Ollier R, Rodriguez E, Alvarez V. Unsaturated polyester/bentonite nanocomposites: influence of clay modification on final performance. Compos Part A: Appl Sci Manuf 2013;48:137–43.
[22] Hunterlab. In: Richard S, Hunter R, Richard W Harold, editors. The Measurement of Appearance. New York: Published by John Wiley & Sons, Inc; 1995.
[23] ASTM. Standard practice for calculation of color tolerances and color differences from instrumentally measured color coordinates (D 2244-02). Pennsylvania: Book of standards. 2013, vol. 11(06).
[24] Vyazovkin S, Sbirrazzuoli N. Isoconversional kinetic analysis of thermally stimulated processes in polymers. Macromol Rapid Commun 2006;27(18):1515–1532.
[25] ASTM. D5266-13. Standard practice for estimating the percentage of wood failure in adhesive bonded joints. Annual book of ASTM standards 2013b, vol. 11(06).
[26] Landry V, Bernard R, Blanchet P. Nanoclay dispersion effects on UV coatings curing. Prog Org Coat 2008;62:400–8.
[27] Gopakumar TG, Lee JA, Kontopoulou M, Parent JS. Influence of clay exfoliation on the physical properties of montmorillonite/polyethylene composites. Polymer 2002;43:5483–91.
[28] Zhu1 L, Xanthos M. Effects of process conditions and mixing protocols on structure of extruded polypropylene nanocomposites. J Appl Polym Sci 2004;93(4):1891–9.
[29] Chaochanchaikul K, Rosarpitak V, Sombatsompop N. Structural and thermal stabilization of PVC and wood/PVC composites by metal stearates and organotin. BioResources 2011;6(3):3115–31.
[30] Awad WH, Beyer G, Benderly D, Ijdo WL, Songtipya P, Jimenez-Gasco MDM, et al. Material properties of nano-clay PVC composites. Polymer 2009;50(8):1857–67.
[31] Samaržija-Jovanović S, Jovanović V, Konstantinović S, Marković G, Marinović-Cincović M. Thermal behaviour of modified urea–formaldehyde resins. J Ther Anal Calorim 2011;104(3):1159–66.
[32] Blazevska-Gilev J, Spaseska D. Thermal degradation of PVAc. J Univ Chem Technol Metall 2005;40(4):287–90.
[33] McNeill IC, Memetea L, Cole WJ. A study of the products of PVC thermal degradation. Polym Degrad Stab 2005;49(1):181–91.
[34] Lee DC, Jang LW. Characterization of epoxy-clay hybrid composite prepared by emulsion polymerization. J Appl Polym Sci 1998;68(12):1997–2005.
[35] Ahamad T, Alshehri SM. Thermal degradation and evolved gas analysis: a polymeric blend of urea formaldehyde (UF) and epoxy (DGEBA) resin. Arab J Chem 2014;7(6):1140–7.
[36] Burnside SD, Giannelis. EP. Synthesis and properties of new poly (dimethylsiloxane) nanocomposites. Chem Mater 1995;7(9):1597–600.
[37] Valera-Zaragoza M, Ramírez-Vargas E, Medellín-Rodríguez FJ, Huerta-Martínez BM. Thermal stability and flammability properties of heterophasic PPeEP/EVA/organoclay nanocomposites. Polym Degrad Stab 2006;91(6):1319–25.
[38] Siimer K, Kaljuvee T, Christjanson P. Thermal behaviour of urea-formaldehyde resins during curing. J Ther Anal Calorim 2003;72(2):607–17.
[39] Roumeli E, Papadopoulou E, Pavlidou E, Vourlias G, Bikiaris D, Paraskevopoulos KM, et al. Synthesis, characterization and thermal analysis of urea–formaldehyde/nanoSiO_2 resins. Thermochim Acta 2012;527:33–9.
[40] Hazarika A, Mandal M, Maji TK. Dynamic mechanical analysis, biodegradability and thermal stability of wood polymer nanocomposites. Compos Part B: Eng 2014;60:568–76.
[41] Cai X, Riedl B, Wan H, Zhang SY, Wang XM. A study on the curing and viscoelastic characteristics of melamine–urea–formaldehyde resin in the presence of aluminium silicate nano-clays. Compos Part A: Appl Sci Manuf 2010;41(5):604–11.
[42] Doğar Ç, Gürses A, Karaca S, Köktepe S, Mindivan F, Güneş K. Investigation of thermal properties of PUF/clay nanocomposites. Appl Surf Sci 2013.

4. Artículo 4. Effects of adding nano-clay in polyvinyl acetate and urea-formaldehyde adhesives on tropical wood shear resistance.

EFFECTS OF ADDING NANO-CLAY IN POLYVINYL ACETATE AND UREA-FORMALDEHYDE ADHESIVES ON TROPICAL WOOD SHEAR RESISTANCE

Róger Moya*, Ana Rodríguez-Zúñiga[2], José Vega-Baudrit[3]

[1]Escuela de Ingeniería Forestal, Instituto Tecnológico de Costa Rica, Apartado 159-7050, Cartago, Costa Rica, Email: rmoya@itcr.ac.cr
[2]Escuela de Ingeniería Forestal, Instituto Tecnológico de Costa Rica, Apartado 159-7050, Cartago, Costa Rica, Email: ana.rodriguez@itcr.ac.cr
[3]Laboratório Nacional Nanotecnologia (LANOTEC), Centro Nacional de Alta Tecnologia-CENAT, San Jose, Costa Rica, email: jvegab@gmail.com

EFFECTS OF ADDING NANO-CLAY IN POLYVINYL ACETATE AND UREA-FORMALDEHYDE ADHESIVES ON TROPICAL WOOD SHEAR RESISTANCE

ABSTRACT

The aim of this study was test the bond strength resistance of polyvinyl acetate (PVAc) and urea-formaldehyde (UF) adhesives modified with nano-clay (montmorillonite) in nine tropical species in 1.0 and 1.5 wt% concentrations. Shear strength (SS), and the percentage of wood failure (PWF) in dry and wet conditions were evaluated. Presence of nano-clay within both adhesives was observed using an AFM and TEM. Viscosity was also evaluated. AFM and TEM observations showed adequate dispersion and impregnation of nano-clay. The viscosity of PVAc-adhesive was not affected, whereas the UF-adhesive was. Adding nano-clay to PVAc- or UF-adhesives has different behavior in SS parameters between the different species. UF-adhesives improved SS for a greater amount of species than PVAc adhesive. Nano-clay added in PVAc and UF-adhesives improves SS and PWF in most species, but when wood humidity increases there is no significant increase in the glue line.

Keywords: Wood adhesives, nanotechnology, tropical species, nano-clay, viscosity

1. Introduction

Wood adhesives and wood products are important for manufacturing products for construction and furniture production (Stoeckel et al., 2013). Adhesives are used to produce wood composed products, such as plywood, fiberboard and oriented strand board (OSB) and also for wood re-use (Kaboorani et al. 2013). Adhesives also improve the usefulness of wood, allowing the use of low-quality wood and small-sized pieces so that wood waste can be more effectively used (Zhao et al., 2011)

Recently, the development of nanotechnology, specifically nano-particles, has helped to produce a new generation of high performance adhesives (Roussak and Gesser, 2013; Peruzzo et al., 2014). Various nano-particles, layered silicates, aluminum oxide and nanocellulose among them, have been used to improve the performance of several wood adhesives (Mohan, 2013).

Organo-clays derived from natural montmorillonite and modified with quaternary ammonium salt (dimethyl benzyl hydrogenated tallow ammonium) have been shown to improve the properties of polyvinyl acetate (Kaboorani et al., 2012; Kaboorani et al., 2013; Pique et al., 2014) and urea-formaldehyde adhesives (Lei et al, 2008; Pirayesh et al., 2013; Xian et al., 2013; Ates et al., 2013). However, the effect of nanoparticle incorporation on the performance of adhesives used with tropical wood is still unknown. While the behavior of adhesives with nano-particles is relatively well understood in temperate countries, in regions of high temperature and high humidity, such as in tropical countries, it can create many problems (Bourreau et al., 2013). Recently, Moya et al. (2015) showed that nano-clay (montmorillonite) improved the performance of polyvinyl acetate (PVAc) and urea-formaldehyde (UF) adhesives in *Carapa guianensis*, which has a high content of extractives and some adhesion problems (Sinha and Okamoto, 2003; Diener and Saklad, 1997). However, there are many species in tropical regions, which have high specific gravity and high shrinkage which, together with the presence of naturally occurring resinous material, could influence glue line integrity characteristics (Gérard, 1999).

The purpose of this work was to study the performance in bond strength of the PVAc- and UF-adhesives modified with nano-clay (montmorillonite) with nine tropical species (*Acacia mangium*, *Cedrela odorata*, *Cordia alliodora*, *Enterolobium cyclocarpum*,

Gmelina arborea, *Goethalsia meiantha*, *Ochroma pyramidale*, *Tectona grandis* and *Vochysia ferruginea*) from low and high density. Also to show changes that occurred in the nano-clay due to modification with benzalkonium chloride and the change in viscosity of the PVAc and UF adhesives modified with nano-clay.

2. Material and methods

2.1. Materials

Commercial clay Closite® Na+, which is an unmodified montmorillonite supplied by Rocwood Clay Based Additives, was used as nanofiller. According to the description of the supplier, the moisture content of the product ranges 4-9%, its density is 2.86 g cm-3 and the size distribution of the particles is: 10% less than 2 µm, 50% less than 6 µm and 90% of the particles are less than 13 µm in size. Benzalkonium chloride (C6H5CH2N+ (CH3)2RCl-) was used to improve miscibility of the layered silicates with the adhesive matrices (PVAc and UF), and it was chosen by several methods proposed by Ray and Okamoto (Sinha and Okamoto, 2003).

Two types of wood adhesive were used. The first type was a water-based polyvinyl acetate (PVAc), ResistolM.R. 850® trademark, produced by Henkel Capital S.A. (http://www.resistol.com.mx/es.html). Technical description of the product indicates that the resin is polyvinyl acetate and water, with 54.5 to 55.5% solid content and a viscosity of 1600 to 2200 cPs. The second type of adhesive used was a water-based urea-formaldehyde (UF), CR-560 UF Resin trademark, produced by Central Chemistry Quibor SA (http://www.agroquibor.com). Technical description of the product indicates that the liquid resin is urea-formaldehyde (UF), with 64 to 65% solids content and 650-900 cPs viscosity.

The species used for the adhesion tests were *Acacia mangium*, *Cedrela odorata*, *Cordia alliodora*, *Enterolobium cyclocarpum*, *Gmelina arborea*, *Goethalsia meiantha*, *Ochroma pyramidale*, *Tectona grandis* and *Vochysia ferruginea*, which are species traditionally used in Costa Rica for manufacturing doors and other wood-based products.

2.2. Preparation of adhesives with nanoclays

Nano-clay was added to both adhesive types in three different concentrations: 0% (or control), 1% and 1.5% (wt.%). According to studies carried out by Kaboorani et al.

(2012) in temperate species, these proportions achieved the best performance. First, commercial nano-clay was modified in order to improve chemical compatibility with both adhesive types. In order to improve affinity, a treatment of cation exchange with benzalkonium chloride was applied, based on the proposal of Ollier et al. (2011; 2013). The proposal was to treat the unmodified montmorillonite with the aqueous solution at 7% of benzalkonium chloride. For this, nano-clay was mixed in a solution of ethanol-water (volume rate at 20:80%) at 60 °C for 1 hour under stirring (solution A). Simultaneously, a solution of 7% benzalkonium chloride (solution B) was prepared at room temperature, also stirring for one hour. After that time, solution A was mixed with solution B. Both were mixed at a temperature of 60 °C with constant stirring for 12 hours. The mixture was then filtered until the chlorides test indicated no presence of chlorine, for this purpose, a solution of saturated silver nitrate, as proposed by Ollier et al. (2011), was used. Finally, the treated nano-clay was left to dry at 105 °C, and once dry, it was pulverized in a mortar to achieve a finely ground nano-clay.

Several adhesive mixtures modified with nano-clay were prepared: (i) PVAc-adhesive was stirred at 1600 rpm for 15 minutes using four 45°-inclined blade impellers at room temperature, during which, nano-clay was slowly added into the PVAc resin; and (ii) with UF adhesive, due to it is a 3-component adhesive (resin, wheat flour, and catalyst of sulfates), the resin and flour were prepared and then mixed with the unmodified nano-clay. As in the previous case, resin was stirred at 1600 rpm for 15 minutes using an inclined blade (45°), while nano-clay and flour were slowly added until disperse in the resin.

2.3. Adhesive characterization

The desperation of nano-clay within the adhesive was verified using the Atomic Force Microscopy (AFM) and Transmission Electron Microscopy (TEM). With both techniques, an appropriate volume of adhesive with either 1% concentration of modified nano-clay (wt.%) or unmodified nano-clay at the same concentration, were prepared. For TEM observations (trademark Jeol and JEM-2100 model), small samples of modified and unmodified nano-clay were placed in the microscope, where a 100-kV acceleration and 10,000X (B and C) and 300,000X (D) amplifications were used. Since AFM observations

were performed in adhesive, they were carried out using a NanoScope V, an atomic force microscope (Asylum Research model MFP 3D) fitted with a Hybrid XYZ scanner. Atomic force microscope measurements were done under ambient air conditions. To measure viscosity, a 0.5-liter sample of the two adhesives in the three concentrations of nano-clay was made and placed in the viscometer, Brokfield-11 + Pro LV. 2.4.4.

2.4. Bond strength

Bond strength assessments for two adhesives modified with nano-clay were evaluated by shear strength of glue line (SS), according to ASTM D-905-98 (ASTM, 2014a). After preparing the two adhesives types with nano-clay, wood of *A. mangium*, *C. odorata*, *C. alliodora*, *E. cyclocarpum*, *G. arborea*, *G. meiantha*, *O. pyramidale*, *T. grandis* and *V. ferruginea* were prepared and bonded according to norm. A total of 90 shear tests were carried out (30 samples per concentrations x 3 concentrations) for each species. Wood was stabilized at a condition of 12% moisture for one week. The adhesive was applied in accordance with the manufacturer's specifications, which recommend an amount of 100 gm-2 for both adhesives. After applying adhesive on the wood surface, samples were pressed in a hydraulic machine at a 0.20 Nmm-2 pressure for 24 hours. Before pressurizing, bonded samples were conditioned to 20 °C and 60% relative humidity for two weeks. Then, 30 samples were extracted and tested for each formulation set. The SS was measured in dry and wet states under ambient air conditions. A Tinus Olsen hydraulic test machine with 50 kN capacity was used for load application and the data were acquired from the computer. Wood failure and maximum load were recorded for each test. Block shear tests were carried out according to ASTM D905-98 (ASTM, 2014a). Samples sizes for ‘‘wet state’’ tests were the same as for “dry state” tests. For ‘‘wet state’’ tests, samples were taken directly out of the water after being immersed for 24 h. Before the tests, excess water was wiped from the samples. During the water immersion period, the water temperature was maintained at 20°C. After each sample was tested in the shear test, the percentage of wood failure (PWF) was evaluated according to ASTM D-5266-13 standard (ASTM, 2014b).

2.5. Analysis of the information

Verification was done according to the assumptions of normal distribution and variance homogeneity of the determined variables, as well as the presence of outliers. Subsequently, a variance analysis (ANOVA) was performed to verify the effect of the nano-clay adhesion (three levels: 0%, 1% and 1.5% nano-clay) on viscosity and SS values. Tukey test at a 99% confidence level was established to determine whether there was a statistically significant difference between the means.

3. Results and discussion

3.1. Adhesive characterization

Regarding the AFM analysis of the nano-clay modified adhesives, the adhesive surfaces with nano-clay were found to be irregular, with the presence of peaks. Figures 1a and 1b show AFM spectra for formulations having nano-clay concentrations of 1.0 wt.% and 1.5 wt.% for the UF adhesive. According to Figure 1a, with the concentration of 1.5 wt.%, the number of peaks is higher than of those occurring in the UF adhesive with a concentration of 1% (Figure 1b). The dispersion of peaks on the surface is uniform at both concentrations.

Figure 2 shows TEM images obtained for the systems studied. First, it was observed that nano-clay particles appear short and tubular in some areas of the PVAc matrix (Figure 2a-2b). These particles are short and their diameter is almost 50 nm (Figure 2a). Additionally, it was observed that typical montmorillonite particles mixed in the PVAc matrix were approximately 1 μm length (Figure 2c) and some montmorillonite particles had little separation between their clay layers (Figure 2d).

Nano-clay addition causes irregularity of the surface (Figure 1b and 1c). The regularity, or lack thereof, is associated with rugosity values. Kaboorani et al. (2013) indicate that low peaks are attributed to wood adhesives without nano-clay, and conversely high peaks are associated with high nano-clay presence. Therefore, the absence of peaks indicated low rugosity values, and high rugosity values indicated nano-clay presence. Another relevant aspect, shown by the AFM images, is that peak distribution is slightly

uniform, showing no agglomerations of the added nano-clay in the adhesive but adequate dispersion instead (Kaboorani et al., 2013; Kaboorani et al., 2012).

In relation to viscosity, nano-clay statistically increases this parameter in the adhesive modified in comparison with the adhesive without nano-clay. For PVAc-adhesive, no significant difference between the adhesive with 1.0 wt.% and 1.5 wt.% nano-clay contents was found regarding viscosity (Figure 3a), whereas for the UF-adhesive, the 3 types of nano-clay content were significantly different (Figure 3b) and : increased with nano-clay content.

The increase in adhesive viscosity is explained by the fact that exfoliation or even intercalation of clay leads to a strong viscosity increase (Landry et al., 2008). Viscosity is highly related to the degree of exfoliation of the clay. Gopakumar et al., 2002, have shown that compounds of polypropylene with several clay types will increase the viscosity of the liquid relative to the increase in exfoliation of the clay. Exfoliation allows an increased adhesion area of the exfoliated clay (Landry et al., 2008). It is important to note that, an increase in viscosity was observed from 1 wt.% to 1.5 wt.% concentration in UF adhesive (Figure 3a), which does not occur with the PVAc adhesive (Figure 3b). Although the effect of the initial viscosity of pure resin on the final viscosity of resin nano-clay adhesive is not tested in this study, most likely the changes in the viscosity for nano-clay adhesion in modified resins are associated with the initial viscosity of the resins. For example, Zhu and Xanthos (2004) found that in resin with higher viscosity, the effect of nano-clay adhesion was greater than resin with lower viscosity. Therefore, the increased amount of nano-clay in PVAc has no effect on viscosity, as occurs with the UF-adhesive.

Likewise, is important to mention that despite viscosity of glue increased, this show no significant effects the penetration of the adhesive in the region near the glue line (Figure 4). Observing glue line with UF-adhesive and its near regions in *C. odorata* a similar glue line was observed for wood that had been glued with the adhesive modified with nano-clay and for the adhesive that had not been modified (Figure 4a and 4b, respectively). It was observed that even for vessels near the glue line a penetration of the adhesive was observed in both modified and unmodified (Figure 4c and 4b, respectively).

3.2. Bond shear strength

Results showed that adding nano-clay to PVAc or UF- adhesives have different behavior in the shear strength of glue line (SS) between the different species (Figure 5). Nano-clay addiction in either adhesive had no significant effects in *A. mangium* wood in dry conditions, but a significant increase in SS occurred for both adhesives in wet condition (Figure 5a). Adding nano-clay in a 1% concentration in PVAc- or UF-adhesive did not increase SS in dry condition for *C. odorata*, *C. alliodora*, *O. pyramidale* and *T. grandis* wood, however 1.5% of nano-clay concentration in both adhesives significantly increases SS in dry condition (Figure 5b-c, 5g-h). SS value for wet condition in these species is different: in PVAc-adhesive nano-clay in 1.5% significantly increased in *C. odorata* wood, but in UF-adhesive, nano-clay addition was not significantly affected (Figure 5b).

For *C. alliodora* and *T. grandis* wood, SS was not affected in PVAc-adhesive in wet condition for either nano-clay concentration, but for UF-adhesive only the de 1.5% concentration significantly increased SS (Figure 5c, 5h). For *O. pyramidale* wood in wet condition, SS was not significantly affected in both adhesives (Figure 5g). Nano-clay addition in concentrations 1.0 and 1.5% in PAVc and UF-adhesives significantly increased SS in *E. cyclocarpum*, *G. meiamtha* and *V. ferruginea* wood (Figure 4d, 4f, 4i). These woods in wet condition did not affect SS in PVAc-adhesive, whereas UF-adhesive significantly increased SS only in the concentration 1.5% (Figure 5d, 5f, 5i). Finally, *G. arborea* wood, SS value with PVAc-adhesive was not significantly affected by nano-clay addition, but in UF-adhesive, nano-clay concentration at 1.0% significantly decreased SS, but concentration at 1.5% significantly increased the resistance (Figure 5e).

Moisture content evaluation showed that in all evaluated species this parameter in dry conditions was statistically equal in all conditions of nano-clay concentrations. However, in wet condition after wood was immersed in water for 24 hours, some differences for this value occurred for some species (Table 1). *A. mangium*, *C. odorata*, *G. arborea*, *E. cyclocarpum*, *G. meiantha*, *T. grandis* and *V. guatemalensis* wood showed no significant differences in MC after water immersion with either adhesives (Table 1). In *C.*

alliodora wood a significant increase occurred in MC in wood glued with UF-adhesive, and in concentration at 1.0% of PVAc-adhesive. For *O. pyramidale* the samples glued with adhesive and nano-clay significantly decreased the moisture content (Table 1).

Percentage of wood failure (PWF) in wood glued line with PVAc-adhesive significantly decreased by adding nano-clay to wood of *A. mangium*, *C. odorata*, *E. cyclocarpum*, *G. arborea*, *T. grandis* and *V. ferruginea* wood in dry condition (Table 1). PWF in dry condition was not significantly affected in wood of *C. alliodora*, *G. meiantha* and *O. pyramidale* when wood is glued with PVAc (Table 1). For wet condition, the addition of nano-clay significantly increased PWF in *C. alliodora*, *E. cyclocarpum*, *G. meintha* and *T. grandis* wood. But, decreased of this percentage in *A. mangium*, C. odorata, *G. arborea*, *O. pyramidale*, and *V. ferruginea* wood in concentration at 1%, but concentration at 1.5% remained similar to the adhesive without nano-clay.

The UF-adhesive with nano-clay, showed that PWF in dry increased in both nano-clay concentrations in wood of *G. arborea*, *T. grandis* and *V. ferruginea*, whereas PWF of *C. odorata*, *E. cyclocarpum* wood increased only in concentration at 1.5% and for the other species (*A mangium*, *G. meintha* and *O. pyramidale*) PWF decreased in some of the concentrations. Furthermore, in *C. alliodora* PWF was not significantly affected (Table 1). For the evaluation of glue line performance using UF-adhesive in wet condition, except for *A. mangium* and *C. odorata*, the PWF decreased, for the other species PWF significantly increased with nano-clay addition to UF (Table 1).

Results showed that adding nano-clay to PVAc or UF adhesives have different behavior in the shear strength of glue line (SS) between the different species, however the UF-adhesives improved SS for a greater amount of species than PVAc-adhesive (Figure 4). In some species, SS increased (for example, *C. odorata* or *C. alliodora* wood with PVAc-adhesive modified with nano-clay), but in others (*A. mangium* wood in both adhesive types and *G. arboorea* wood in PVAc-adhesive) the SS was not affected with the addition of nano-particles (Figure 4).

The increase of SS found in *C. odorata*, *C. alliodora*, *O. pyramidale* and *T. grandis* wood agrees with the results from other studies using PVAc-based adhesives (Kaboorani et

al., 2013; Kaboorani et al., 2011; Pique et al., 2014; Peruzzo et al., 2014). Likewise, the increase of SS with nano-clay concentration agrees with the results of Moya et al (2015), in *Carapa guianensis*, is also a tropical species and with adhesion problems. The increase of SS in all species (except for *A. mangium* wood) in the present study (Figure 4) with UF-adhesive modified with nano-clay is consistent with the results obtained for *Populus deltoides* (Ashori and Nourbakhsh, 2009) and *Paulownia fortunei* (Salari et al., 2012), but these authors investigated medium density fiberboard (MDF) and oriented strand board (OSB) respectively.

The improvement of SS can be explained based on the study conducted by Kaboorani et al. (2012). They mentioned that nano-clay can modify the response of a polymer to a load through several mechanisms. Nano-clay particles have an inherently high surface area to volume ratio, leading to a large interfacial area between fillers and matrix. This in turn leads to a suggestion that there is an interaction zone surrounding each filler particle that substantially alters the physical properties relative to the neat polymer matrix, such as higher or lower polymer mobility, entanglement density and altered modulus. Additionally, the polymer–clay nanocomposites exhibit extremely strong interfaces with polymers due to the confinement of polymer chains within the galleries of clay platelets. It is possible that the confinement of polymer–clay interactions could affect the local chain dynamics to a certain extent.

Although, the addition of nano-clay has no implications for SS in *A. mangium* and *G. arborea* wood in dry condition (Figure 4). This contradictory result regarding the other species indicates that the adhesive modified with nano-clay is affected by intrinsic characteristics of these species, where extractives, wettability and chemical composition stand out (Nussbaum and Sterley, 2002).

The PVAc-adhesive is the less resistant to water in relation to UF-adhesive (Roussak and Gesser, 2013). However, nano-clay failed to modify resistance significantly in wet condition, counter to the increase achieved in dry condition, except for *A. mangium* and *C. alliodora* (Figure 4a and 4c). In UF-adhesive, SS is more resistant to water than

PVAc-adhesive for the different species, since the differences in dry condition are maintained (Figure 4).

The percentage of nano-clay addition with the results found seems to indicate that the highest resistance increase is achieved when the proportion of nano-clay is 1.5% in both adhesive types, since for most species a significant increase of SS was achieved with this percentage.

Another important aspect regarding the results of wet conditions is that the addition of nano-clay improves the behavior of the PWF, particularly with the UF-adhesive, not with the PVAc one (Table 1). Lei et al. (2008) presented a hypothesis that first, all montmorillonite nano-clay itself is water repellent, and second, the observed reinforcement effect induced by the presence of filler may also be attributed to a percolation phenomenon between the nano-clay particles. Montmorillonite nano-clay particles may be modeled as thin disks. When dispersed inside a continuous medium such as a UF-adhesive, the particles are expected to touch each other, thus forming a connected and infinite cluster even at low concentrations. Thus, the water resistance increased in the UF-adhesive, but most likely the affinity of PVAc-adhesive with water did not permit adequate resistance.

4. Conclusions

The montmorillonite type nano-clay modified with benzalkonium chloride ($C_6H_5CH_2N(CH_3)$ 2RCl) and added to polyvinyl acetate (PVAc) and urea-formaldehyde (UF) slightly increased the viscosity of the resin, but has no negative effects in the penetration of the adhesive within wood, since penetration similar as when the adhesive has not been modified.

Adding nano-clay to PVAc or UF adhesives has different behavior in the shear strength of glue line (SS) between the different species, UF-adhesives improved SS for a greater amount of species than PVAc adhesive. Nano-clay added in PVAc-adhesives improved shear strength of the SS and the percentage of wood failure (PWF) in most tropical species studied (except for *A. mangium* and *G. arborea* wood), however, when the

glue line is subjected to a wet condition, this fails to improve the resistance of glue line due to this factor.

Nano-clay addition in UF-adhesive, significantly improves SS in most species, again with the exception of *A. mangium* wood. Whereas glue line acquires moisture, the resistance of glue line significantly improves in the different tropical species, especially when nano-clay addition is 1.5%.

Acknowledgments

The authors wish to thank the Vicerrectoría de Investigación y Extensión at the Instituto Tecnológico de Costa Rica (ITCR) for financial support for the study.

References

Ashori, A., Nourbakhsh, A. (2009) 'Effects of nanoclay as a reinforcement filler on the physical and mechanical properties of wood-based composite'. *Journal of composite materials*, **43**, 1869-1875.

ASTM-American Society for Testing and Materials (2014a) *Standard test method for strength properties of adhesive bonds in shear by compression loading*; D-905-08, Vol. 11.06; Philadelphia, PA, USA.

ASTM-American Society for Testing and Materials (2014b) *Standard practice for estimating the percentage of wood failure in adhesive bonded joints*, D-5266-13, Vol. 11.06; Philadelphia, PA, USA.

Ates, E., Uyanik, N., Kizilcan, N. (2013) 'Preparation of urea formaldehyde resin/layered silicate nanocomposites'. *Pigment Resin Technology*, vol. 42, pp. 283-287.

Bourreau, D., Aimene, Y., Beauchêne, J., Thibaut, B. (2013) 'Feasibility of glued laminated timber beams with tropical hardwoods'. *European Journal of Wood Products*, vol. 71, pp. 653-662.

Diener, B. J., Saklad, H. (1997) 'Portico, SA.' *Journal Business Research*, vol. 38, pp.89-96.

Gérard, J. (1999) 'Specific features of tropical hardwoods bondability: adding values to secondary wood species and multi-species gluing (In French) '. *Annales Génie Civil Bois Collage Structural*, vol. 1, pp.15–30

Gopakumar, T.G., Lee, J.A., Kontopoulou, M., Parent, J.S. (2002) 'Influence of clay exfoliation on the physical properties of montmorillonite/polyethylene composites'. *Polymer*, vol. 43, pp. 5483-5491.

Kaboorani, A., Riedl, B., Blanchet P. (2013) 'Ultrasonication technique: a method for dispersing nano-clay in wood adhesives'. *Journal of Nanomaterials*, vol. 3, pp.1-9.

Kaboorani, A., Riedl, B. (2011) 'Effects of adding nano-clay on performance of polyvinyl acetate (PVA) as a wood adhesive'. *Composites Part A: Applied Science Manufacturing*, vol. 42, pp.1031-1039.

Kaboorani, A., Riedl, B., Blanchet, P.., Fellin, M., Hosseinaei, O., Wang, S. (2012) Nanocrystalline cellulose (NCC): A renewable nano-material for polyvinyl acetate (PVA) adhesive. *European Polymer Journal*, vol. 48, pp. 1829–1837

Landry, V., Bernard, R., Blanchet, P. (2008) 'Nanoclay dispersion effects on UV coatings curing'. *Progress Organic Coating*, vol. 62, pp. 400-408.

Lei, H., Du, G., Pizzi, A., Celzard, A. (2008) 'Influence of nano-clay on urea-formaldehyde resins for wood adhesives and its model'. *Journal Apply of Polymer Science*, vol. 109, pp. 2442-2451.

Mohan, P. (2013) 'A Critical Review: The modification, properties, and applications of epoxy resins'. *Polymer-Plastics Technology and Engineering*, vol. 52, pp. 107-125.

Moya, R., Rodríguez-Zúñiga, A.L., Vega-Baudrit, J., Álvarez, V. (2015) 'Effects of adding nano-clay (montmorillonite) on performance of polyvinyl acetate (PVAc) and urea-formaldehyde (UF) adhesives in *Carapa guianensis*, a tropical species'. *International Journal of Adhesion and Adhesives*, vol. 59, pp. 62-70.

Nussbaum, R. M., Sterley, M. 2002. 'The effect of wood extractive content on glue adhesion and surface wettability of wood'. *Wood Fiber and Science*, vol. 34, pp. 57-71.

Ollier, R., Rodriguez, E., Alvarez, V. (2013) 'Unsaturated polyester/bentonite nanocomposites: Influence of clay modification on final performance'. *Composites Part A: Apply Science Manufacturing*, vol. 48, pp. 137-143.

Ollier, R., Vázquez, A., Alvarez V. (2011) 'Biodegradable nanocomposites based on modified bentonite and policaprolactone'. *Advances of Nanotech*, vol. 1, pp. 1-10.

Peruzzo, P. J., Bonnefond, A., Reyes, Y., Fernández, M., Fare, J., Ronne, E., Leiza, J. R. (2014) 'Beneficial in-situ incorporation of nano-clay to waterborne PVAc/PVOH

dispersion adhesives for wood applications'. *International Journal of Adhesion and Adhesives*, vol. 48, pp.295-302.

Pique, T. M., Pérez, C. J., Alvarez, V. A., Vázquez, A. (2014) 'Water soluble nanocomposite films based on poly (vinyl alcohol) and chemically modified montmorillonites'. *Journal of Composite Materials*, vol. 48, pp. 545-553.

Pirayesh, H., Khanjanzadeh, H., Salari A. (2013) 'Effect of using walnut/almond shells on the physical, mechanical properties and formaldehyde emission of particleboard'. *Composites Part B: Engineering*, vol. 45, pp. 858-863.

Ray, S.; Okamoto, M. (2003) Polymer/layered silicate nanocomposites: a review from preparation to processing. *Progress in Polymer Science*, vol. 28, pp. 1539-1641.

Roussak, O.V. Gesser, H.D. (2013) Adhesives and Adhesion. In *Applied Chemistry: A Textbook for Engineers and Technologists*, Roussak, O.V. Gesser, H.D. Springer Science & Business Media, New York, pp. 219-232.

Salari, A., Tabarsa, T., Khazaeian, A., Saraeian, A. (2012) 'Effect of nanoclay on some applied properties of oriented strand board (OSB) made from underutilized low quality paulownia (*Paulownia fortunei*) wood'. *Journal of Wood Science*, vol. 58, pp. 513-524.

Stoeckel, F., Johannes, K. (2013) Wolfgang, G. 'Mechanical properties of adhesives for bonding wood—A review'. *International Journal of Adhesion and Adhesives*, vol. 45, 32-41.

Xian, D., Semple, K. E., Haghda, S., Smith, G. D. (2013) Properties and wood bonding capacity of nano-clay-modified urea and melamine formaldehyde resins. *Wood Fiber Science*, vol. 45, pp. 383-395.

Zhao, L.F., Liu, Y., Xu, Z.D.; Zhang, Y. Z., Zhao, F., Zhang, S.B. (2011) 'State of research and trends in development of wood adhesives', *Forestry Studies in China*, vol. 13, pp. 321-326.

Zhu, L., Xanthos, M. (2004) 'Effects of process conditions and mixing protocols on structure of extruded polypropylene nanocomposites', *Journal of Apply Polymer Science*, vol. 93, pp. 1891–1899.

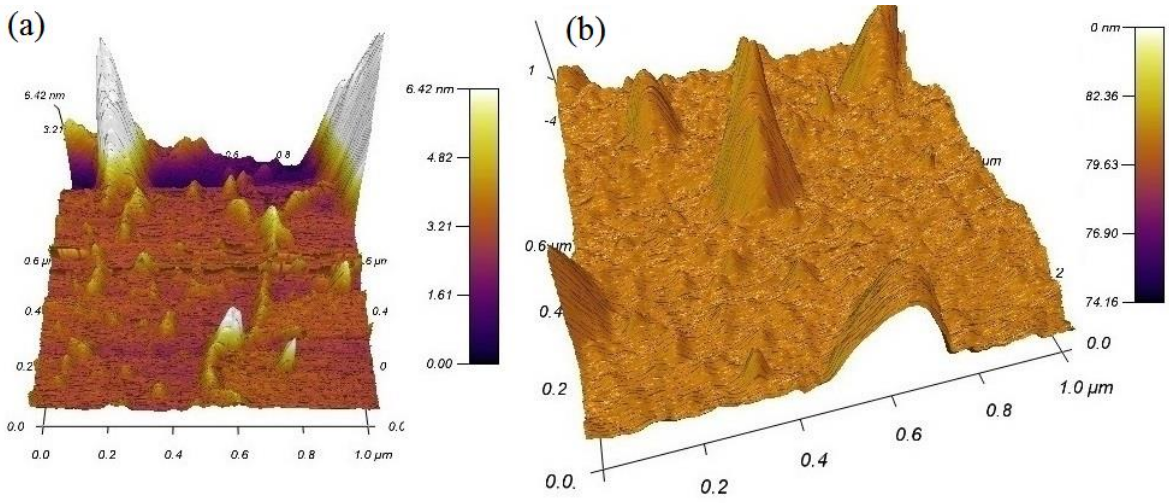

Figure 1 - Atomic force microscope-AFM spectra of nano-clay particles utilized in PVAc-adhesive: (A) 1.5% with nano-clay and (B) 1.0 nano-clay

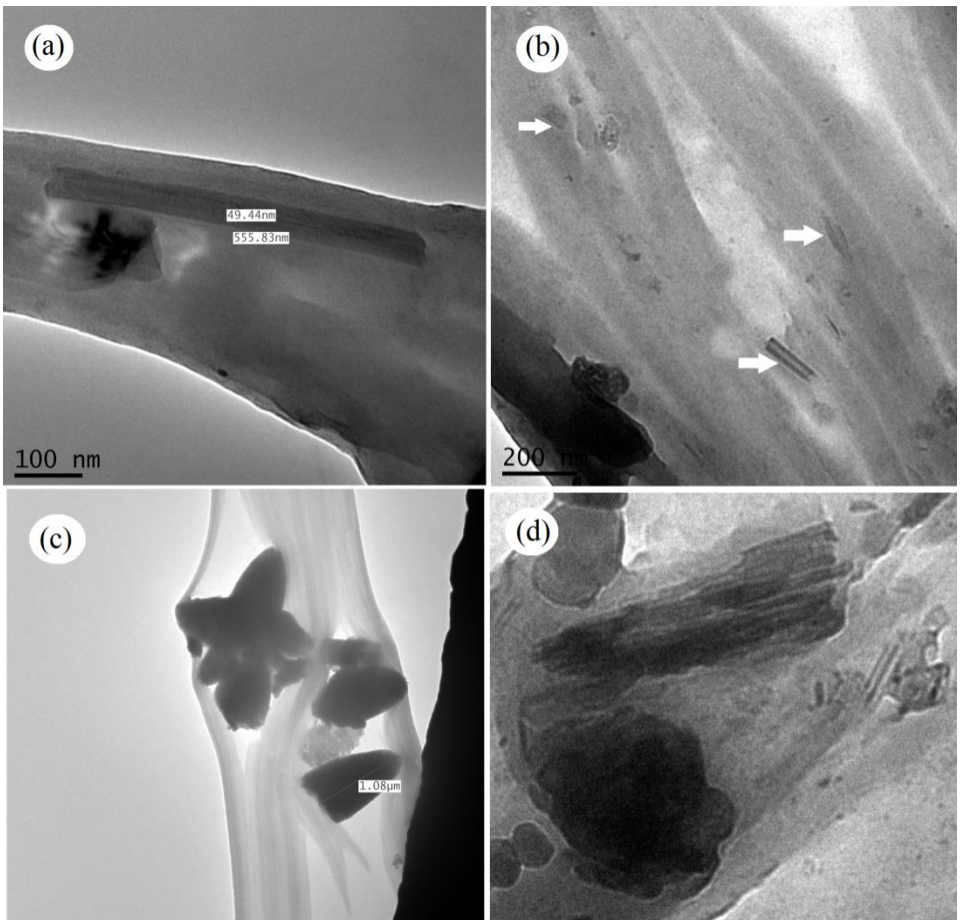

Figure 2 - Transmission Electron Microscopy (TEM) images of PVAc/nano-clay composites: (a-b) short-tubular of nano-clay mixed into PVAc polymers, (c) typical montmorillonite particles inside of two PVAc chain and (d) nano-clay in layers and particles mixed into PVAc-adhesive

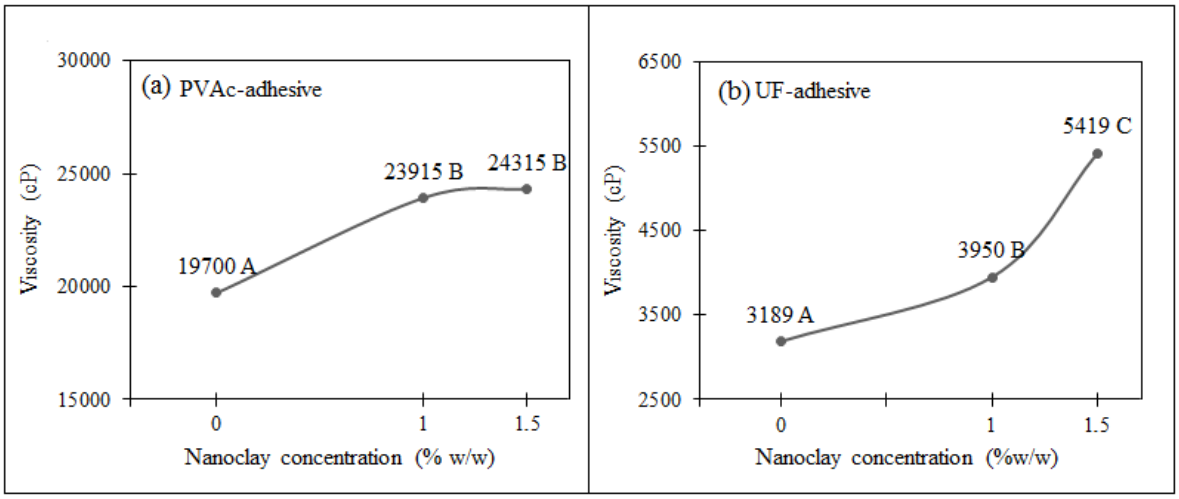

Figure 3 - Viscosity values of PVAc-adhesive and UF-adhesive, adding different concentrations (wt.%) of nano-clay

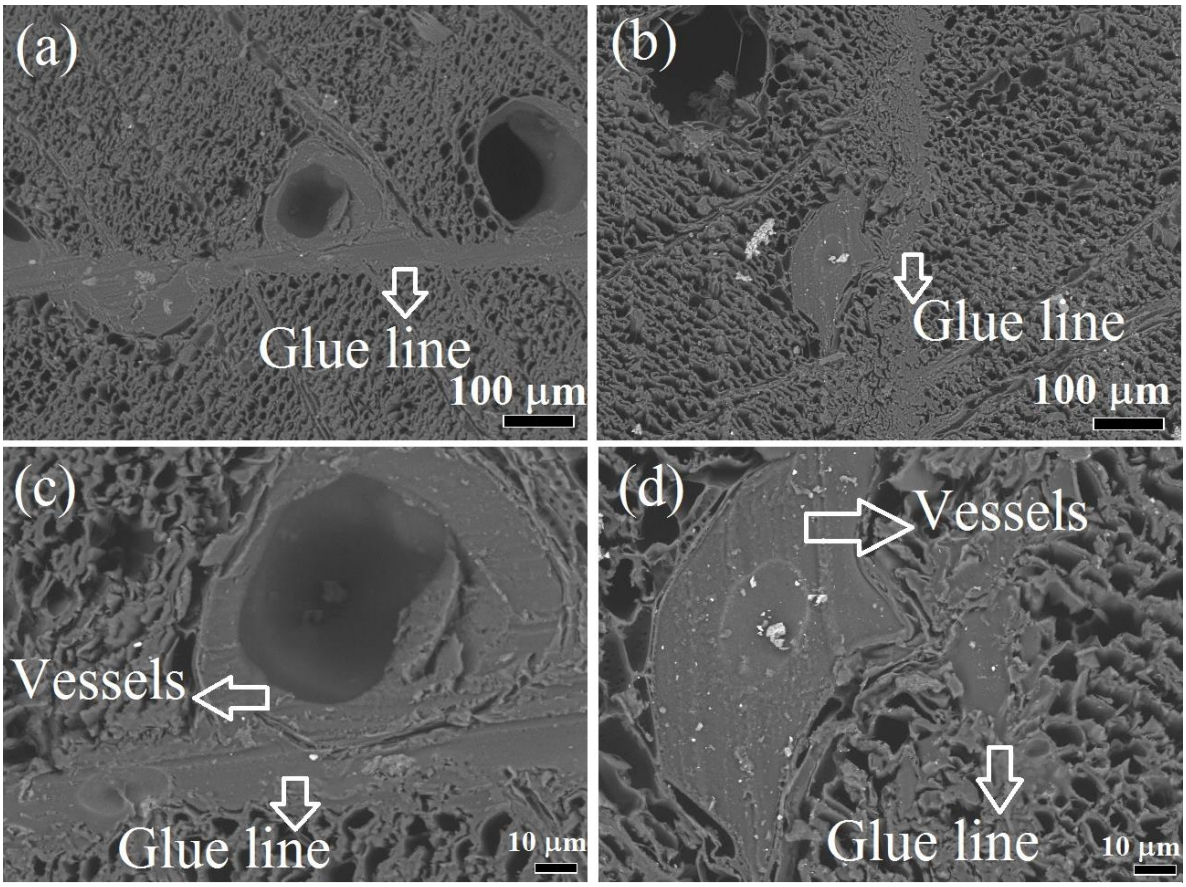

Figure 4 - Glue line in *Cedrela odorata* wood glued with PVAc-adhesive modified without nano-clay (a) and with nano-clay (b). Vessel of wood with PVAc-adhesive modified without nano-clay (c) and with nano-clay (d).

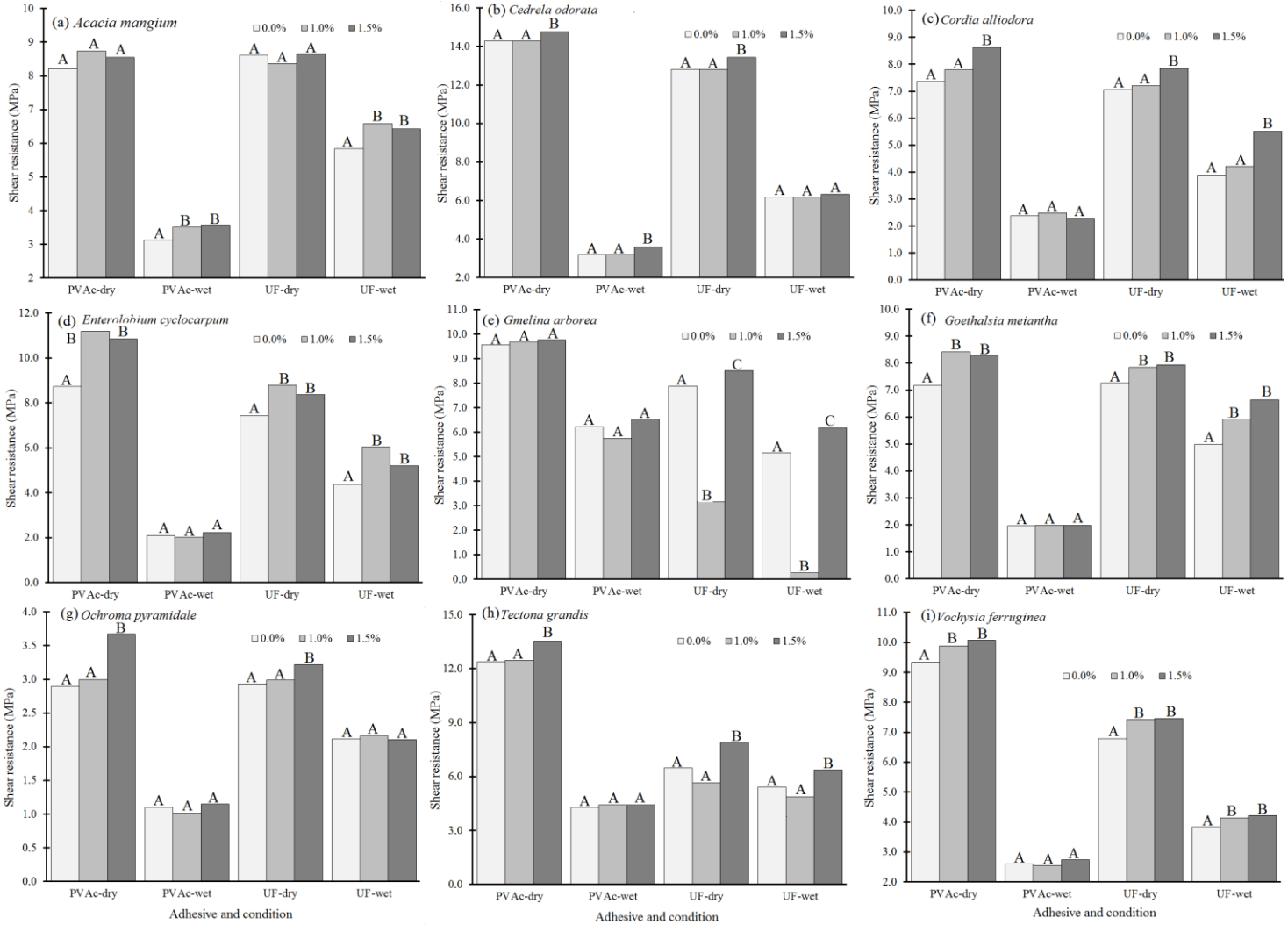

Figure 5 - Resistance of shear strength for dry and wet condition for ten tropical species glued with PVA and UF-adhesive with and without nano-clay

Table 1 Moisture content and failure area percentage in shear test of PVAc and UF-adhesives using different concentrations (weight/ weight) of nano-clay

Species	Nano-clay (wt.%)	Moisture content (%)				Failure area percentage			
		PVAc adhesive		UF adhesive		PVAc adhesive		UF adhesive	
		Dry	Wet	Dry	Wet	Dry	Wet	Dry	Wet
Acacia mangium	0.0	9.7^{A}	21.3^{A}	10.1^{A}	22.8^{A}	32.8^{A}	24.9^{A}	42.7^{A}	71.9^{A}
	1.0	9.7^{A}	20.4^{A}	11.1^{A}	22.6^{A}	31.7^{A}	32.6^{AB}	12.7^{B}	20.7^{B}
	1.5	10.2^{A}	20.7^{A}	10.8^{A}	20.5^{A}	25.5^{B}	38.1^{B}	10.7^{B}	47.3^{C}
Cedrela odorata	0.0	12.1^{A}	25.5^{A}	11.9^{A}	24.0^{A}	72.7^{A}	30.1^{A}	53.2^{A}	50.9^{A}
	1.0	12.7^{A}	25.5^{A}	11.7^{A}	24.9^{A}	25.5^{B}	33.7^{B}	53.3^{A}	65.8^{B}
	1.5	12.2^{A}	25.2^{A}	12.1^{A}	25.0^{A}	42.9^{C}	34.1^{B}	59.9^{B}	68.3^{B}
Cordia alliodora	0.0	10.2^{A}	32.3^{A}	10.7^{A}	29.2^{A}	100.0^{A}	16.8^{A}	100.0^{A}	92.0^{A}
	1.0	10.3^{A}	34.7^{B}	11.1^{A}	36.9^{B}	100.0^{A}	21.9^{B}	97.3^{A}	72.5^{B}
	1.5	9.8^{A}	31.6^{A}	10.2^{A}	34.8^{B}	97.7^{A}	29.4^{B}	100.0^{A}	63.1^{C}
Enterolobium cyclocarpum	0.0	9.4^{A}	30.9^{A}	8.9^{A}	30.3^{A}	95.8^{A}	2.6^{A}	1.1^{A}	7.7^{A}
	1.0	9.7^{A}	28.5^{A}	8.7^{A}	31.9^{A}	84.0^{B}	9.4^{B}	0.7^{A}	8.5^{A}
	1.5	10.2^{A}	28.2^{A}	8.6^{A}	30.2^{A}	90.3^{C}	12.0^{B}	7.8^{C}	11.4B
Gmelina arborea	0.0	9.6^{A}	17.9^{A}	9.0^{A}	22.5^{A}	25.8^{A}	8.8^{A}	53.9^{A}	35.8^{A}
	1.0	10.2^{A}	17.5^{A}	9.9^{A}	22.0^{A}	12.8^{B}	8.5^{A}	79.7^{B}	47.0^{B}
	1.5	9.4^{A}	17.0^{A}	10.1^{A}	23.0^{A}	13.0^{A}	7.6^{A}	79.7^{B}	50.6^{B}
Goethalsia meiantha	0.0	9.0^{A}	36.5^{A}	9.2^{A}	35.4^{A}	89.7^{A}	43.8^{A}	95.5^{A}	89.5^{A}
	1.0	8.7^{A}	37.0^{A}	8.9^{A}	36.8^{A}	94.5^{A}	50.2^{B}	91.3^{AB}	94.0^{B}
	1.5	9.4^{A}	37.8^{A}	9.9^{A}	34.7^{A}	92.4^{A}	50.1^{B}	87.0^{B}	98.5^{B}
Ochroma pyramidale	0.0	9.3^{A}	52.9^{A}	8.6^{A}	64.6^{A}	54.6^{AB}	33.8^{A}	61.9^{A}	27.6^{A}
	1.0	9.3^{A}	55.3^{A}	9.1^{A}	52.7^{B}	57.0^{A}	44.9^{B}	49.6^{B}	99.3^{B}
	1.5	9.0^{A}	54.9^{A}	10.0^{A}	53.7^{B}	52.7^{B}	41.0^{B}	37.0^{C}	88.3^{B}
Tectona grandis	0.0	10.6^{A}	21.2^{A}	9.6^{A}	21.4^{A}	82.1^{A}	4.8^{A}	21.4^{A}	14.8^{A}
	1.0	11.0^{A}	21.7^{A}	9.3^{A}	19.5^{A}	74.0^{B}	31.7^{B}	31.3^{B}	18.4^{B}
	1.5	10.6^{A}	23.2^{A}	9.6^{A}	22.0^{A}	64.4^{C}	28.0^{B}	32.2^{B}	26.6^{C}
Vochysia ferruginea	0.0	9.8^{A}	29.1^{A}	9.01^{A}	30.3^{A}	82.6^{A}	49.1^{A}	74.0^{A}	59.0^{A}
	1.0	9.7^{A}	28.4^{A}	9.97^{A}	30.5^{A}	51.8^{B}	51.6^{A}	82.7^{B}	74.0^{B}
	1.5	9.4^{A}	29.4^{A}	9.93^{A}	30.9^{A}	63.4^{C}	49.2^{A}	82.3^{B}	69.2^{C}

Legend: the letters next to this value indicates that the values are statistically different at a confidence level of 95%.

5. Artículo 5. Effects of adding Multiwall carbon-nanotubes (MWCNT) on performance of polyvinyl acetate (PVAc) and Urea-Fprmaldehyde (UF) adhesive in Costarican tropical timber species

Effects of adding multiwall carbon-nanotubes (MWCNT) **on performance of polyvinyl acetate (PVAc) and Urea-formaldehyde (UF) adhesives in *tropical timber species* in Costa Rica.**

Efecto de la adición de nanotubos de carbono (MWCNT)**, sobre el comportamiento de adhesivos para madera de tipo polivinilo acetato (PVAc) y urea-formaldehído en *especies tropicales de Costa Rica***

Abstract

In this work, multiwall carbon-nanotubes functionalized with hydroxyl groups (MWCNTs-OH) have been incorporated into polyvinyl acetate (PVAc) and urea-formaldehyde (UF) adhesives utilized in tropical wood gluing. The RAMAN spectroscopy, the Atomic Force Microscopy (AFM) and the Transmission Electron Microscopy (TEM) were used to describe the MWCNTs-OH. The adhesives were evaluated in three concentrations of MWCNTs-OH: 0% (control), 0.05 % and 0.1% (weight weight^{-1}). The evaluation included color, the distribution of MWCNT-OH by TEM and AFM, thermal stability and viscosity of the adhesives, and shear strength of the glue line (SS) for nine tropical woods. AFM and TEM confirmed interaction of MWCNT-OH with adhesives. The viscosity of the PVAc adhesive increases with added MWCNTs-OH. The incorporation of MWCNTs-OH in PVAc and UF resin produces wood adhesives with less brightness, less yellowness, and increased redness. The nanotubes in the adhesive improved the thermal stability of the composites, and increased the entropy factor and energy of activation in the kinetic decomposition of the resin. In relation to SS, MWCNTs-OH in any of the two concentrations had no significant effect in SS in dry condition in half of the species studied glued with PVAc adhesive, whereas for UF-adhesive, the SS and percentage of wood failure improved in most of the 9 species studied.

Keywords: Wood adhesives, nanotechnology, tropical species, multiwall carbon nanotubes, thermo-analysis.

Introduction

Adhesives play an important role in the wood industry; 75% of the products manufactured with this material are joined together by means of adhesives (Pizzi y Mittal, 2011); among those products are composites like plywood, fiberboards and OSB (Kaboorani et al., 2013, Stoeckel et al., 2013). The employment of adhesives has also facilitated wood utilization to make good quality products (Zhao et al., 2011). Due to their importance, production of new or enhanced adhesives has incentivized the search for new methods to increase added value in the applications (Pizzi and Mittal, 2011).

Application of nanotechnology to adhesive manufacturing allows the development of new characteristics and properties in these polymers that increase their performance (Roussak and Gesser, 2013; Kaboorani et al., 2013). Nanoclay, aluminum oxide nanoparticles, cellulose nanocrystals, zinc oxide nanoparticles and carbon nanotubes are among the nanofillers utilized to enhance adhesives (Mohan et al,. 2013).

The unique properties of carbon nanotubes have attracted great interest since its discovery in 1991. Carbon nanotubes can be used to store fuel such as hydrogen; for new compound materials; in catalytic applications, among others (Yudianti et al., 2001). Carbon nanotubes are graphene tubular structures that may be composed of a single layer (single-wall carbon nanotubes, SWNTs) or several concentric layers (multi-wall carbon nanotubes, MWCNTs) (Fraczek, 2008).

Despite the versatility of carbon nanotubes, dispersion into different polymer matrices has posed a challenge since it is composed only of carbon. However, a number of techniques have been developed to achieve compatibility of the nanotubes with other materials. One of these techniques consists of performing chemical modification of the nanotube surface, by adding functional groups such as hydroxyl (–OH) or carboxyl groups (-COOH), when polar polymer matrixes are to be used (Yudianti et al., 2001).

Numerous studies have shown that adding carbon nanotubes to different polymer matrices improves the properties of materials. For example, Du et al. (2003) showed improvement of the modulus of elasticity, electrical conductivity, and thermal stability of

poly (methyl methacrylate) matrix resins, by adding single-wall carbon nanotubes. Similarly, Ghasemi et al. (2012), showed improvement of the morphological and mechanical properties of foams based on poly(vinyl chloride)/wood flour with the dispersion of functionalized MWCNTs. Likewise, Fu et al. (2010) concluded that adding carbon nanotubes to polypropylene/wood flour composites increases the thermal stability of these materials according to the concentration of the nanotubes, confirming that the use of nanotubes as nanofillers in polymers modifies and improves the properties of the latter.

Thus, the present work aims at showing the performance of two adhesive types —polyvinyl acetate (PVAc) and urea-formaldehyde (UF)— with added multiwall carbon nanotubes functionalized with –OH groups in two concentrations (0.05% and 0,1%, w/w) as nanofiller and the effect of this nanofiller on shear resistance (effort and percentage of wood failure) of the glue line in nine (9) tropical species: *Acacia mangium, Cedrela odorata, Cordia alliodora, Enterolobium cyclocarpum, Gmelina arborea, Goethalsia meiantha, Ochroma pyramidale, Tectona grandis and Vochysia ferrugia*. In addition to presenting the resistance values, this study aims at characterizing the MWCNTs-OH, and observe the color change of the adhesives, the variation of viscosity, thermal stability, entropy factor and activation energy in the decomposition kinetics, the shear strength of the glue line and the percentage of wood failure.

Materials and methods

Materials

Multiwall carbon nanotubes functionalized with hydroxyl groups (MWCNTs-OH) were used, provided by Cheap Tubes Inc. (Cambridgeport, USA). In addition, multiwall carbon not-functionalized nanotubes from the same company were used to compare functionalization of nanotubes in RAMAN. Information provided by the manufacturer of both products indicates an external diameter of approximately 50 nm, 10-20 µm long, 95% pureness and –OH groups concentration ranging from 0.5-1.0% in weight.

Two types of wood adhesives were employed: the water based polyvinyl acetate (PVAc) Resistol M.R. 850®, produced by Henkel Capital S.A (http://www.resistol.com.mx/es.html). The technical description of the product indicates that the resin is polyvinyl acetate and water, presenting 54.5-55.5% solid content and 1600-2200 cPs viscosity. The second type is water based urea-formaldehyde adhesive (UF) of the commercial brand Resina CR-560 U-F, manufactured by Química Centroamericana, Quibor, S.A. (http://www.agroquibor.com). This is a three-component *in situ*-prepared adhesive: resin, wheat flour, and catalyst of sulphate type, with weight proportions of 41%, 24.8% and 0.32%, respectively, plus 34% water. The technical description indicates that the product presents 64-65% solid content and 650-900 cPs viscosity.

The species utilized to test the modified adhesive were *Acacia mangium, Cedrela odorata, Cordia alliodora, Enterolobium cyclocarpum, Gmelina arborea, Goethalsia meiantha, Ochroma pyramidale, Tectona grandis* and *Vochysia ferrugia*, all of them woods traditionally used in Costa Rica to manufacture doors and other wood products, or products for engineering that demand intensive use of adhesives (Diener and Saklad, 1997). Some of these species have shown gluing problems (Chahud, et al., 2009). The woods were obtained at different lumber stores.

MWCNTs-OH characterization

The structure of the MWCNTs-OH was evaluated by means of the RAMAN spectra and the Thermogravimetric analyzer. The Raman spectra of the nanotubes were collected on a DXR Raman Microscope Thermo Scientific, the samples were excited at 532 nm from the laser line and 2.5 mW power, with a spectrograph aperture of 25 µm pinhole. Next, the analysis of the variation in the intensities of the bands characteristic in MWCNTs-OH (D, G and G') is carried out. Measurements of TGA were carried out using 10-12 mg of MWCNTs and MWCNTs-OH in order to determine the thermal stability, at a heating rate of 50 °C/min in a nitrogen atmosphere reaching a temperature of 800 °C in 35 minutes. A Thermogravimetric Analyzer model TGA 5000, brand Instrument NBr was used. In order to avoid unwanted oxidation, TGA measurements were conducted with the composite placed in high quality nitrogen (99.5% nitrogen and 0.5% oxygen content) atmosphere.

Spectra obtained with the RAMAN and the curves in the TGA of the MWCNT-OH were compared with the spectra of the MWCNTs without functionalizing.

Preparation of adhesive with MWCNTs-OH

The two types of adhesives (PVAc and UF) were added MWCNTs-OH in three concentrations: 0% (control), 0.05 % and 0.1% (weight weight^{-1}). The addition of the MWCNTs-OH to the adhesive was carried out in two stages. Firstly, the weight of the MWCNTs-OH necessary to prepare the 0.05% and 0.1% concentrations in the adhesives was calculated. Then, the nanotubes were dispersed in a volume of water (5% weight weight^{-1} with respect to the PVAc adhesive) by sonication (dispersion A), following the method proposed by Khan et al. (2012). The second stage consisted of mixing the aqueous dispersion of functionalized nanotubes in the PVAc, which was performed mechanically. In the case of the UF-adhesive, it differs from the PVAc: firstly, the mass of nanotubes corresponding to concentrations 0.05% and 1% was sonicated in the volume of water to be added in the preparation of the adhesive (54% w/w water). Following, the weight of the resin and of the other components was calculated according to the proportions indicated and then mixed.

Sonication of the MWCNTs-OH in water was performed at an amplitude of 75% for 30 minutes, at intervals of 45 seconds with 15-second breaks. For sonication the equipment Ultrasonic processor model CV18 was used. To add the dispersion A into the PVAc adhesive and the MWCNTs-OH mixture into the UF resin, both mixtures were stirred at 1600 rpm with the aid of four 45°-inclined blade impeller for 15 minutes. During that time, the nanotube dispersion was added slowly to attain a homogeneous mixture.

Characterization of the adhesive

First, the MWCNTs-OH were observed in the adhesive. For this, samples were observed by means of the transmission electron microscope (TEM) and the atomic force microscope (AFM). Later, the two types of adhesives (PVAc and UF) in both concentrations of MWCNTs-OH (0.05% and 0.1%) and the respective controls, were

evaluated for viscosity, color and thermal behavior by means of thermogravimetric analyzes (TGA).

TEM images were obtained using a Jeol JEM 2100F TEM. These images were taken with a bean current of 52 µm at 100 kV. The AFM observations performed in the wood adhesive were carried out using a NanoScope V, an atomic force microscope (model Asylum Research model MFP 3D), fitted with a Hybrid XYZ scanner. Atomic force microscope measurements were done under ambient air conditions in tapping mode. The sensitivity of the tip deviation and the scanner resolution was 0.3 nm. The resolution was set to 250 lines by 256 pixels for all observations.

Measurement of viscosity was performed using a 600 mL Low Form Griffin Beaker using 500 mL of the adhesives in the Brokfield-11+ Pro LV. 2.4.4 viscometer, according to the ASTM D2256-11 standard (ASTM, 2011). The spindler number 4 for the PVAc adhesives and the spindler number 3 for the UF adhesives were used during the measurements.

As for color, a film sample (3 cm wide x 10 cm long x 2 mm thick) was prepared on glass with each adhesive. Once the film was dry (approximately 72 hours later), its color was measured. Color measurement of the MWCNTs-OH in solid condition was also performed, for which purpose powder samples of the MWCNTs-OH were used. A Hunter Lab, Scan XE Plus mini model spectrophotometer was used to obtain the L*, a* and b* parameters. The conditions for color measurement are detailed in Moya et al. (2015). The index of color difference (ΔE*), according to the ASTM D2244 standard (ASTM, 2014), was used to compare color parameters between adhesives with different concentrations of MWCNTs-OH. This index defines the color difference magnitude between two adhesives using CIELab's color systems according to equation 1. This index was calculated using the average color values for all samples from each adhesive.

$$\Delta E^* = \sqrt{(\Delta L^*)^2 + (\Delta a^*)^2 + (\Delta b^*)^2} \qquad \text{(Equation 1)}$$

Where: $\Delta L^* = L^{*M} - L^{*P}$, $\Delta a^* = a^{*M} - a^{*P}$, $\Delta b^* = b^{*M} - b^{*P}$, M = Average value for adhesive

without MWCNTs-OH and P = Average value for adhesive with MWCNTs-OH.

The thermal stability was analyzed for the two types of adhesives with the 3 concentrations. Measurements of TGA were carried out using 10-12 mg of each adhesive in each concentration, at a heating rate of 50 °C/min in a nitrogen atmosphere reaching a temperature of 800 °C in 35 minutes. A Thermogravimetric Analyzer model TGA 5000, Instrument NBr brand, was used. TGA measurement conditions are detailed in Moya et al. (2015). Two decomposition reactions were identified in the case of PVAc; in the case of UF only the second reaction was analyzed because the first one corresponds to water elimination.

For each reaction, the temperature and the remnant mass at the start of the decomposition, at the maximum reaction point and at the end of the reaction, were identified. Then kinetics was calculated for each reaction (Equation 2) by means of lineation (Equation 3), according to Vyazovkin and Sbirrazzuoli (2006), where the differential isoconversional method of Friedman is utilized.

$$K = K_0 * e^{(\frac{-E}{RT})} \qquad \text{(Equation 2)}$$

$$\ln\left(\frac{d\alpha}{dt}\right) = lnK_0 + \left(\frac{-E}{RT}\right) + nln(1-\alpha) \qquad \text{(Equation 3)}$$

Where: α: degraded mass, dα/dt: percentage of the degraded sample in unite time, K_0: entropy factor, E: energy of activation, T: temperature, R: Gas constant.

Bond strength resistance

Shear strength of glue line (SS) of PVAc and UF adhesives modified with MWCNTs-OH in both concentrations was evaluated by the shear test according to the ASTM D-905-98 (ASTM, 2013a) standard. The adhesive containing MWCNTs-OH was applied to *Acacia mangium*, *Cedrela odorata*, *Cordia alliodora*, *Enterolobium cyclocarpum*, *Gmelina arborea*, *Goethalsia meiantha*, *Ochroma pyramidale*, *Tectona grandis* and *Vochysia ferrugia*. A total of 90 shear samples were prepared, using 3 concentrations of MWCNTs-

OH (0.00, 0.05 and 0.10%), with 30 samples for each concentration. During preparation, the wood samples were stabilized at 12% moisture content for one week. The adhesive was applied according to the manufacturer's specifications, i.e., an amount of 100 g m^{-2} in both types of adhesive. After applying glue on the surface of the wood, the samples were pressed in a hydraulic machine at 2.0 kg cm^{-2} pressure, maintaining the pressure for 24 hours. After pressure application, glued samples were conditioned to 20 °C and 60% relative humidity for two weeks. Then 30 samples were extracted from the glued samples and tested for each set of formulation. The evaluation of shear resistance was measured in dry and wet condition. The Tinus Olsen hydraulic test machine with 10 kN capacity was used for load application and the data were entered into a computer. The percentage of wood failure and maximum load were recorded for each test. The block shear tests were carried out according to the ASTM D905-98 (ASTM, 2013a) standard. The sizes of samples for ''wet condition'' were the same as "dry condition tests". For ''wet condition'', the samples were taken directly out of the water after being immersed in water for 24 h. Before the tests, excess water was wiped off from the samples. During the water immersion period, temperature of water was maintained at 20 °C. After each sample was tested in the compression test, the percentage of wood failure was evaluated according to the ASTM D-5266-13 standard (ASTM, 2013b).

Analysis of the information

Compliance of the determined variables with the assumptions of normal distribution, homogeneity of the variances, and with the presence of extreme data, was verified. Following, a variance analysis was applied to verify the effect of adhesion of the MWCNTs-OH concentration (0%, 0.05% and 0.1%) on viscosity, values of entropy factor, activation energy, function of decomposition, and temperature and remnant mass in different reactions of kinetics of decomposition and shear strength of the wood. The Tukey test at 99% confidence level was established to determine the statistical difference between the means.

Results and discussion

MWCNT characterization

Figure 1a shows the comparison between the MWCNT and MWCNTs-OH. As expected, the bands D, G and G' were detected in both types of nanotubes. However, a difference in the RAMAN intensity of the functionalized nanotubes in the three bands was observed. In band D, located close to 1350 cm^{-1}, the increase in the intensity represents a ringbreathing mode from sp^2 carbon rings and indicates the presence of some disorder in the graphene structure in the nanotubes, attributed to other forms of carbon that contaminate the sample, to defects in the walls of the nanotubes or heteroatoms added to the structure of the nanotubes (Hodkiewicz, 2010, Lonkar et al., 2012). Meanwhile, Datsyuk et al.(2008) mention that increases in the intensities of band G, located after 1500 cm^{-1}, and band G', are produced by in-plane stretching of carbon-carbon bonds in the graphene sheets; they also point out disorders and defects of the carbon nanotubes. The above results showed that MWCNTs-OH presented an increment in all the bands with respect to MWCNT, and increased defects in the walls of the nanotubes, probably due to the presence of –OH groups added to multiwall nanotubes (Hodkiewicz, 2010, Lonkar et al., 2012).

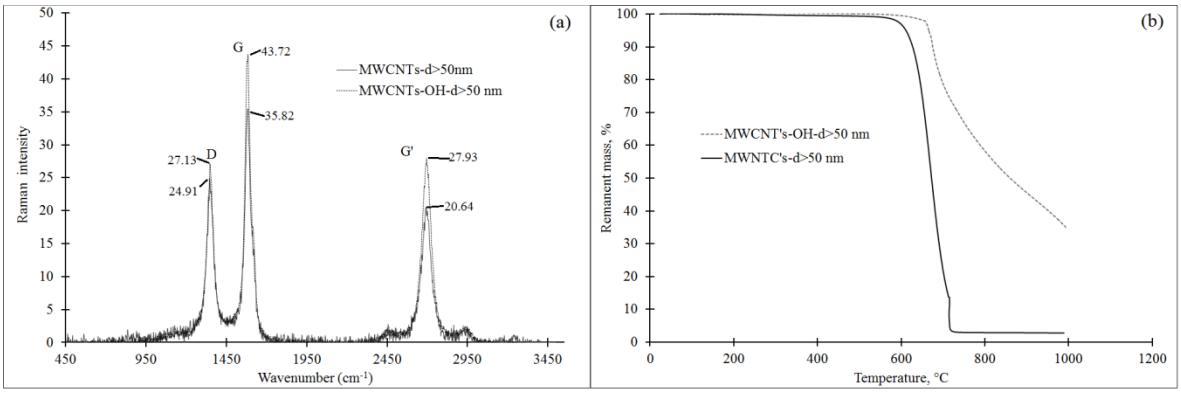

Figure 1. Raman spectra (532nm excitation) (a) and TGA (b) of MWCNTs and MWCNTs-OH.

The evaluation of the thermal stability measured by TGA shows a difference between MWCNTs-OH and MWCNTs. For MWCNT, maximum decomposition occurs close to 660 °C, while for MWCNTs-OH, decomposition is slower, around 700 °C (Figure 1b). The difference in the thermal stability in the MWCNTs-OH can be linked to the temperatures of synthesis of the nanotubes, or to the presence of defect sites along the walls and at the ends of the nanotubes (Peng et al., 2006). This result confirms the findings in the RAMAN spectra relative to modification of MWCNTs-OH.

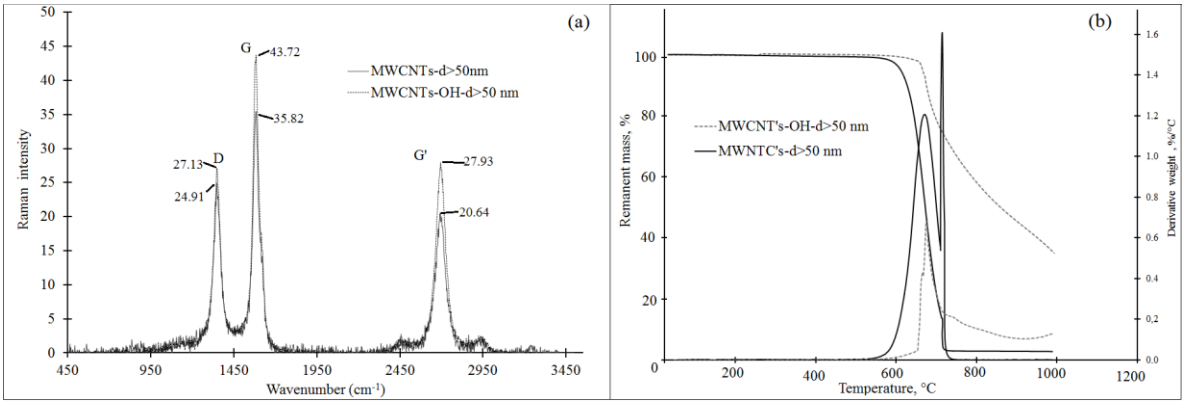

The evaluation of the thermal stability measured by TGA shows a difference between MWCNTs-OH and MWCNTs (Figure 1b). Two oxidations are observed in MWCNTs: the first one presented at 671 °C and the second one occurred at 714 ° C; with a residual mass of 2.82%. For MWCNTs-OH, the maximum decomposition temperature occurred at 675 °C and residual mass was 35% (Figure 1b). It is also observed that the initial decomposition temperatures differ for both CNT, in MWCNTs was approximately 597 °C and for MWCNTs-OH was 659 °C.

The temperature ranges observed agree with other report of MWCNTs, which reports a range of 600 °C to 750 °C (Yudianti *et al.* 2011, Lehman *et al.* 2011, Osswald *et al.* 2007). The small differences observed in this temperature and in decomposition temperatures can be linked to the temperatures of synthesis of the nanotubes, to the presence of defect sites along the walls and at the ends of the nanotubes, the number of walls in MWCNTs and the presence of the catalyst composition and the presence of other materials in the sample (Sun *et al*. 2002, Hui-Wang and Guan-Ben 2011). The crystallinity of the nanotubes gives great stability and increases the resistance they present to oxidation;

when subjected to a functionalization process, nanotubes change their size, they may lose some layers and increase the number of defects (Yudianti *et al.* 2011, Lehman *et al.* 2011). This characteristics implies a loss in the crystallinity and therefore the resistance oxidation, this should be reflected in a decrease in the maximum temperature of decomposition (Osswald *et al.* 2007, Yudianti *et al.* 2011, Sun *et al*. 2002, Peng and Liu 2006). However, this behavior of MWCNTs-OH does not agree with expected. This difference could be due to two samples don't belong to the same batch and the number of walls before functionalization differs with the MWCNTs used for this comparison.

Regarding the peak at 714 ° C in the MWCNTs and lightly observed in MWCNTs-OH can be associated to material purity and associated with the presence of other types of complex materials such as fullerenes (Lehman *et al.* 2011, Peng and Liu 2006). Similarly, the difference between the residual masses (MWCNTs: 2.82%; MWCNTs-OH: 35%) may be associated with the metal type used for catalysis in the synthesis process as well as oxidation products of that catalyst. This reflects a difference in the quality and homogeneity between both materials Lehman et al. (Lehman *et al.* 2011)

Adhesive characterization

TEM and AFM

Figures 2a and 2b show MWCNT-OH TEM images where the dimensions and irregularities of the external wall of the nanotubes can be observed. Figure 2c reveals the interaction of the MWCNT-OH with the PVAc; the MWCNT-OH has a tubular structure while the PVAc can be perceived as spherical particles (Hui-Wang et al., 2011), with diameters ranging between 35.0 and 45.0 nm. Figure 2d, meanwhile, shows the corresponding AFM image of the PVAc-MWCNTs-OH film, where zones of high and low rugosity can be observed. High rugosity zones could be associated to presence of MWCNT-OH, while low rugosity areas could be linked to PVAc particles (Kaboorani et al., 2013), which tend to be more homogeneous in shape and rugosity, thus coinciding with the observations from the TEM.

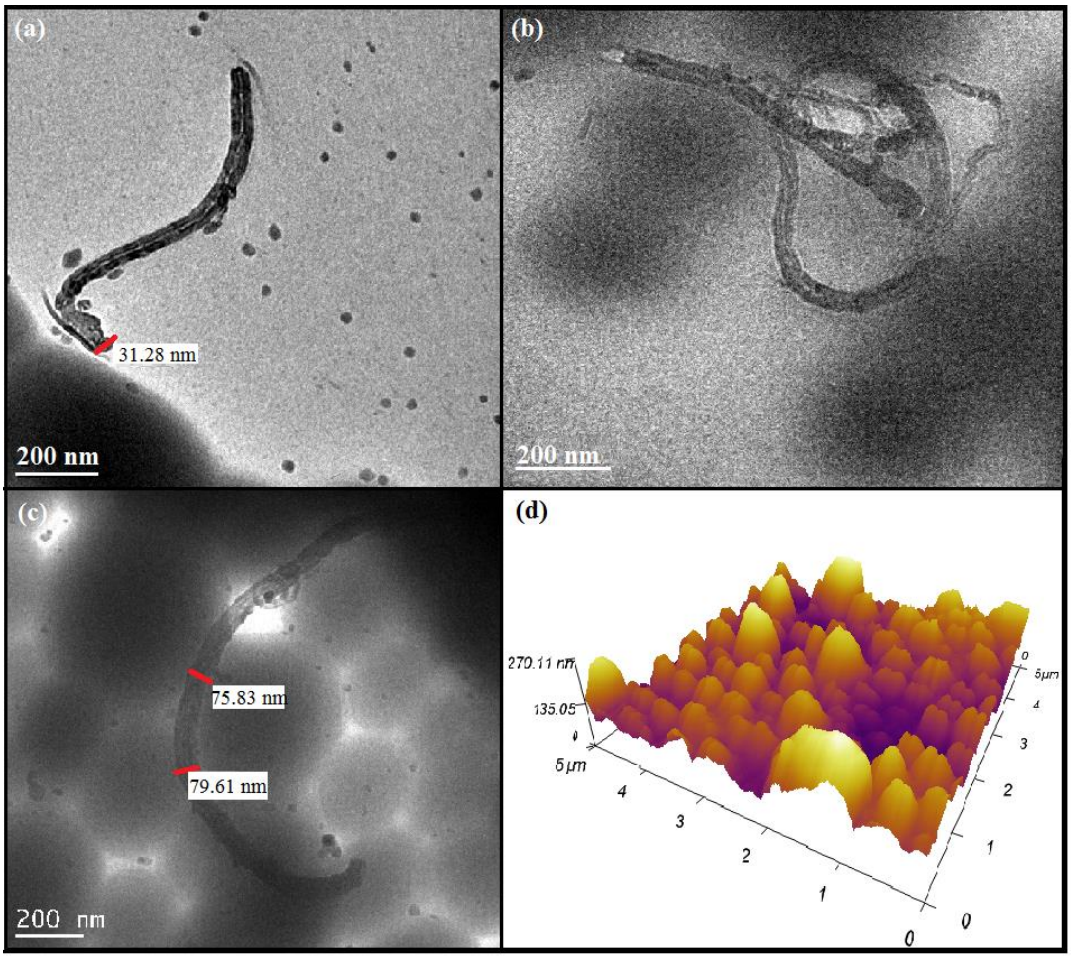

Figure 2. TEM micrographs (a), (b), (c) and AFM photo (d) of MWCNTs-OH/PVAc films

Viscosity

Viscosity decreases as the rotational speed increases in both types of adhesives and the 3 concentrations of MWCNT-OH (Figure 3). This behavior is known as "shear-thinning", which is characteristic of pseudoplastic fluids (Barnes et al., 1989). For PVAc adhesives, viscosity is greater when MWCNTs-OH are added, and greater at 0.05% concentration than at 0.1% concentration (Figure 3a). This behavior was not observed for the UF adhesive. No differences in viscosity were observed between the adhesive without MWCNT-OH and the adhesive with 0.05% concentration at low rotational speeds, as opposed to high speeds

where differences are evidenced. Meanwhile, there was difference between the adhesive without MWCNT-OH at 0.1% and 0.05% concentrations (Figure 3b).

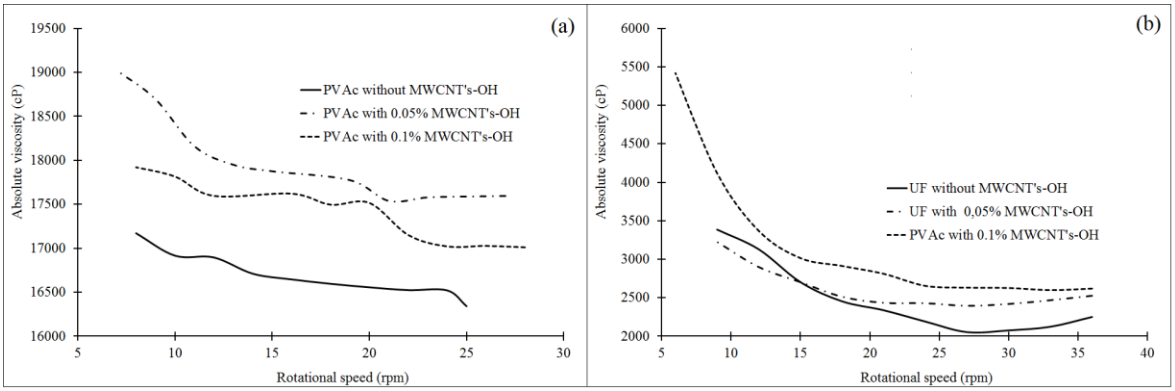

Figure 3. (a) Absolute Viscosity of PVAc with MWCNTs-OH at 22.5 ±0.5 °C and (b) Absolute Viscosity of UF with MWCNTs-OH at 21.8 ±0.5 °C

The increase in viscosity with increasing amount of added MWCNT-OH, especially the UF-adhesive, coincides with observations made by Pötschke et al. (2002) and Du et al. (2003) in polymers with MWCNT-OH. However, the behavior found in the concentrations of the PVAc adhesive (greater viscosity at 0.05% concentration relative to 0.1% concentration) could be associated to the fact that the mixture between the PVAc and MWCNT-OH at 0.1% concentration was not satisfactorily homogeneous (Sherman, 1994).

2.2 Color

Relative to color parameters of the different adhesives with different proportions of MWCNTs-OH, luminosity (L*) and yellowness (b*) for both adhesives decreased statistically, whereas redness (a*) increases with added MWCNTs-OH (Table 1). However, the change in L* differed in each resin: no differences were observed in PVAc with the proportions 0.05% and 0.1%. Parameter a* (redness) increases in PVAc adhesive, while diminishing in UF adhesive. On the other hand, color change (ΔE*) varied from 24.88 to 25.50 in the PVAc adhesive and from 26.67 to 28.53 in the UF adhesive as the amount of added MWCNT-OH increases (Table 1)

Table 1. Viscosity and color of the adhesive modified with MWCT's-OH

Adhesive	Concentration (%)	L* color parameter	a* color parameter	b* color parameter	ΔE*
MWCNTs-OH	-	1.08	0.27	0.34	-
PVAc	0.00	37.40A	-3.30A	-2.06A	-
	0.05	12.75B	-0.24B	-0.68B	24.88
	0.10	12.13B	0.06C	-1.80C	25.50
UF	0.00	39.90A	7.76A	14.46A	-
	0.05	17.90B	0.15B	1.45B	26.67
	0.10	15.90C	0.44C	0.88C	28.53

According to the above results the addition of MWCNTs-OH tends to noticeably change the color parameters in both adhesives used, producing ΔE* values above 12 (Gonnet, 1993). This variation can be explained by the fact that unmixed MWCNTs-OH show values of L*, a* and b* close to zero, distinctive of black. When adding the MWCNTs-OH to both resins, a suspension instead of a mixture is created, producing change in the tonality of the adhesive from white (Figure 4a) to gray (Figure 4b).

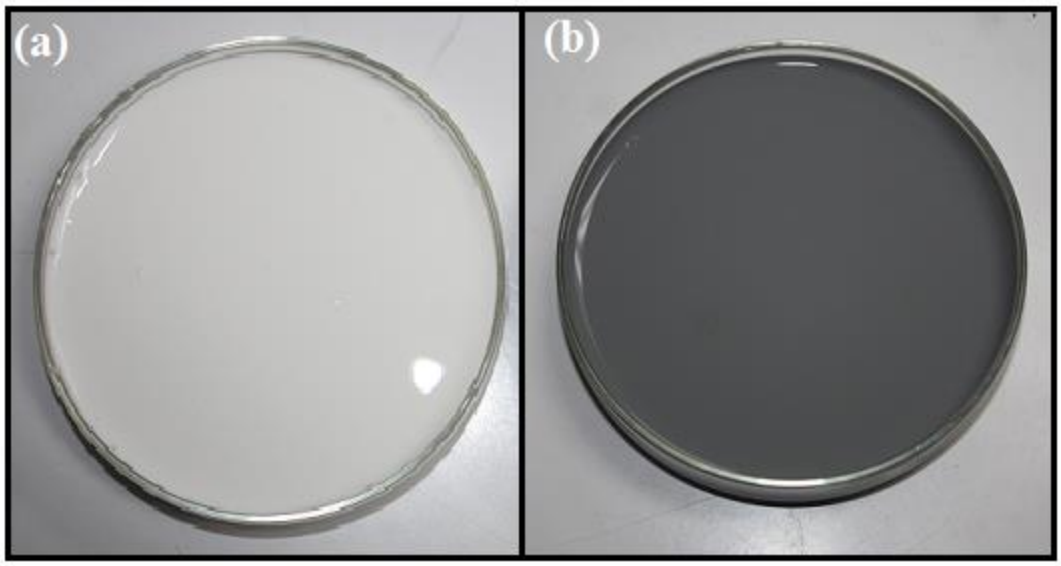

Figure 4. (a) PVAc sample without MWCNTs-OH and (b) PVAc with MWCNTs-OH showing color change.

2.3 Thermal stability of the adhesive

TGA analysis of the PVAc modified with and without MWCNTs-OH (0.05% w/w, 0.1% w/w) show two inflexions (Figure 5a). These inflexions are related to chemical reactions of decomposition that occur in each adhesive (Kaboorani and Riedl, 2011). The first inflexion in PAVc adhesive, around 310 °C, corresponds to the greatest weight loss and to structural decomposition of the adhesive, which according to McNeill et al. (1995) is linked to decomposition of acetic acid. The second inflexion, close to 430 °C (Figure 4a), could be the result of decomposition of organic additives utilized in the formulation of the PVAc emulsion (Matoso, 2008; McNeill et al. 1995). Regarding the UF adhesive (Figure 4b), small inflexion occurs before reaching 100 °C, which is linked to loss of water contained in the UF adhesive (Samaržija-Jovanoviĉ et al., 2011). A second decomposition within the range of temperature of 235 °C and 262 °C, is also observed, resulting mainly from resin degradation. As a result, a series of components are liberated: methylene, methylol, dimethylene ethers, methylene methyl ethers, methylene glycols (formaldehyde), components with carbonyl groups and triazine, among others (Siimer et al., 2003).

The values of temperature and remnant mass at each inflexion where decomposition of each adhesive starts (Figures 4c and 4d) indicate that there is slight difference between the PAVc adhesive with MWCNTs-OH and without MWCNTs-OH in the first and second decomposition. In the first decomposition, the temperature (initial, peak maximum and final point) presents no variation, but the remnant mass in those points is higher in adhesives containing MWCNTs-OH. A slight increase is observed with increasing concentration (Table 2). In the second reaction of the PVAc adhesive with and without MWCNTs-OH, little difference is again observed with the different temperatures. However, for remnant mass differences can be observed. The PVAc adhesive without MWCNTs-OH and the PVAc adhesive with 0.1% concentration of MWCNTs-OH presented differences in the remnant mass relative to the adhesive with 0.05% concentration of MWCNTs-OH.

The addition of any of the two concentrations of MWCNTs-OH to the UF adhesive produces noticeable alteration in temperature and increase of the remnant mass in reaction 2, with the exception of the remnant mass at the initial point (Table 2). Furthermore, no

differences were found in the various parameters evaluated for adhesives with 0.05% and 0.1% concentration of MWCNTs-OH (Table 2).

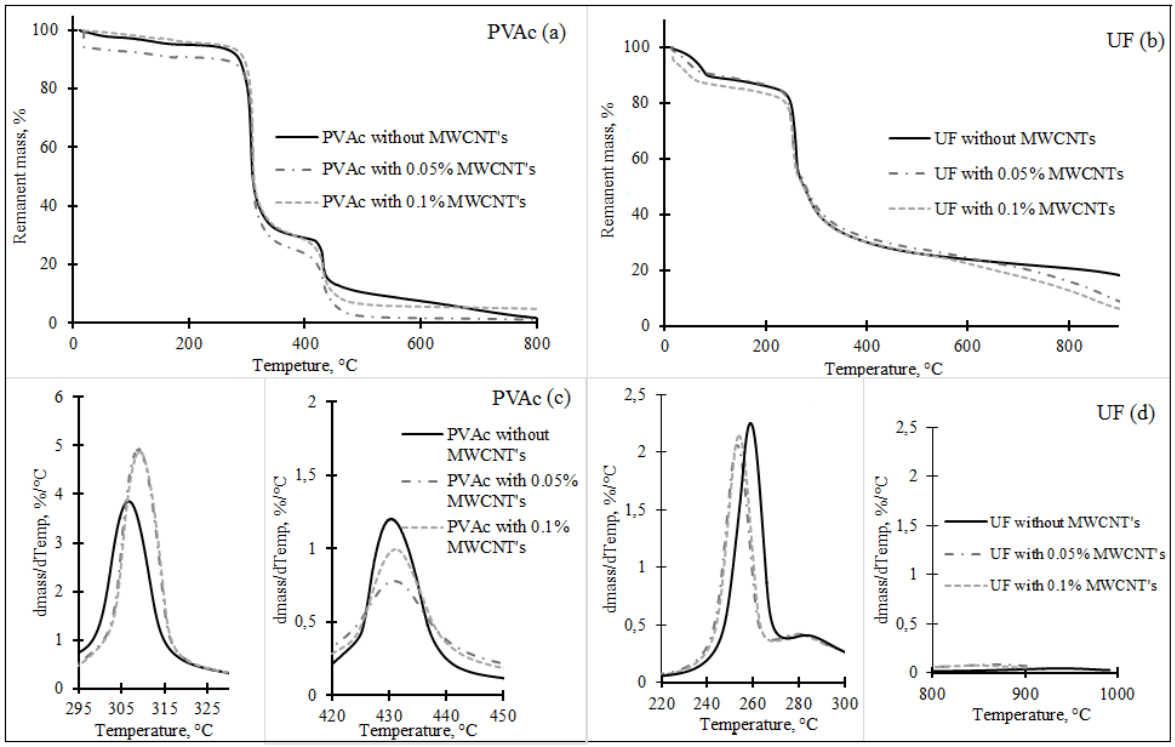

Figure 5. TGA (a, b) and DTG of the different reaction (c, d) curves of PVAc and UF wood adhesives adding different concentrations of MWCNTs-OH; measured under N_2 atmosphere with a heating rate of 50 °C/min.

Table 2. Temperature and remnant mass in different reactions of decomposition kinetics of PVAc and UF adhesives adding different concentrations (weight weight^{-1}) of MWCNTs-OH.

Adhesive	MWCNTs-OH concentration (%)	Reaction 1						Reaction 2						Ash content at 900 °C (%)
		Initial point		Peak maximum		Final point		Initial point		Peak maximum		Final point		
		Temp (°C)	RM (%)	Temp (°C)	RM (%)	Temp (°C)	RM (%)	Temp (°C)	RM (%)	Temp (°C)	RM (%)	Temp (°C)	RM (%)	
PVAc	0.00	298	85.36	309	64.50	315	44.34	414	27.63	431	21.71	450	12.47	0.97
	0.05	298	86.32	308	65.20	316	41.50	415	24.66	431	17.46	450	8.99	3.53
	0.10	298	87.57	309	66.73	315	43.80	415	26.59	422	19.28	449	10.40	4.40
UF	0.00	-	-	-	-	-	-	237	81.34	258	66.83	246	53.80	6.54
	0.05	-	-	-	-	-	-	243	81.57	253	69.60	262	57.59	10.10
	0.10	-	-	-	-	-	-	245	79.45	254	67.80	262	55.98	11.63

Temp: temperature, RM: Remnant mass.

The analysis of the apparent combustion kinetics modelling of both types of adhesives with the different concentrations of MWCNTs-OH (Table 3), showed that the activation energy in the adhesive without MWCNTs-OH is lower than in the adhesive with concentrations of MWCNTs-OH at 0.05% and 0.1%, increasing as the concentration of MWCNTs-OH increases (Table 3). Moreover, differences were found between the entropy factor of the combustion kinetics in the different reactions of the adhesives. The entropy factor was statistically higher in the PVAc adhesive with MWCNTs-OH in the first reaction, while the degree of the decomposition function tends to be stable for the three adhesives. Meanwhile, the entropy factor increases again with increasing concentration of MWCNTs-OH (0.05 % and 0.1%) added to the UF adhesive, as occurs with the activation energy and the degree of the decomposition function (Table 3).

As regards to the final ash content an increase was observed as concentration of MWCNTs-OH in the adhesives increased, which is attributed to the presence of MWCNTs-OH at finalization of the decomposition of the adhesive (Table 2).

Table 3. Values of entropy factor, activation energy, degree of the function of decomposition and correlation coefficient of kinetics of decomposition of PVAc and UF adhesives adding different concentrations of MWCNTs-OH.

Adhesive	Reaction	MWCNTs concentration (%)	Entropy factor (K_0 in S^{-1})	Activation energy (E in kJ mol^{-1})	Degree of the function of decomposition (n)	Correlation coefficient (R)
PVAc	First	0.00	$^{A}4.33 \times 10^{15}$	$^{A}189.34$	$^{A}2.0$	0.77
		0.05	$^{B}5.35 \times 10^{16}$	$^{B}204.67$	$^{A}2.1$	0.83
		0.10	$^{C}6.53 \times 10^{18}$	$^{C}227.28$	$^{A}2.3$	0.82
	Second	0.00	$^{A}6.76 \times 10^{37}$	$^{A}403.94$	$^{A}4.6$	0.75
		0.05	$^{B}4.38 \times 10^{20}$	$^{B}232.27$	$^{B}2.3$	0.83
		0.10	$^{C}6.69 \times 10^{23}$	$^{C}323.01$	$^{B}2.9$	0.71
UF		0.00	$^{A}2.03 \times 10^{23}$	$^{A}237.6$	$^{A}6.83$	0.98

	0.05	$^{B}2.72 \times 10^{33}$	$^{B}333.16$	$^{B}9.7$	0.95
	0.10	$^{C}1.01 \times 10^{41}$	$^{C}414.63$	$^{B}10.8$	0.96

TGA spectra (Figure 4a and 4b) showed that addition of MWCNTs-OH caused no modification in the decomposition reaction of any of the two types of adhesives evaluated, although modification of the thermal stability is observed (Table 3), which is due to increased activation energy and maximum temperature (Table 2). The same behavior was observed by Du et al. (2003) and Fu et al. (2010), although these authors added single-wall carbon nanotubes (SWCNs). According to Fu et al. (2010) thermal stability could be attributed to the barrier effects and radical-trapping effects of CNTs.

Wood penetration

Likewise, it is important to mention that, despite the increased viscosity of the glue (Figure 3), no significant effects in the penetration of the adhesive into the region near the glue line (Figure 6) are observed. Moreover, it was observed that the glue line area of *Vochysia guatemalensis* wood glued with PVAc adhesive modified with MWCNTs-OH was similar to wood glued with the unmodified adhesive (Figures 6a and 6b, respectively). Even for vessels near the glue line, penetration of the adhesive was observed in both modified and unmodified.

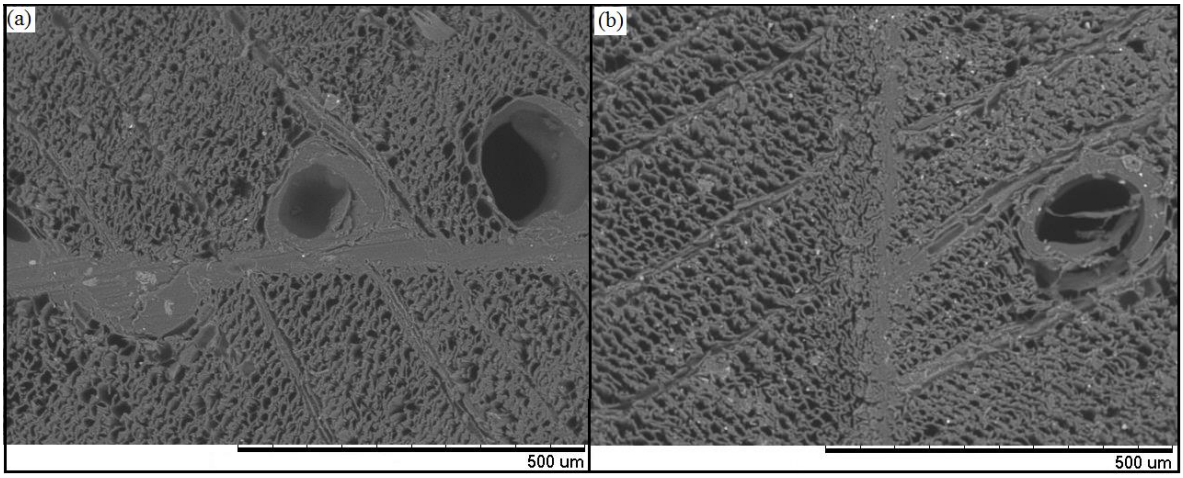

Figure 6. (a) Glue line in *Vochysia guatemalensis* wood glued with PVAc adhesive without (a) and with MWCNTs-OH (b).

Bond shear resistance

The results showed that adding MWCNTs-OH to PVAc or UF adhesives produces different behaviors in the shear strength of the glue line (SS) among species (Figure 7). As expected, the highest values of SS appeared when the different types of woods were glued with the UF adhesive compared to the PVAc adhesive. The MWCNTs-OH in any of the concentrations had no significant effect on SS in the species *C. alliodora*, *E. cyclocarpum*, *G. arborea*, *O. pyramidale* and *T. grandis* in dry condition, glued with PVAc adhesive (Figures 7c-e, g-h). *E. cyclocarpum* glued with PVAc adhesive modified with MWCNTs-OH was the only species significantly unaffected in wet condition (Figure 7d). The SS for *T. grandis*, *G. meiantha*, *O. pyramidale* and *T. grandis* glued with UF adhesive modified with MWCNTs-OH were not significantly affected in wet condition (Figure 7f-i). For the remaining conditions and species, SS augmented significantly in at least one concentration, the adhesive with 0.1% concentration of MWCNTs-OH being the one with the highest values of SS, in many conditions and species.

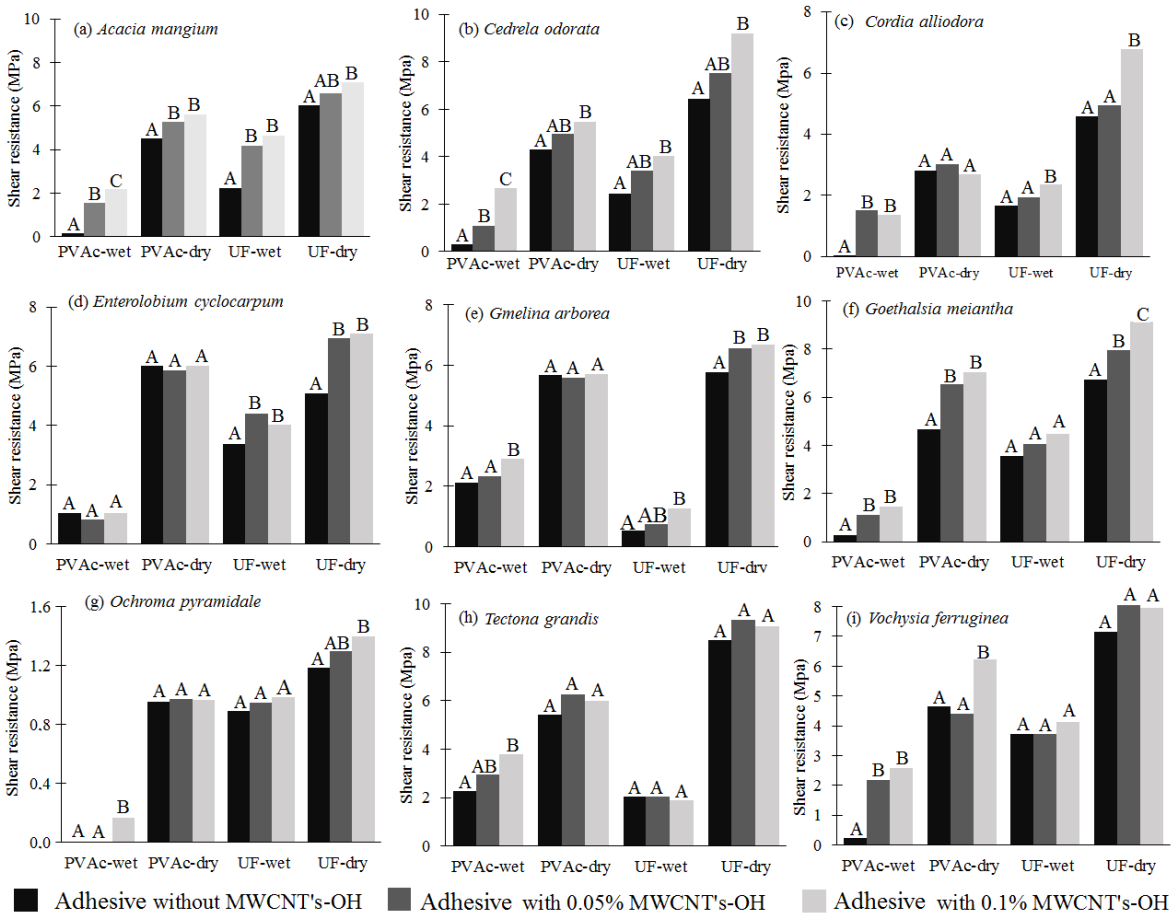

Figure 7. Resistance of shear strength for dry and wet condition for ten tropical species glued with PVA and UF-adhesive with and without MWCNTs-OH

.

In all evaluated species moisture content in dry condition was statistically equivalent for all conditions of concentration of MWCNTs-OH and species (Table 4). However, no differences were observed in this property in some species or adhesives in wet condition (MC), after the wood was immersed in water for 24 hours (Table 4). Where the PVAc adhesive is modified with MWCNTs-OH, significant decrease of the moisture absorption, i.e., less MC, occurs only in *C. alliodora* and *O. pyramidale*. Meanwhile, where the UF adhesive is modified with MWCNTs-OH, moisture content decreases in the wood of *A. mangium*, *G. arborea* and *O. pyramidale*. For the rest of the species, the value of moisture content remains statistically unaffected (Table 4).

The percentage of wood failure (PWF) in wood glued with PVAc adhesive with added MWCNTs-OH diminished significantly in the woods of *A. mangium*, *C. alliodora*, *G. arborea*, and *O. pyramidale* in dry condition (Tabla 4). Meanwhile, for *A. mangium*, *E. cyclocarpum*, *G. meiantha*, *T. grandis* and *V. guatemalensis* in wet condition, the wood failure percentage increased with added MWCNTs-OH. For the rest of conditions and species, PWF was not significantly affected by the addition of MWCNTs-OH to the PVAc.

For *C. odorata* in wet condition and for *G. meiantha* in both moisture conditions (dry and wet), PWF diminished significantly with the UF-adhesive with MWCNTs-OH (Table 4). On the other hand, the PWF increased in the glue line with the UF-adhesive modified with MWCNTs-OH in *A. mangium* and *E. cyclocarpum* in both moisture conditions (dry and wet); in *C. odorata* and *C. alliodora* in dry condition and 0.1% concentration of MWCNTs-OH and in *T. grandis* and *V. guatemalensis* in dry condition.

Table 4. Moisture content and percentage of wood failure in shear test of PVAc and UF wood

Species	MWCNTs (wt.%)	Moisture content (%)				Percentage of wood failure			
		PVAc adhesive		UF adhesive		PVAc adhesive		UF adhesive	
		Dry	Wet	Dry	Wet	Dry	Wet	Dry	Wet
Acacia mangium	0.00	11.5A	32.6A	12.4A	35.7A	72.7A	4.3A	32.2A	19.5A
	0.05	11.7A	32.8A	12.4A	31.7B	26.3B	0.0A	36.5B	34.0B
	0.10	12.1A	31.6A	12.4A	31.7B	31.4B	27.3B	43.0C	34.0B
Cedrela odorata	0.00	10.8A	31.0A	12.7A	28.0A	66.5A	0.0A	30.7A	27.8A
	0.05	11.5A	32.0A	12.6A	29.3A	70.3A	0.0A	27.8A	6.7B
	0.10	12.5A	30.9A	12.3A	29.8A	68.3A	8.3B	49.1B	9.4B

adhesive adding different concentrations of MWCNTs-OH

Cordia alliodora	0.00	10.5A	32.5A	12.7A	32.8A	81.3A	1.5A	38.9A	31.0A
	0.05	11.4A	26.9B	11.7A	33.0A	68.5B	6.9B	41.9A	32.7A
	0.10	9.9A	25.7B	12.1A	31.3A	68.5B	15.4C	61.9B	32.6A
Enterolobium cyclocarpum	0.00	10.8A	40.4A	11.7A	41.4A	76.6A	84.8A	59.6A	41.0A
	0.05	10.4A	42.3A	11.4A	42.4A	97.7B	37.8B	55.7A	55.0B
	0.10	10.3A	41.6A	11.3A	42.3A	89.0C	54.8C	53.3A	52.7B
Gmelina arborea	0.00	10.0A	20.5A	12.3A	26.1A	52.6A	9.1A	2.6A	3.6A
	0.05	10.0A	21.6A	11.9A	23.4B	4.8B	1.0B	1.3A	2.1A
	0.10	10.7A	22.0A	11.5A	22.5B	0.0B	0.2B	0.8A	2.0A
Goethalsia meiantha	0.00	9.8A	38.1A	12.3A	39.1A	37.5A	15.4A	55.7A	60.6A
	0.05	9.7A	38.8A	11.8A	38.5A	93.3B	75.5B	41.8B	33.2B
	0.10	10.5A	39.2A	11.7A	37.0A	96.0B	69.2B	19.0C	52.2C
Ochroma pyramidale	0.00	10.8A	65.1A	12.2A	57.1A	99.6A	1.3A	68.2A	48.8A
	0.05	11.3A	58.0B	11.0A	58.8A	44.0B	44.0B	68.7A	52.4A
	0.10	11.7A	58.5B	11.8A	50.7B	69.9C	14.2B	73.2A	80.8B
Tectona grandis	0.00	10.9A	23.1A	12.0A	26.0A	16.7A	0.0A	8.0A	10.1A
	0.05	11.9A	25.1A	12.2A	26.1A	27.7B	0.0A	12.1B	10.0A
	0.10	11.9A	24.0A	12.0A	27.0A	21.6B	0.0A	13.5B	9.7A
Vochysia ferruginea	0.00	10.2A	32.7A	11.7A	32.1A	38.5A	50.0A	53.5A	37.3A
	0.05	10.5A	30.9A	10.6A	33.5A	55.0B	81.3B	79.1B	36.0A
	0.10	11.7A	32.1A	10.8A	32.5A	56.3B	78.7B	76.9B	56.6A

Addition of graphene components or nanotubes (CNT or MWCNT) has proved to help improve adhesion properties of different types of adhesives (Fu et al., 2010, Ghasemi et al., 2012, Sydlik et al., 2013, Pinto et al., 2013, Jakubinek at al., 2015), as observed in several of the species evaluated in the present study (Figure 5). However, few studies have utilized MWCNT in wood adhesives. One of them is the one conducted by Fu et al. (2010), who found that incorporating CNTs and CNT–OH could effectively reduce the flammability of WPC, and CNT–OH conferred better flame retardancy on WPC relative to pristine CNTs due to its improved interfacial compatibilization between CNT–OH and wood flour.

Meanwhile, Pinto et al. (2013) found that 50% increase of shear strength on veneer lap joints occurs by increasing concentration of graphene nanoplatelets from 0.1% a 0.3% in poly(vinyl acetate) latex. Those investigations agree with the results obtained when adding MWCNTs-OH

to a base of either PVAc or UF in *A. mangium*, *C. odorata*, *C. alliodora* and *G. meiantha* (Figure 7a-c, f); and in *E. cyclocarpum*, *G. arborea* and *O. pyramidale* with UF-adhesive (Figures 7d-e, g). However, an increase in SS was only observed in *G. meiantha* while changing from 0.05 to 0.1% concentration in the UF-adhesive (Figure 7c) and in *V. ferruginea* with PVAc (Figure 7i), as observed by Pinto et al. (2013) while changing from 0.1% to 0.3% graphene nanoplatelets in poly(vinyl acetate) latex to increase shear resistance.

Shear resistance increment occurring in most of the species when adding MWCNTs-OH, particularly in the case of UF resin in some concentrations, can be explained by the conclusions in Pinto et al. (2013), who mention a significant mechanical reinforcement that can be attributed to strong interfacial interactions between polymer chains and the graphene surface. Likely, affinity of the surface of the material and good dispersion of the nanotubes inside the polymeric matrix produces cohesive reinforcement of the adhesive layer, resulting in greater joint resistance (Wang et al., 2010).

The less significant effectivity observed in the PVAc adhesive relative to the UF adhesive may be explained by agglomeration of the MWCNTs-OH in the PVAc adhesive that reduces SS, as occurred in *C. alliodora*, *E. cyclocarpum*, *G. arborea*, *O. pyramidale* and *T. grandis* (Figure 7), resulting in values of SS statistically equivalent between the control and the different concentrations. Therefore, according to the results, incorporating nanotubes was more effective in the UF adhesive, probably because of less agglomeration of nanotubes in this type of resin.

It is known that the performance of the PVAc and UF adhesives depends on moisture absorption by the material. Presence of water, which works as a plasticizer, increases elongation and tear strength, but reduces the tensile strength, limiting the structural behavior of the adhesive (Wang et al., 2011). This is therefore the cause for reduction of the SS in all of the species after immersing the samples in water during 24 hours (Table 3).

However, addition of MWCNTs-OH slightly increases SS or percentage of wood failure in all species; for example, an increase was obtained in *C. alliodora* and *O. pyramidale* with the PVAc adhesive and in *A. mangium*, *G. arborea* and *O. pyramidale* with UF adhesive (Table 4). For the remaining conditions it is not possible to achieve this. These results confirm the findings for SS in dry condition: for some species the increment is achieved, whereas not for others, indicating that the adhesive modified with MWCNTs-OH fails to achieve adequate

interaction between the surface of the substrate and the modifications carried out to the adhesive. Therefore, other types of functionalization of MWCNTs-OH will be necessary.

Conclusion

Multiwall carbon-nanotubes functionalized with hydroxyl groups (MWCNTs-OH) incorporated to polyvinyl acetate wood adhesives (PVAc) and urea-formaldehyde (UF), improve the thermogravimetric properties of those adhesives (increase of the initial temperature, increase of the maximum peak temperature, increase of the remnant mass in the different periods of temperature studied in the reactions of the adhesives and increase of the entropy factor and activation energy of the kinetics of decomposition of the resin). Other physical aspects affected by the addition of MWCNTs-OH to PVAc and UF adhesives were increased resin viscosity, decreased brightness and adhesive yellowness, and increased redness, especially in the proportion of 1.5%. AFM and TEM showed that the MWCNTs-OH are appropriately distributed into the two types of adhesives and the SEM showed no penetration problems of the modified adhesives into the different types of wood.

As for the behavior of the modification of adhesives, increased shear strength of the glue line and percentage of wood failure of most tropical species occurs, especially when using the UF-adhesive. By increasing the moisture in the wood, the modified adhesive increases the strength of the glue line in half of the species studied, indicating that, in some species, an adequate interaction between the substrate surface and the adhesive modified with MWCNTs-OH is not achieved.

Acknowledgement

The authors wish to thank the *Vicerrectoría de Investigación y Extensión* at the *Instituto Tecnológico de Costa Rica (ITCR)* for financial support for the study.

References

ASTM. 2013a. D905-08 Standard test method for strength properties of adhesive bonds in shear by compression loading. Annual Book of ASTM Standards. Vol. 11.06. Philadelphia, US, 5 p. (Reaproved 2013)

ASTM. 2013b. D5266-13 (1995) Standard practice for estimating the percentage of wood failure in adhesive bonded joints. Annual Book of ASTM Standards. Vol. 11.06. Philadelphia, US, 8p.

ASTM. D2556-11(2011) Standard test method for apparent viscosity of adhesives having shear-rate-dependent flow properties. Book of Standards. Vol. 15.06. Philadelphia, US, 7 p.

ASTM-American Society for Testing and Materials. Standard practice for calculation of color tolerances and color differences from instrumentally measured color coordinates. ASTM D-2244-11, American Society for Testing and Materials, West Conshohocken, PA.2014.

Barnes, H. A., & Hutton, J. F. (1989). An introduction to rheology (Vol. 3). Elsevier.

Chahud, E., Rocco, F.A. and Rosi, R.R.. (2009). O uso de espécies nativas comercializadas em Belo Horizonte na composição de madeira laminada colada. Construindo 1: 42-49.

Datsyuk, V., Kalyva, M., Papagelis, K., Parthenios, J., Tasis, D., Siokou, A., Galiotis, C. (2008). Chemical oxidation of multiwalled carbon nanotubes. *Carbon*, *46*(6), 833-840.

Diener, B. J., & Saklad, H. (1997). Portico, SA. Journal of Business Research, 38(1), 89-96.

Du, F., Fischer, J. E., & Winey, K. I. (2003). Coagulation method for preparing single-walled carbon nanotube/poly (methyl methacrylate) composites and their modulus, electrical conductivity, and thermal stability. Journal of Polymer Science Part B: Polymer Physics, 41(24), 3333-3338.

Fraczek, A., Menaszek, E., Paluszkiewicz, C., & Blazewicz, M. (2008). Comparative in vivo biocompatibility study of single-and multi-wall carbon nanotubes. *Acta Biomaterialia*, *4*(6), 1593-1602.

Fu, S., Song, P., Yang, H., Jin, Y., Lu, F., Ye, J., & Wu, Q. (2010). Effects of carbon nanotubes and its functionalization on the thermal and flammability properties of polypropylene/wood flour composites. Journal of materials science, 45(13), 3520-3528.

Ghasemi, I., Farsheh, A. T., & Masoomi, Z. (2012). Effects of multi-walled carbon nanotube functionalization on the morphological and mechanical properties of nanocomposite

foams based on poly (vinyl chloride)/(wood flour)/(multi-walled carbon nanotubes). Journal of Vinyl and Additive Technology, 18(3), 161-167.

Gonnet JF (1993) CIELab measurement, a precise communication in flower colour: an example with carnation (*Dianthus caryophyllus*) cultivars. J Hort Sci 68: 499–510.

Hodkiewicz, J. (2010). Characterizing carbon materials with raman spectroscopy. *Thermo Scientific Application Note*, *51946 and 51946*.

Hui-Wang, C., & Guan-Ben, D. (2011). Preparation and characterization of exfoliated nano-composite of polyvinyl acetate and montmorillonite. Journal of Chemical Engineering and Materials Science, 2(8), 122-128.

Jakubinek, M. B., Ashrafi, B., Zhang, Y., Martinez-Rubi, Y., Kingston, C. T., Johnston, A., & Simard, B. (2015). Single-walled carbon nanotube–epoxy composites for structural and conductive aerospace adhesives. *Composites Part B: Engineering*, *69*, 87-93.

Kaboorani, A., & Riedl, B. (2011). Effects of adding nano-clay on performance of polyvinyl acetate (PVA) as a wood adhesive. Composites Part A: Applied Science and Manufacturing, 42(8), 1031-1039.

Kaboorani, A., Riedl, B., Blanchet, P. (2013). Ultrasonication technique: a method for dispersing nanoclay in wood adhesives. Journal of Nanomaterials, 2013, 3: 1-9.

Khan, U., May, P., Porwal, H., Nawaz, K., Coleman, J. N. (2013). Improved adhesive strength and toughness of polyvinyl acetate glue on addition of small quantities of graphene. *ACS applied materials & interfaces*, *5*(4), 1423-1428.

Lehman, J. H., Terrones, M., Mansfield, E., Hurst, K. E., & Meunier, V. (2011). *Evaluating the characteristics of multiwall carbon nanotubes*. Carbon, 49(8), 2581-2602.

Lonkar, S. P., Kushwaha, O. S., Leuteritz, A., Heinrich, G., & Singh, R. P. (2012). Self photostabilizing UV-durable MWCNT/polymer nanocomposites.*RSC Advances*, *2*(32), 12255-12262.

Matoso, E., & Cadore, S. (2008). Development of a digestion method for the determination of inorganic contaminants in polyvinyl acetate (PVAc). Journal of the Brazilian Chemical Society, 19(7), 1284-1289.

McNeill, I. C., Memetea, L., Cole, W. J. (1995). A study of the products of PVC thermal degradation. Polymer degradation and stability, 49(1), 181-191.

Mohan, P. (2013) "A Critical Review: The modification, properties, and applications of epoxy resins." Polymer-Plastics Technology and Engineering 52,2, 107-125.

Moya, R., Rodriguez-Zuñiga, A., Vega-Baudrit, J., Álvarez, V., 2015. Effect of silver nanoparticles on white-rot wood decay and some physical properties of three tropical wood species. International Journal of Adhesion and Adhesives 59: 62-70.

Osswald, S., Havel, M., & Gogotsi, Y. (2007). *Monitoring oxidation of multiwalled carbon nanotubes by Raman spectroscopy*. Journal of Raman Spectroscopy, 38(6), 728-736.

Peng, Y., & Liu, H. (2006). Effects of oxidation by hydrogen peroxide on the structures of multiwalled carbon nanotubes. *Industrial & engineering chemistry research*, *45*(19), 6483-6488.

Pinto, A. M., Martins, J., Moreira, J. A., Mendes, A. M., & Magalhães, F. D. (2013). Dispersion of graphene nanoplatelets in poly (vinyl acetate) latex and effect on adhesive bond strength. *Polymer International*, *62*(6), 928-935.

Pizzi, A., & Mittal, K. L. (Eds.). (2011). *Wood adhesives*. CRC Press. Macel Dekker, Inc. New York, USA.

Pötschke, P., Fornes, T. D., & Paul, D. R. (2002). Rheological behavior of multiwalled carbon nanotube/polycarbonate composites. Polymer, 43(11), 3247-3255.

Roussak, O. V., and H. D. Gesser. "Adhesives and Adhesion." Applied Chemistry. Springer US, 2013. 219-232.

Samaržija-Jovanović S, Jovanović V, Konstantinović S, Marković G, Marinović-Cincović M. Thermal behaviour of modified urea–formaldehyde resins. J Ther Analysis Calorimetry 2011;104(3):1159-1166.

Sun, Y. P., Fu, K., Lin, Y., & Huang, W. (2002). *Functionalized carbon nanotubes: properties and applications*. Accounts of Chemical Research,35(12), 1096-1104.

Sydlik, S. A., Lee, J. H., Walish, J. J., Thomas, E. L., & Swager, T. M. (2013). *Epoxy functionalized multi-walled carbon nanotubes for improved adhesives*. *Carbon*, *59*, 109-120.

Yudianti, R., H. Onggo, Y.S: Sudirman, Y. S., Iwata, T., and J.I. Azuma, "*Analysis of functional group sited on multi-wall carbon nanotube surface,"* Open Materials Science Journal, vol.5, pp. 242-247, 2011.

6. Artículo 6. Aplicación de nanotubos multicapa en la resistencia mecánica de nueve maderas comerciales de Costa Rica

Aplicación de nanotubos multicapa en la resistencia mecánica de nueve maderas comerciales de Costa Rica

Resumen

Los nanotubos de carbono multicapa (MWCNT) por su versatilidad se han utilizado en el refoerzamiento de materiales, sin embargo poco se conoce de su uso en maderas tropicales. En el presente estudio se introdujeron MWCNT funcionalizados con un grupo hidroxilo en una solución de agua a dos concentraciones, de 0,005% y 0,01%. Estos fueron inyectados utilizando el método vacío-presión utilizando comúnmente en la preservación de la madera. Nueve especies de importancia forestal en Costa Rica: *Acacia mangium*, *Cedrela odorata*, *Cordia alliodora*, *Enterolobium cyclocarpum*, *Gmelina arborea*, *Goethalsia meiantha*, *Ochroma pyramidale*, *Tectona grandis* y *Vochysia ferruginea* fueron probada la efectividad de lo MWCNT en 5 tipos de resistencia mecánica (compresión perpendicular a la fibra, flexión estática a la fibra, corte paralelo a la fibra, dureza lateral y axial y tensión paralela a la fibra) para probar su efectividad. En los resultados de absorción *Vochysia ferruginea* fue la especie que más absorbió con 455,45 L/m^3 en 0,005% y 466,40 L/m^3 en 0,01%, *Ochroma pyramidale* fue la especie que más retuvo MWCNT con 15,34 mg$_{MWCNT}$/kg$_{madera}$ en 0,005% y 21,49 mg$_{MWCNT}$/kg$_{madera}$, mientras que *Cedrela odorata* fue la especie que menos absorbió con 215,78 L/m^3 en 0,05% y 213,75 en 0,01% y *Tectona grandis* fue la que menos MWCNT retuvo con 2,27 mg$_{MWCNT}$/kg$_{madera}$ y 5,23 mg$_{MWCNT}$/kg$_{madera}$. En las pruebas mecánicas no hubo un patrón de mejoramiento en ninguna de las especies por lo que los resultados no son los esperados esto debido a varias razones, la procedencia del material, la funcionalización con grupo hidroxilo en los nanotubos o hasta la composición química de las especies.

Palabras claves: MWCNT, funcionalizado, hidroxilo, pruebas mecánicas, absorción.

Abstract

Multilayer carbon nanotubes (MWCNT) have been used in the reinforcement of materials due to its versatility, however little is known about their use in tropical timber. In the present study, functionalized MWCNT's were introduced with a hydroxyl group in a water solution at two concentrations, 0.005% and 0.01%. These were injected using the vacuum pressure method commonly used in wood preservation. Nine species of trees of importance to Costa Rica were used to prove the effectiveness of the MWCNT in 5 types of mechanical strength (perpendicular compression to the fiber, the fiber static bending, parallel cut to the fiber, lateral and axial hardness and tension parallel to grain). These species are: *Acacia mangium, Cedrela odorata, Cordia alliodora, Enterolobium cyclocarpum, Gmelina arborea, Goethalsia meiantha, Ochroma pyramidale, Tectona grandis and Vochysia ferruginea*. The results of absorption was that *Vochysia ferruginea* absorbed most with 455.45 L/m^3 at 0.005% and 466.40 L/m^3 at 0.01%, *Ochroma pyramidale* retained more MWCNT with 15.34 mg$_{MWCNT}$/kg$_{wood}$ 0.005% and 21.49 mg$_{MWCNT}$/kg$_{wood}$, while the species *Cedrela odorata* was the one that absorbed less with 215.78 L / m3 at 0.05% and 215.78 215.78 L/m3 0.01% and

Tectona grandis was the one that retained less MWCNT with 2.27 mg_{MWCNT}/kg_{wood} in 0,005% and 5.23 mg_{MWCNT}/kg_{wood}. In the mechanical tests there was no pattern of improvement in either species so the results were not as expected, due to several reasons; the origin of the material, functionalization with hydroxyl group nanotubes or the chemical composition of the species.

Keywords: MWCNT, functionalized, hydroxyl, mechanical tests, absorption.

Introducción

Los nanotubos de carbono (NTC´s) son alótropos de carbono como el diamante, el grafito o los fulerenos, su estructura puede ser procedente de una lámina de grafeno enrollada sobre sí misma (Lariza *et al,* 2012). El interés mundial comercial en los nanotubos de carbono (NTC) se ve reflejado en una capacidad de producción en la actualidad que supera los varios de miles de toneladas por año. Los NTC son cilindros de una o más capas con los extremos abiertos o cerrados (De Volder *et al,* 2013). Poseen un diámetro del orden del nanómetro y su longitud puede alcanzar hasta un milímetro, por lo que la relación entre longitud-anchura es muy alta (Pérez, 2010).

Algunas de las ventajas de los NTC es que presentan una alta resistencia mecánica y estabilidad térmica, con su estructura y forma presenta la posibilidad de crear sitios de anclaje para soportes convencionales como el carbono, el óxido de aluminio y sílice (Orináková , 2011). Su fuerza y conducción térmica son otras ventajas que lo hacen un producto importante en el ambiento científico, ya que un NTC perfecto es de 10 a 100 veces más fuerte que el acero cuando se considera el peso de unidad (Pérez, 2010). Entre las desventajas que presenta NTC es que la producción masiva de nanotubos se introducen pentágonos y heptágonos, en lugar del hexágono que es la unión perfecta del NTC, por lo que las propiedades deseadas se pueden degenerar (De Volder *et al*, 2013). La falta de solubilidad en disolventes orgánicos o disoluciones acuosas es otra de las desventajas que presentan estas estructuras aunque pueden sufrir reacciones químicas que los hacen solubles en diversos disolventes, pudiéndose integrarse a sistemas inorgánicos, orgánicos e incluso biológicos (Gómez, 2011), proceso conocido como funcionalización de los nanotubos.

Los usos para NTC son varios, como por ejemplo en la medicina se puede utilizar para los diagnósticos y tratamiento de cáncer, desordenes en el sistema nervioso y enfermedades infecciosa (Yi *et al,* 2010). También podemos encontrar nanotubos en materiales compuestos como cargas conductoras eléctricamente en plásticos. Así mismo las resinas de NTC´s se utilizan para mejorar los compuestos de fibra, entre los que destaca las aspas fuertes y ligeras de los aerogeneradores y en algunos casos en aspas de barcos. También se utilizan en las pinturas que ayudan a reducir la contaminación biológica de los cascos de los barcos al ser una alternativa a pinturas que contienen biocidas peligroso para el medio ambiente (De Volder *et al*, 2013). Un uso importante es en recubrimiento de anticorrosivo para los metales puede

mejorar la rigidez de revestimiento y la fuerza que proporciona una vía eléctrica para la protección catódica (De Volder *et al*, 2013)

La estructura compleja de una célula de madera que define muchas de las propiedades físicas y mecánicas ha llamado la atención de los científicos, recientemente herramientas que permitan obtener imágenes y medir estructuras sumamente pequeñas ha llevado a estos científicos a incursionarse en la nanotecnología. Están comenzando a ver a la madera y la posibilidad de trabajar con ella en una escala nano para lograr la creación de productos más absorbentes, ligeros y fuertes. (shmulsky *et al,* 2011). Experimentos en los cuales se unen las fibras leñosas, cemento y NTC´s han demostrado la multifuncionalidad de los NTC´s haciéndolos ideal para este tipo de trabajos. El experimento consistió en tres concentraciones de nanotubos multicapa 0,5%, 1% y 1,5% revueltos con 10% y 20% de fibra de bagazo en una mezcla normal de cemento. La mezcla de 1,5% de nanotubos multicapa (MWCNT) y 20% de fibra tuvo el valor más alto en la prueba de flexión aumentando las características del cemento en un 43%. (Younesi *et al,* 2011).

La madera del ficus (*Ficus hispida)* es un tipo de madera suave, que se encuentra en los trópicos, no es apropiada para aplicaciones estructurales debido a sus pobres propiedades físicas y mecánicas, sin embargo esta madera puede tener un valor agregado si se utiliza para la formación de compuestos con polímeros. En una investigación realizada por Hazarika y Maji (2014) agregaron 5g de nanotubos multicapa a una disolución de etanol e hidróxido de potasio para obtener nanotubos multicapa con grupo hidroxilo (MWCNT-OH) para luego aplicárselo un copolimero de melanina y formaldehído (MFFA). Se varió entre 0,5 y 1,5 phr de concentración de MWCNT. Otro componente importante en este experimento fue la nanoarcilla, esta mantuvo un valor constante de 3 phr. Luego de reunir los componentes se dimensionaron las piezas de *Ficus hispida* de acuerdo a las especificaciones de ASTM y se hicieron 6 tratamientos, madera tratada con MFFA y 1,3-dimetilol urea 4,5-dihidroxietileno (DMDHEU), MFFA/DMDHEU/nanoacrilla/MWCNT (0,5 phr), MFFA/DMDHEU/nanoacrilla/MWCNT (1 phr), MFFA/DMDHEU/MWCNT (1,5 phr), MFFA/DMDHEU/nanoacrilla/MWCNT (1,5 phr) y el testigo. Los resultados fueron positivos para el tratamiento con mayor concentración de MWCNT y nanoarcilla ya que presentaron los mayores valores en las pruebas de dureza, flexión y tensión.

En Costa Rica el uso de madera se distribuye de la siguiente forma: 45,9% en tarimas, 22,5% construcción, 13,6% muebles 17,5% exportación y 0,3% otros (ONF, 2013). Las nueve

especies a utilizar en este trabajo se encuentran entre la lista de especies que se comercian actualmente en el país ya sea en pie o aserrada. Sin embargo los precios de ciertas especies están cayendo como es el caso de la *Gmelina arborea y Cedrela odorata* en el área de la construcción (ONF, 2013). No obstante con la finalidad de contar con productos de mayor resistencia y mejor desempeño es que la utilización de MWCNT permitiría dar un valor agregado estas maderas.

Por esta razón, el objetivo de este trabajo fue estudiar el comportamiento de las propiedades mecánicas (compresión perpendicular a la fibra, flexión estática a la fibra, corte paralelo a la fibra, dureza lateral y axial y tensión paralela a la fibra) por la introducción de soluciones de nonotubos de carbono multicapas funcionalizados con grupos hidroxilos (MWCNT-O) en dos concentraciones (0,005 y 0,01%) en nueve especie tropicales (*Acacia mangium, Cedrela odorata, Cordia alliodora*, *Enterolobium cyclocarpum*, *Gmelina arborea, Goethalsia meiantha*, *Ochroma pyramidale*, *Tectona grandis* and *Vochysia ferruginea*).

Materiales y métodos

1. **Materiales utilizados**

Primeramente fueron utilizado MWCNT funcionalizados con grupos hidroxilo (MWCNT's-OH), suministrados por CheapTubes.Inc (Cambridgeport, USA). La información suministrada por el fabricante es: diámetro externo de aproximadamente de 50 nm, longitud de 10-20 µm, pureza del 95% y una concentración de grupos –OH de 0.5-1.0% en peso.

En cuanto a las especies de madera utilizadas son de uso forestal maderable en Costa Rica. Se subdividen en tres grupos: las más usadas en los programas de reforestación *Gmelina arborea* (melina*)*, *Tectona grandis* (teca), y *Acacia magnium* (acacia), de las más usadas en la fabricación de muebles *Cordia alliodora* (Laurel), *Cedrela odorata* (Cedro amargo) y *Enterolobium cyclocarpum* (Guanacaste) y madera con potencial en bosque secundario *Vochysia ferruginea* (botarrama), *Ochroma pyramidale* (balsa) y *Goethalsia meiantha* (guacimo blanco). Estas maderas fueron obtenidas de aserraderos y depósitos de madera cercanos a las instalaciones del Instituto Tecnológico de Costa Rica.

Las piezas de madera utilizada presentaba un espesor de 6 cm de grueso, en la mayoría de los casos el ancho correspondía al ancho de la troza que es comúnmente el patrón utilizado para madera para mueblería (Serrano y Moya, 2011). La madera estaba seca al aire. Luego fueron preparadas 45 muestras por tipo de ensayo con las siguientes dimensiones:

- Compresión paralela a la fibra: probetas de 2,5 cm x 2,5 cm x 6 cm
- Flexión estática a la fibra: probetas de 2,5 cm x 2,5 cm x 41 cm.
- Cortante paralelo a la fibra: 5,5 cm x 5,5 cm x 6,3 cm
- Dureza axial y lateral: con probetas de 5 cm x 5 cm x 15 cm
- Tensión paralela a la fibra: con probetas de 2,5 cm x 2,5 cm x 46 cm

2. Caracterización de nanotubos de carbono multicapa funcionalizados (MWCNT´s-OH)

El detalle de las características, dimensiones y demás aspectos de MWCNT-OH son detallados ampliamente en Moya et al. (2015). El resumen de la anterior se indica que los MWCNT-OH presentan las 3 bandas características de los nanotubos multicapas, llamadas D, G, G´ (Figura 1), y los cuales se diferencias de los nanotubos no funcionalzados en la banda D, l atribuida esta diferencia a defectos en las paredes de los nanotubos o heteroátomos que han sido añadidos a la estructura de los nanotubos, y las diferencias en las bandas G y G´ se producen por los estiramientos en el plano de los enlaces carbono-carbono en las hojas de grafeno; e indica también desordenes y defectos en los nanotubos de carbono.

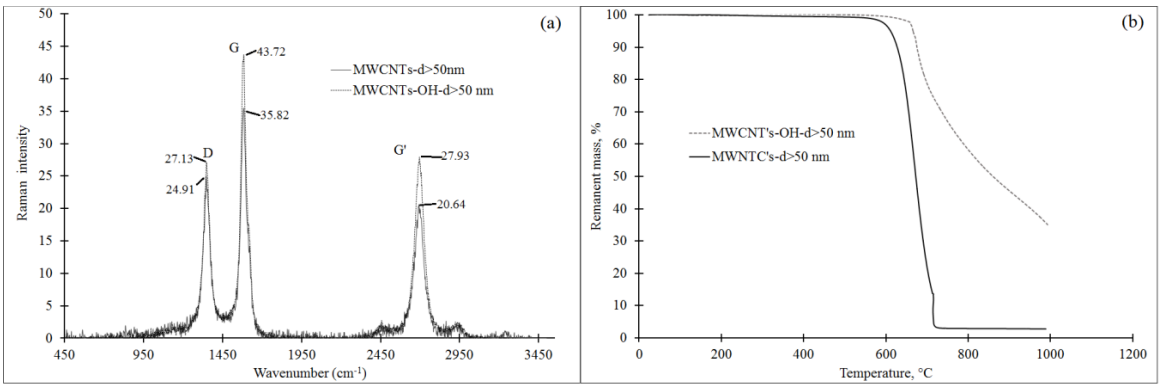

Figura 1. Espectro Raman (532 nm excitación) (a) y análisis termográfico para MWCNT´s y MWCNT´s-OH

Los MWCNT´s-OH utilizados en la evaluación de la estabilidad térmica presentan una descomposición máxima alrededor de 600 °C, mostrando que estos son de menor estabilidad térmica a los nanotubos no funcionalizados.

3. Preparación de la solución de MWCNT´s-OH

Primeramente fue preparada una solución de los nanotubos de 0,03 g para la solución de 0,01% y de 0.015 g para la concentración de 0,005% en 200 ml de agua. Esta cantidad de

nanotubos fueron sonificados. Se utilizó un Ultrasonic Processor modelo CV18 para la sonificación de la disolución de nanotubos. Luego se sometieron a una sonificación por cinco minutos con una amplitud del 75% con intervalos de 45 segundos y descansos de 10 segundos para mezclar los nanotubos. Los 200 ml zonificados se vertieron en tres litros de agua y se volvieron a zonificar por 25 minutos, esto se repitió hasta obtener 15 litros de disolución ya zonificada. Una vez obtenidos los 15 litros de disolución zonificada, estos se vertieron en 15 litros de agua para obtener 30 litros de disolución.

4. Tratamiento de la madera con MWCNT´s-OH

Las muestras se colocaron en un tanque de presión experimental como el que se muestra en la figura 2a, comúnmente utilizado para la conservación de la madera. El proceso de introducción de las solución con MWCNT´s-OH consta de 30 min de vacío a -78 kPa, dos horas de presión a 690 kPa, y 15 min de vacío a -78 kPa. Luego las muestras humedad se colocan en un ambiente controlado para lograr un contenido de humedad de equilibrio de 12% (madera seca al aire) por un periodo de 6 meses.

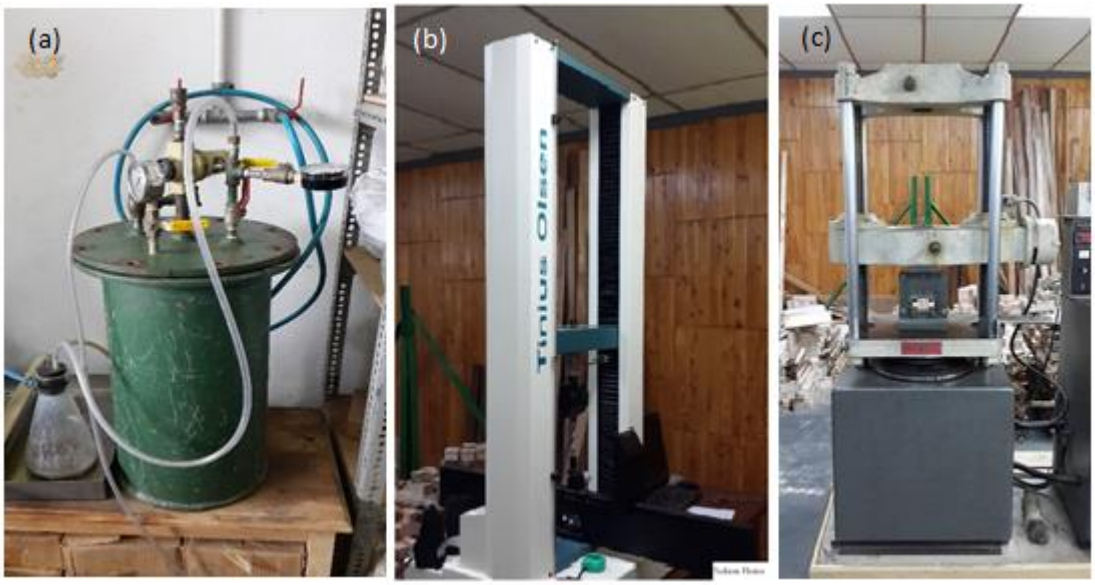

Figura 2. (a) Bomba de inyección, (b) Maquina Tinius Olsen H10KTy (c) Maquina Tinius Olsen

5. **Capacidad de absorción y retención de MWCNT´s-OH en las muestras de madera**

Las Muestras fueron pesadas antes y después del proceso de preservación y se generaron dos parámetros: la capacidad de absorción y retención de MWCNT´s. La capacidad de absorción para cada muestra se calculó como la absorción de la solución en litros por volumen de madera

(Ecuación 1), mientras que la retención de MWCNT´s fue determinada considerando la absorción MWCNT´s en peso por la madera en peso, de acuerdo con la Ecuación 2.

$$\text{Capacidad de absorción } \left(\frac{L_{solución}}{m^3}\right) = \frac{\text{(Peso antes de la penetración -peso después de la penetración) (kg)} * \text{densidad solución } \left(\frac{kg}{m^3}\right)}{\text{Volumen de la muestra } (m^3)} * \frac{L_{solución}}{1\ m^3} \quad (1)$$

$$\text{Capacidad de retención} = \frac{\text{Capacidad de absorción } \left(\frac{L_{solución}}{m^3}\right)}{\text{Volumen de la muestra } (m^3)} * \text{Concentración de nanotubos } \left(\frac{mg}{L_{solución}}\right) \quad (2)$$

6. Ensayos mecánicos

El efecto de las nanotubos de carbono multicapas en mejoramiento de la resistencia fue evaluado por medio de 5 pruebas mecánicas: compresión paralela a la fibra, flexión estática a la fibra, cortante paralelo a la fibra, dureza axial y lateral y tensión paralela a la fibra. Estas pruebas mecánicas fueron realizadas acorde a la norma ASTM D-143 (ASTM, 2014). Para cada tipo de ensayo fueron utilizadas un total de 45 muestras, 15 por cada tipo de concentración de nanotubos Los ensayos de flexión, tensión y dureza Fueron realizados en una maquina universal de ensayo máquina Tinius Olsen modelo H10KT (Fig. 2b) en tanto que los ensayos de corte y compresión fue utilizada nuevamente una máquina de ensayo universal Tinius Olsen modelo 4022 (Fig. 2c).

7. Análisis estadístico

Un análisis descriptivo se desarrolló (media y desviación estándar) de los parámetros de esfuerzo. Además, se comprobó si las variables cumplen los supuestos de distribución normal, la homogeneidad de las varianzas y la presencia de datos extremas. Posteriormente, se aplicó un Análisis de varianza (ANDEVA) para verificar el efecto de la concentración de los nanotubos sobre las propiedades mecánicas estudiadas. Luego fue establecido las diferencias estadísticas entre las media por una prueba de Tukey en un nivel de confianza del 95%. Para el estadístico se utilizó el programa SAS y se hizo una comparación entre las medias, para las figuras y tablas se utilizó Excel 2013.

Resultados

1. Absorción y retención de MWCNT´s

A continuación se presenta el cuadro 1 en el cual se muestran las absorciones de la disolución con nanotubos y retenciones de nanotubos de las nueve especies forestales. De las nueve especies *Cordia alliodora, Goethalsia meiantha* y *Ochroma pyramidale* fueron las que retuvieron la mayor cantidad de nanotubos. *Ochroma pyramidale* fue la que retuvo más nanotubos entre las nueve especies en el tratamiento de 0,01%. *Tectona grandis* fue la especie que presentó menor absorción de nanotubos en ambos tratamientos.

Cuadro 1. Retención y absorción de nanoparticulas en nueves especies tropicales de Costa Rica para dos concentraciones de nanotubos de carbono

Especies	Absorción ($L_{disolucion}/m^3_{madera}$)		Retención de nano-carbono ($g_{nanotubos}/m^3_{madera}$)		Retención de nano-carbono ($mg_{nanotubos}/kg_{madera}$)		Densidad antes de ser impregnados (kg/m3)
	0,005%	0,01%	0,005%	0,01%	0,005%	0,01%	
Acacia magnium	360,76	315,85	1,80	3,16	3,38	5,93	533
Cedrela odorata	215,78	213,75	1,08	2,14	2,76	5,47	391
Cordia alliodora	435,17	511,96	2,18	5,12	6,29	14,80	346
E. cyclocarpum	307,11	328,48	1,54	3,28	4,44	9,49	346
Gmelina arborea	283,24	256,76	1,42	2,57	2,86	5,19	495
Goethalsia meiantha	447,04	593,39	2,24	5,93	5,60	14,87	399
Ochroma pyramidale	380,44	266,53	1,90	2,67	15,34	21,49	124
Tectona grandis	271,10	311,43	1,36	3,11	2,27	5,23	596
Vochysia ferrugia	455,45	466,40	2,28	4,66	4,19	8,57	544

2. Flexión perpendicular a la fibra

En esta prueba mecánica, *Ochroma pyramidale, Vochysia ferruginea, Enterolobium cyclocarpum, Cordia alliodora, Gmelina arborea* y *Tectona grandis* no presentan diferencias significativas en ninguna de las concentraciones de MWCNT´s-OH (Figura 3). Mientras que *Acacia magnium, Cedrela odorata* y *Goethalsia meiantha* si presentan diferencias estadística. En la madera de *A. mangium*, el MOE de la madera tratada con MWCNT´s-OH a 0,005% presenta diferencias más bajas comparada con el testigo, mientras que el tratamiento de 0,01% no presenta diferencia significativa al compararlo con la madera no tratada. Lo mismo sucede en el MOR de la madera tratada con una concentracción de 0,005% MWCNT´s-OH, que el MOR es estadísticamente más bajo que la madera sin nanotubos. En *Cedrela odorata* las diferencias se presentan cuando hay nanotubos presentes en la madera. Estadísticamente el MOR en la madera con 0,005% de MWCNT´s-OH es mayor que la madera con 0,01% de nanotubos. Sin embargo ninguna concentración de nanotubos, presenta diferencias con el testigo en el MOR. En *Goethalsia meiantha* en el MOR se presenta un valor estadísticamente mayor en la madera tratada con 0,01% de MWCNT´s-OH, mientras que la madera tratada 0,005% de MWCNT´s-OH no se encuentran diferencias significativas en el MOE.

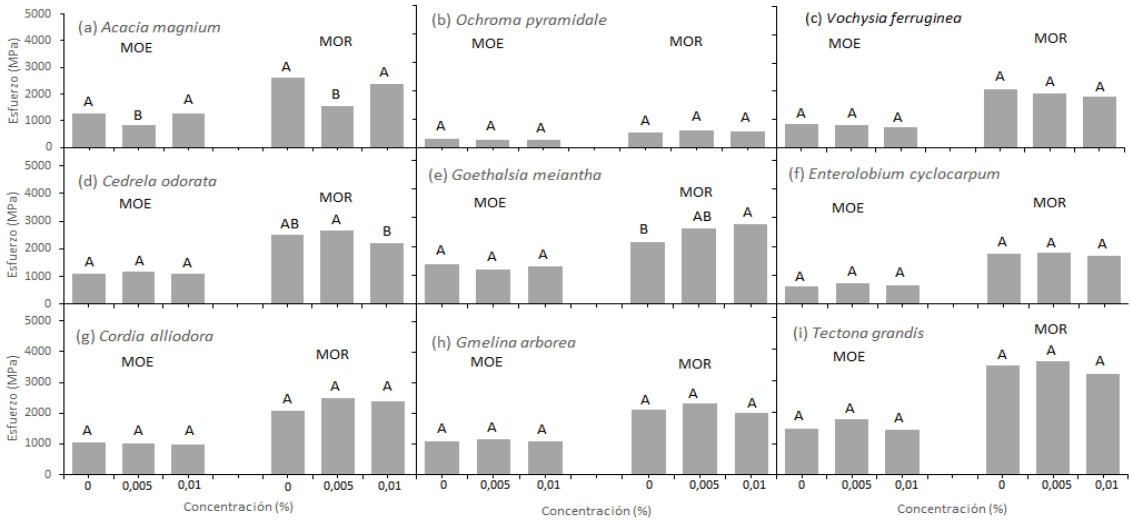

Figura 3. Esfuerzo (MPa) promedio de los módulos de ruptura (MOR) y módulo de elasticidad (MOE) para nueve especies forestales con tres tratamientos de concentración de MWCNT´s-OH (0, 0,005 y 0,01%).

Nota: Los valores medios identificados con las letras A y B son estadísticamente diferentes en $\alpha = 99$ %.

3. Tensión paralela a la fibra

Los ANDEVA mostraron que las especies *Acacia magnium, Cordia alliodora*, *Enterolobium cyclocarpum, Gmelina arborea, Ochroma pyramidale, Vochysia ferrugia* no presentan valores con diferencias significativas entre las tres diferentes concentraciones, mientras que el resto de las especies si presentan diferencias (Cuadro 2). Ambos tratamientos en *Cedrela odorata* presentan diferencias muchos más altas que el testigo. El tratamiento que presenta un valor estadísticamente mayor en el caso de *Goethalsia meiantha* es el de 0,005%, el tratamiento de 0,01% no presento diferencias con el testigo. Caso similar en *Tectona grandis*, el tratamiento 0,005% presentó un valor mayor significativo comparado con el otro tratamiento y el testigo.

Cuadro 2. Esfuerzo en tensión en madera de nueves especies tropicales con diferentes concentraciones de MWCNT´s-OH.

Especie	Esfuerzo (MPa)		
	0%	0,005%	0,01%
Acacia magnium	95,87^{A}	87,97^{A}	79,55^{A}
Cedrela odorata	37,30^{B}	69,91^{A}	77,02^{A}
Cordia alliodora	62,13^{A}	66,06^{A}	63,19^{A}
Enterolobium cyclocarpum	30,59^{A}	31,51^{A}	35,84^{A}
Gmelina arborea	66,56^{A}	65,59^{A}	61,49^{A}
Goethalsia meiantha	57,07^{B}	75,79^{A}	61,99^{B}
Ochroma pyramidale	30,75^{A}	26,32^{A}	31,01^{A}
Tectona grandis	95,63^{B}	151,99^{A}	113,59^{B}
Vochysia ferruginea	45,92^{A}	44,69^{A}	40,78^{A}

Nota: Los valores medios identificados con las letras A y B son estadísticamente diferentes en $\alpha = 99$ %.

4. Dureza

En este ensayo mecánico, de las nueve especies tropicales fueron *Acacia magnium, Vochysea ferruginea, Goethalsia meiantha, Cordia alliodora* y *Gmelina arborea* presentaron diferencias significativas en al menos uno de los tratamientos. *Acacia magnium* presentó mayor dureza lateral en la concentración de 0,005%, mientras que 0,01% no presento diferencia tanto con el testigo como la concentración de 0,005%. *Vochysia ferruginea* presentó diferencia en la dureza

axial. La madera tratada con nanotubos a 0,001% presentó menor dureza lateral, pero solamente menor a la concentración de 0,001%. *Goethalsia meiantha* presenta diferencias significativas mayores al testigo en la madera tratada con una concentración de 0,01% de la dureza axial. *Cordia alliodora* tiene diferencias tanto en dureza axial como lateral y en ambos casos el tratamiento de 0,005% presenta un valor estadísticamente mayor al testigo. Mientras que *Gmelina arborea* también presenta diferencias en dureza lateral y axial, en este caso las diferencias se presentan en el tratamiento de 0,01% y es mayor estadísticamente que el testigo.

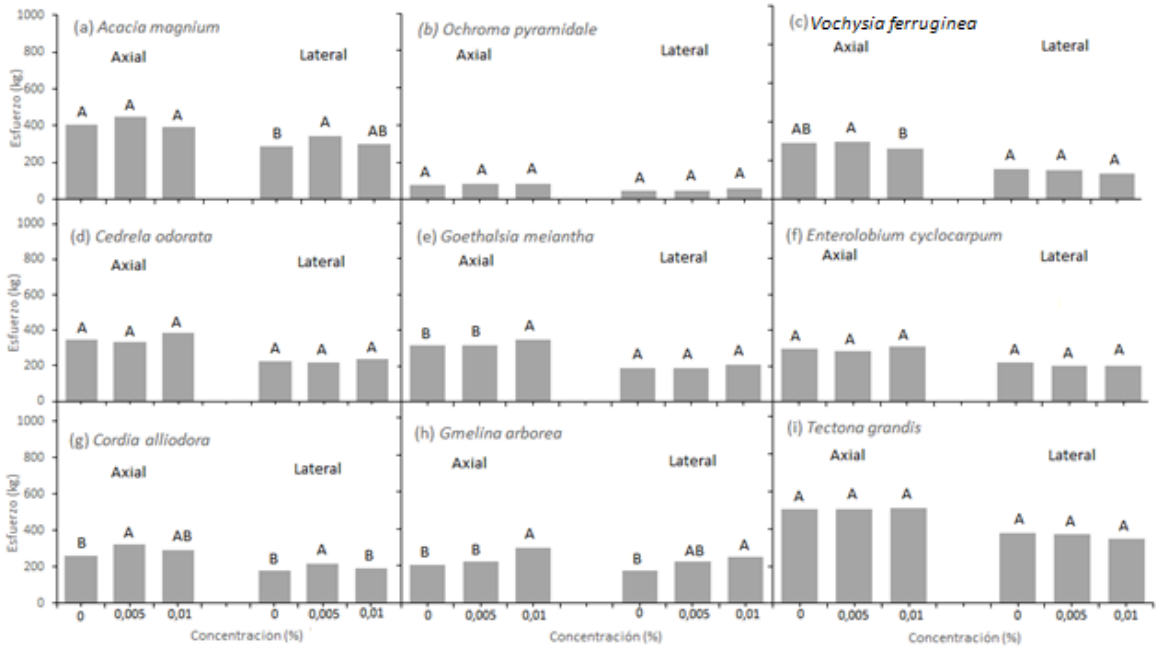

Figura 4. Esfuerzo promedio de la dureza axial y lateral en madera de nueve especies tropicales con diferentes concentraciones de MWCNT´s-OH.

Nota: Los valores medios identificados con las letras A y B son estadísticamente diferentes en $\alpha = 99$ %.

5. Compresión paralela a la fibra

En la compresión las maderas de *Gmelina arborea, Goethalsia meiantha* y *Ochroma pyramidale* son las únicas que presentan diferencias significativas entre sus tratamientos (Cuadro 3). *Gmelina arborea* presenta un valor mayor en el tratamiento de 0,005%, *Goethalsia meiantha* no presenta diferencias cuando la madera es tratada con nanotubos, pero se si presenta diferencias entre menor esfuerzo de compresión en la madera tratada con una 0,005% de concentración en relación con la concentración de 0,001%. Finalmente en la madera de

Ochroma pyramidale presenta cuando es tratada con nanotubos valores de resistencia en compresión debajo del valor del testigo.

Cuadro 3. Esfuerzo en la compresión paralela a la fibra en madera de nueve especies tropicales con diferentes concentraciones de MWCNT´s-OH.

Especie	Esfuerzo (MPa)		
	0%	0,005%	0,01%
Acacia magnium	44,27^{A}	45,95^{A}	42,57^{A}
Cedrela odorata	37,68^{A}	38,31^{A}	38,99^{A}
Cordia alliodora	36,06^{A}	31,85^{A}	35,24^{A}
Enterolobium cyclocarpum	29,41^{A}	33,58^{A}	33,70^{A}
Gmelina arbórea	37,21^{B}	48,75^{A}	40,69^{B}
Goethalsia meiantha	35,89^{AB}	30,73^{B}	36,84^{A}
Ochroma pyramidale	11,48^{A}	6,60^{B}	7,23^{B}
Tectona grandis	40,83^{A}	42,11^{A}	41,55^{A}
Vochysia ferrugia	28,89^{A}	25,81^{A}	27,59^{A}

Nota: Los valores medios identificados con las letras A y B son estadísticamente diferentes en $\alpha = 99$ %.

6. Esfuerzo cortante paralelo a la fibra

En este prueba de resistencia mecánica las maderas de *Acacia magnium* y *Cordia alliodora* fueron las únicas especies, en las cuales hubo diferencias significativas. En ambos especies cuando la madera es tratada con MWCNT´s-OH a una concentración de 0,005% da como resultado madera con mayor resistencia al cortante en relación a la madera sin nanotubos y tratada con MWCNT´s-OH a una concentración de 0,01%.

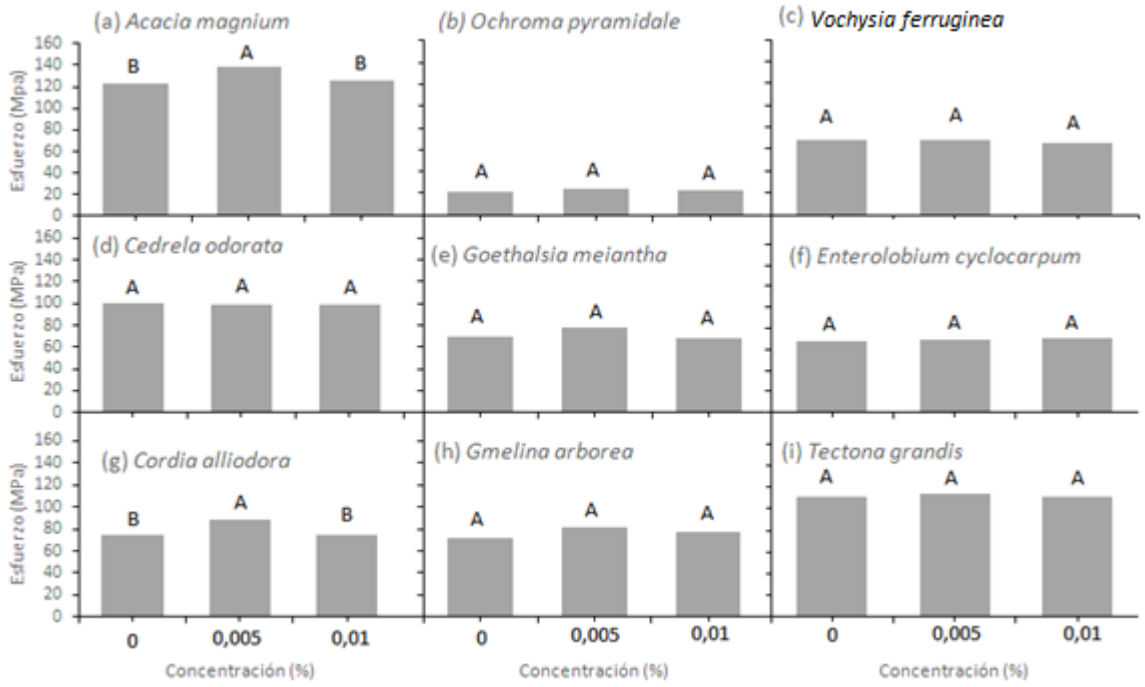

Figura 7. Esfuerzo cortante paralelo a la fibra en madera de nueve especies tropicales con diferentes concentraciones de MWCNT´s-OH.

Nota: Los valores medios identificados con las letras A y B son estadísticamente diferentes en $\alpha = 99$ %.

Discusión

1. Absorción y retención de MWCNT´s

El comportamiento encontrado en la absorción (Tabla 1) aumentó de esta con la disminución de la densidad, concuerdan con los resultados encontrado en otras investigaciones donde sean utilizado algún tipo de nanoparticulas en la madera (Moya et al., 2011). Consecuente a lo anterior, se encontró que una mayor cantidad de MWCNT/kg de madera fueron absorbidos en madera de menor densidad, como es el caso de *O. pyramidale*, *C. alliodora* y *G. meiantha*, mientras que especies como *T. grandis* y *A. mangium*, de mayor densidad, la absorción fue menor y retuvieron menos cantidad de MWCNT/kg de madera (Tabla 1).

La madera de *V. ferruginea* fue la especie que más disolución absorbió a diferencia de *O. pyramidale* que es otra especie también con baja densidad. La baja retención de MWCNT en la madera *T. grandis* es explicado al hecho que esta madera presenta alto porcentaje de albura.

Moya *et al* (2011) reportan que en el tratamiento de vacío-presión la penetración es nula cuando hay madera de duramen; pero con adecuada penetración en la albura.

.

2. Pruebas mecánicas

Aunque varios autores han mostrado que la utilización de MWCNT –OH mejora las propiedades de la madera (Hazarika y Maji, 2014; Younesi *et al*., 2011), los resultados obtenidos en la presente investigación no son congruentes con esos resultados, esto por en la mayoría de las especies no hubo una mejora significativa en las cinco pruebas mecánicas realizadas. Al respecto se establece que las imperfecciones e impurezas en los MWCNT –OH no permiten un adecuado unión de estos con algunos sustractos (De Volder, 2013), por lo que esta situación puede están influenciando el comportamiento de los los MWCNT –OH con las diferentes maderas.

Un aspecto importante también de destacar de los resultados, es la irregularidad que se presentan en las pruebas mecánicas, por ejemplo en algunas pruebas la concentración de 0,005% presentó mayor resistencia que la concentración de 0,01%, como por ejemplo *Gmelina arborea* en la prueba de compresión el mayor valor de esfuerzo se da en el tratamiento de 0,005%, pero en la dureza de esa misma especie se presentó el efecto contrario, el valor de esfuerzo fue mayor en el tratamiento de 0,01%. Esta irregularidad puede ser explicada por el hecho que la madera al ser comprada en depósitos alrededor del Instituto Tecnológico de Costa Rica, no se garantizó una misma procedencia o no se consideró la variación de las propiedades en muchas de estas especies (Moya y Muñoz, 2010)

Otro aspecto que contribuye a la poca efectividad en el reforzamiento de la madera por la inyección de MWCNT –OH dentro de la madera es el tipo de funcionalización utilizado. El grupo hidroxilo, con el cual nos MWCNT fueron funcionalizados, es una de las formas de funcionalizaciones que sirven como precursora (Xie *et al* 2010) Aunque este tipo de grupo funcional utilizado permite interactuar con los cuatro grupos hidroxilo de los polímeros de la pared celular y por lo tanto puede ser utilizado como un agente de reticulación para modificar las fibras de madera (Xie, et al., 2010), esta no fue tan efectiva. O bien la composición química de estas especies, que son muy diferentes entre ellas (Moya et al., 2014), también no permite la interacción adecuada entre los grupos funcionales de lo MWCNT y los de la madera.

Conclusiones

El método de vacío-presión es posible de utilizar para la inyección MWCNT dentro de la madera, no obstante la funcionalización con grupo hidroxilo en los nanotubos no es apta para lograr un reforzamiento de las propiedades mecánicas de 9 especies comerciales de Costa Rica.

Los valores de resistencia mecánica en la madera de las 9 especies de madera no fueron homogéneas por lo que para llegar a establecer verdaderamente el efecto de los MWCNT deben ser considerados algunos aspectos como uniformizar la procedencia del material y utilizar un tipo de funcionalización que permite una mayor interacción con los grupos OH de la madera.

Bibliografía

De Volder, M., Tawfick, S., Baughman, R., & Hart, J. (2013). *Science Journals.* Obtenido de Science Mag: http://www.sciencemag.org/content/339/6119/535.full

Gómez, V. (2011). *Trabajos academicos.* Obtenido de Universidad Politécnica de Valencia: https://riunet.upv.es/handle/10251/13099?show=full

Harazarika, A., & Maji, T. (2014). *Chemical Engineering Journal.* Retrieved from Science Direct: http://www.sciencedirect.com/science/article/pii/S1385894714002277

Lariza, M., López , I., & Sáenz, A. (2012). Obtenido de research gate: http://www.researchgate.net/profile/Marlene_Andrade/publication/257573326_Nanotubos_de_carbonoFuncionalizacin_y_aplicaciones_biologicas/links/004635256f2c5912f1000000.pdf

Moya, R., & Muñoz, F. (2010). Physical and mechanical properties of eight species from fast-growth plantaion in Costa Rica. *Journal of Tropical Forest Science 22(3)*, 317-328.

Moya, R., Muñoz, F., Salas, C., Berrocal, A., Leandro, L., & Esquivel, E. (2011). *Tecnología de madera de plantaciones forestales: fichas técnicas*. Obtenido de Revista Forestal Mesoamericana Kurú: http://tecdigital.tec.ac.cr/servicios/ojs/index.php/kuru/article/view/383/316

Moya, R., Tenorio, C., Berrocal , A., & Salas, C. (2015). *Informe Final de Proyecto.* San José.

ONF. (2013). *Usos y aportes de la madera*. Obtenido de Oficina Nacional Forestal: http://onfcr.org/media/uploads/documents/uyam_onf_2014_3_af_ultimo.pdf

Orináková , R. (2011). *Fuel*. Obtenido de Science Direct: http://www.sciencedirect.com/science/article/pii/S0016236111003693

Pérez, A. (2010). *Revista de Información, Tecnología y Sociedad.* Obtenido de Revistas Bolivianas: http://www.revistasbolivianas.org.bo/scielo.php?pid=S1997-40442010000200003&script=sci_arttext&tlng=es

Serrano, R., & Moya, R. (2011). Procesamiento, uso y mercado de la madera en Costa Rica: Aspectos historicos y analisis crítico. *Revista Forestal Mesoamericana*, 12.

Shmulsky, R., & Jones, D. (2011). *Forest Products and Wood Science.* Obtenido de https://books.google.es/books?hl=es&lr=&id=RvEXYftWIHMC&oi=fnd&pg=PT9&dq=uses+of+CNT+in+wood+fibers&ots=yRvy7ShTKD&sig=VP_7n7WwAxmbcKoDYYm00OUemBg#v=onepage&q=carbon%20nanotubes&f=false

Xie, Y., Zefang , X., Timo, G., Militz, H., Hill, C., Steuernagel, L., & Mai, C. (2010). *Composites Science and Technology*. Retrieved from ELSEVIER: http://ac.els-cdn.com/S0266353810002939/1-s2.0-S0266353810002939-main.pdf?_tid=e955515c-0f86-11e5-be47-00000aab0f02&acdnat=1433950962_c84b246cc91db2ce2502d89874a0e9d4

Yi, Z., Bai, Y., & Bing, Y. (2010). *Drug discovery today*. Retrieved from Science Direct: http://www.sciencedirect.com/science/article/pii/S1359644610001480

Younesi, H., Hiziroglu, S., & Farsi, M. (2011). *Materials and Designs.* Obtenido de Science Direct: http://www.sciencedirect.com/science/article/pii/S0261306911002822

7. Artículo 7

Effects of adding TiO_2 nanoparticles in natural accelerated weathering in nine tropical species of Costa Rica.

Resumen

En este estudio nanoparticulas de oxido de titanio (TiO_2) han sido incorporado en un barniz a base de agua y utilizado en acabado de maderas comerciales. Las TiO_2-nanopartículas fueron evaluado en tres concentraciones: 0%, 1.0 % y 1.5%. las nanoparticulas fueron caracterizadas por Transmission Electron Microscopy (TEM) y X-ray diffractometer (XRD). Los barnices preparados fue evaluado su viscosidad, la adhesión de la película en la madera, la permeabilidad, y los efectos del intemperismo natural sobre color y calidad del acabado. Fue encontrado que la viscosidad disminuye con las TiO_2-nanoparticulas, pero a pesar de esta variación no se produce cambios en el espesor de la película que puede formar sobre la madera. Así mismo adhesión test también no se vio afectado estadísticamente, a excepción de *G. arborea* y *T. grandis*, donde la adhesión aumentó con la incorporación de las TiO_2-nanopartículas. En las 9 especies probadas se encontró que la incorporación de las TiO_2-nanoparticulas disminuye los valores de wáter permeability. En la evaluación del intemperismo natural fue encontrado que cuando no se aplica las nanopartículas la película de barniz se degrada completamente luego de 1 año de exposición, pero la película de barniz modificado se mantiene. El cambio de color, utilizando el sistema Lab (ΔE^*), fue menor en la madera que han sido tratada barniz con TiO_2-nanoparticulas, con la excepción de *E. Cyclocarpum* y *T. grandis* que no presentaron diferencia entre los tres tipos de acabados. EL mejor comportamiento del barniz en las 9 maderas tropicales utilizadas es cuando se le agrega las nanoparticulas a una concentración de 1.5%.

Keywords: coating, nanotechnology, tropical species, aditives, XDR spectro.

Introduction

Las construcciones en madera están generalmente expuestas a un número de factores que deterioran su apariencia y su performance, tales como moisture, UV-radiation, temperature or mechanical stresses. (Veigel *et al.,* 2014). Dentro de la variedad de productos aplicados a la superficie de la madera, varnishes and coatings are used to protect and to enhance the beauty, color and la apariencia natural de la madera (Kaygin and Akgun, 2008). Hoy en día, productos que presten mayor protección y durabilidad en la madera abren la posibilidad de desarrollar nuevas formulaciones en las cuales la utilización de la nanotecnología representa una gran alternativa (Fufa et al., 2012).

The development of nanotechnology, has helped to satisfy the continuous improvement of adhesives and coatings industry (Corcione and Frigione, 2012; Roussak and Gesser, 2013; Peruzzo et al., 2014). Fufa *et al.* (2012) menciona que less than 10% of nanoparticles in the coatings pueden mejorar significativamente las propiedades de la madera.

Nanofillers pueden ayudar a crear una película del barniz o del recubrimiento más resistente al UV-radiation, water, fungal growth, stains and grease (Vlad-Cristea *et al.*, 2012). Numerosos estudios muestran como la adición de nanoclays, nanosilica, nanocellulose, TiO_2 and ZnO nanoparticles,and other kind of nanofillers, incrementan the performance of varnishes and coatings (Gornicka and Sieradzka, 2009; Cristea *et al.*, 2010; Salla *et al.*, 2012; Veigel *et al.*, 2014).

La adición de nanopartículas de TiO_2 in coatings such as UV blocking agents is an extended practice. The TiO_2 nanoparticles además de bloquear grandes proporciones de radiación solar, proporciona photostabilization as a coating. (Fufa *et al.*, 2012; Nikolic *et al.,* 2015). Asimismo antimicrobial and bactericide activity hacen del TiO_2 nanoparticles una opción para la protección de madera expuesta al daño producido por condiciones ambientales (Cristea *et al.*, 2010).

Las condiciones ambientales presentes en la región tropical, altas temperaturas y la presencia de precipitaciones casi durante todo el año, permiten que en países como Costa Rica se pueda desarrollar una gran variedad de especies arbóreas maderables (Thompson 1995). Sin embargo, una limitante que se ha encontrado con el uso y aprovechamiento de muchas especies utilizadas en la reforestación según Moya y Muñoz (2010), ha sido los pocos conocimientos

acerca de las propiedades químicas, secado, preservado, durabilidad natural de la madera y resistencia o cambio de color de los acabados aplicados en estas especies de madera.

En general los estudios del deterioro del color y del acabado mismo en la superficie de la madera con nanopartículas o sin ellas, están orientados a especies de regiones templadas tales como: *Betula pendulata* (Oltean et al. 2008), *Cryptomeria japonica* (Tovaj y Mitsui 2005) y *Picea albies* (Petric et al. 2004, Deka et al. 2008, Oltean et al. 2008, Ahajji et al. 2009, Fufa et al., 2012). Esta orientación ha hecho que muchas de las fábricas de acabados, incluidas las de Costa Rica, desarrollen sus productos con base en el comportamiento en maderas de climas temperados. No obstante, algunos pocos estudios del comportamiento de los acabados en maderas que crecen en el trópico han sido llevados a cabo, entre los cuales se destacan los estudios en *Cedrela odorata*, *Carapa guianenesis*, *Tectona grandis* y *Acacia mangium* (Valverde y Moya, 2010, 2013) con viarios acabados y evaluados en intemperie natural y acelerado.

La degradación de la superficie del acabado sobre la madera (color y degradación) expuesta a la intemperie, es una de las limitantes de los coatings (Schnabel et al. 2009). Diferentes estudios (Ahajji et al., 2009; Deka et al., 2008; Oltean et al., 2008), han encontrado que la luz ultravioleta (UV), la luz visible y la infrarroja son las que generan las mayores reacciones químicas en los componentes de la madera y el acabado mismo, lo cual provoca su degradación.

The purpose of this work was to study the effect of the addition of TiO_2 nanoparticles en la resistencia a los rayos UV de un recubrimiento para madera a base de agua aplicado sobre nine tropical species (*Acacia mangium, Cedrela odorata, Cordia alliodora, Enterolobium cyclocarpum, Gmelina arborea, Goethalsia meiantha, Ochroma pyramidale, Tectona grandis and Vochysia ferruginea*) from low and high density. Also to show changes that occurred en la viscosidad, nivel de adhesion y permeabilidad de los acabados. The durability of nanocomposites coatings was evaluated through aging behavior in artificial and natural weathering.

Materials and methods

Materiales

Se utilizó nanopartículas de dióxido de titanio (TiO2 nps) con marca comercial Hombitec RM 400 ® (http://www.sachtleben.de/fileadmin/pdf_dateien/brochures/043_HOMBITEC.pdf) , suministrados por Sachtleben Chemie (Germany). La información suministrada por el fabricante indica que es una nanoparticula de TiO_2 de long-term UV-absorbers para ser utilizado en acabados para madera, con tamaño de partículas de approximate primary particle size of 10 nm, specific surface area of 110 m^2 g^{-1}, yellowish in powder appearance and TiO_2 percentage of 78%.

Las nanopartículas fueron probadas en un acabado para madera suministrado por la empresa Xilo Química (Costa Rica), el acabado es marca comercial de Barnizol®, dicho barniz es a base agua y contiene 3-10% dispersante acrílico, 1-5% Natrasol 250, 1-8% de Texanol, 1-5% Propilenglicol, 0.1-3% Triton X-100, 1-5% de Trietanolamina y 1-5% de Poliacrilato de sodio y comúnmente se utiliza pigmentos de TiO_2 (http://www.grupoxilo.com/app/files/chemicalproducts/files/26_techfile_barnisoluv.pdf).

Las especies utilizadas para probar el acabado con nanopartícula fueron *Acacia magnimum, Cedrela odorata, Cordia alliodora, Enterolobium cyclocarpum, Gmelina arborea, Goethalsia meiantha, Ochroma pyramidale, Tectona grandis and Vochysia ferrugia*, las cuales son maderas utilizadas tradicionalmente en Costa Rica para la fabricación de puertas y productos a base de madera o bien en productos de ingeniería que demanda el uso intensivo de acabados (Diener and Saklad, 1997, Moya et al., 2015a-b). Estas maderas fueron obtenidas de diferentes sitios de comercialización de madera aserrada.

Coating preparation with TiO_2 nps

Al barniz se le agregó las nanopartículas de TiO2 nps en dos concentraciones en relación al peso: 1% y 1.5%. Las evaluaciones se realizan con respecto a un barniz al que no se le agregan TiO_2-nanoparticle. Por tanto 3 tipos de barniz fueron preparados: 2 con nanopartículas (1.0 y 1.5%) y uno sin nanopartículas. La incorporación de los la nano-partículas de TiO2 en la resina fue realizada en dos etapas: en la primera parte fue calculado el weigth de las nanopartículas necesarias para preparar 4 litros del acabado con las concentraciones de 1% y 1.5%. Luego, esta cantidad de nanopartículas fueron diluidas en 100 mL de agua (dispersión A), utilizando una agitación mecánica. La segunda etapa, la mezcla de

la dispersión acuosa de nanopartículas fue mezclada en la pintura. Para ello los diferentes componentes del acabado (resina, agua diluyente y aditivos) fueron calculados sus proporciones. La resina iba siendo agregada lentamente en el diluyente hasta lograr la suspensión total, luego los aditivos fueron siendo agregados lentamente y paralelamente las nanopartículas fueron agregadas también lentamente hasta garantizar su dispersión.

Caracterización del barniz

Primeramente la estructura y presencia de las nanopartículas en el coating, fueron observadas mediante el uso de Transmission Electron Microscopy (TEM), X-ray diffractometer (XRD) y su viscosidad. TEM fue utilizado fue utilizado un equipo Hitachi HT-7700. nanopartículas de TiO_2 fue tomado una muestra de 1.1 mg y se agregó 1 mL de Etanol al 95 % y ultrasonifico por 20 minutos. Luego se tomó una muestra de 2 μL y se colocó en una Cu-600 mesh grid recubierta con una película de Collodion.

For X-ray diffraction patterns, cured varnishes were obtained with the PANalytical Empyrean Series 2 diffraction meter (Cu-Kα, 6°-40° 2θ) using the PANalytical-High Score Plus software. El análisis de las muestras se estudió en el rango de bandas características del TiO_2, que es de 2θ con un rango de 20° a los 80°. Las muestras para el estudio de XRD diffraction patterns fue necesario preparar un film de aproximadamente 1 mm de espesor X 26 mm de largo X 76 mm ancho. Para sobe una lámina de vidrio fue formado un rectángulo con neopreno de 1.5 mm. Luego fue vertido el coating sobre este rectángulo. Esta muestra se dejó secando temperatura ambiente por dos días.

En el caso de la viscosidad, se realiza utilizando a 600 mL Low Form Griffin Beaker having a working volumen of 500 mL de los adhesivos en el viscosímetro de Brokfield-11+ Pro LV. 2.4.4. (ASTM, 2014). Se utiliza the spindler number 3 para los 3 tipos de acabado according to the ASTM D2256-11 standard (ASTM, 2011). Se evaluaron viscosidades en las velocidades de 2, 5,8, 11, 14, 17, 20, 26, 29 and 35 rpm.

Wood species, surface preparation and application of coating:

El comportamiento de los tres tipos de acabados (2 con nanopartículas y 1 sin ellas) fueron evaluados en 9 especies tropicales (*Acacia magnimum, Cedrela odorata, Cordia*

alliodora, Enterolobium cyclocarpum, Gmelina arborea, Goethalsia meiantha, Ochroma pyramidale, Tectona grandis and *Vochysia ferrugia*). En cada especie fueron preparados 945 muestras con dimensiones de 150 mm de largo X 65 mm ancho X 4.3 mm espesor.

Prior to application of the coatings, the all sample surfaces were polished using a sandpaper #100. y two layer coatings fueron aplicadas with a Laboratory Lacquer Roller Coater machine (BKL Burkel). Todas las muestras fueron acondicionadas por una semana a una condición de 12% de contenido de humedad.

Dry film thickness, adhesion test and water permeability

El comportamiento de los tres tipos de acabados (2 con nanopartículas y 1 sin ellas) en las 9 especies tropicales fue evaluado el espesor del film del recubrimiento en seco (dry film thickness), adhesión, absorción de humedad. Primeramente fue medido el espesor de dry film thickness de acuerdo con ASTM D6132-13 standard (ASTM, 2014a). Y para ello fue utilizado el medidor PosiTector® 200 series ultrasonic coating thickness gage (DeFelsko, USA). Esta prueba fue medido en 81 muestras de las preparadas con acabado y en cada muestra fue medido en 2 diferentes puntos (9 especies x 3 acabados x 3 muestras x 2 puntos diferentes=162 mediciones).

Luego estas muestras fueron partidas en dos partes: una parte fue utilizada para medir la adhesion by tape test fue realizada according to the ASTM D3359-09 standard (ASTM, 2014a), la cual consiste en rajar la película de acabado con cross hatch cutter handle en dos sentido (uno perpedicular a la otra), luego en le punto de cruce se coloca una adhesive tape y luego se procede a remover the tale by pulling in a single smooth action. El daño provocado en la pelicula del acabado es clafisicado 6 clases en relación al aréa removida y detallada en la norma ASTM D3359-09.

La otra parte de la muestra fueron utilizadas para medidar la absorcion de agua acorde a la metodologia propuesta por Kowalczyk (2014) and Ekstedt and Östberg (2001). Las muestras con el acabado en sus edges and back side were coated with paraffin wax para evitar el ingreso de agua a través de las zonas desprovistas de barniz. Luego que esas partes estuvieran secadas (24 horas despues), las muestras fueron pesadas y colocadas con la superficie con el acabado en contacto de distilled wáter. Las muestras fueron nuevamente pesadas en peridoo de 24 y 72 horas y finalmente se peso y terminó el periodo de absorción de agua a los 7 days. The water

permeability (WP) was determined as the increase weight of the test samples, according to the following equation:

$$WP\ (\frac{g}{m^2}) = \frac{m_2 - m_1}{A} \qquad \text{(Equation 1)}$$

Where: m_1 is the mass of a sample (before testing), m_2 is the mass of water-treated sample, A is the area of a tested varnished surface.

Wood color evaluation

El color fue evaluado por medio de la exposición de las 9 especies de madera con los 3 tipos de acabados con nanopartículas (0.0%, 1.0% y 1.5%) por weathering**.** Two kinds of weathering exposure were tested: natural and artificial: A total of 432 samples were tested (9 especies x 3 acabados x 16 muestras) para cada condicion de exposición. In natural weathering (NW), wood samples are exposed for 365 days (1 years) with an inclination of 15º south in an area free of shade and where the rain, sun and wind impacted directly upon the samples. The test began in November 2013 and finished in November 2014. Wood samples were exposed in the Cartago province of Costa Rica (9°50'59"N; 83°54'37"W). The climatic conditions were widely detailed by Valverde and Moya (2014) and Salas et al. (2015). For the artificial weathering (AW), UV exposure was administered by means of a weathering Q-Lab camera (QUV/spray model). The ASTM G-154 standard was applied for this test (ASTM 2013a). The exposure consisted of 4-hour cycles in two phases: first, 4 hours of UV radiation at 50 ºC and 0.71 W/m^2 (with mercury bulb type UVB 313L and wave length 310 nm), then a second phase of condensation that took two hours and consisted of using evaporated water at 50ºC. The total exposure amounted to 500 hours for each species. For AW, the color was measured al final de las 500 horas de exposición, but para NW el color fue evaluado en diferentes periodos de tiempos. Wood samples in this condition were evaluated between the 10th and 12th hour in the morning and without any event of rain before the measurement. And the color of the surface were measured each 15 days during the first 3 months, afterwards color was measured month until exposure time was up each month.

Color measuring was done with a Hunter Lab mini Skan XE Plus spectrophotometer. The CIE Lab standardized chromatologic system was used. The range of this measurement is from 400 to 700 nm with an opening at the point of measurement of 11 mm. For the observation of reflection, the specular component (SCI mode) was included at a 10º angle,

which is normal for the specimen surface (D65/10); a field of vision of 2º (Standard observer, CIE 1931) and an illumination standard of D65 (corresponding to daylight in 6500 K). The mini Skan XE Plus generated three parameters for each measurement, namely: L*(luminosity), a* (tendency of color from red to green), and finally b*(tendency of color from yellow to blue).

Color change (ΔE*)**: ***)**:** It was determined as the color net variation for each finish in a period of time. This difference was determined according to the ASTM D 2244 standard formula is detailed in equation 1 (ASTM 2013b). The color difference was determined for each type of finish in each species in the different types of exposure.

$$\Delta E^* = \sqrt{(\Delta L)^2 + (\Delta a)^2 + (\Delta b)^2} \qquad (1)$$

Where:

ΔE*= wood color difference; ΔL= L* value before weathering – L* value in different types of exposure; Δa= a* value before weathering - a* value in different types of exposure; Δb= b* value before weathering - b* value in different types of exposure.

Evaluation of the quality of finish: The evaluation of the quality of finish in each species and their behavior to weathering (NW as well as AW) the ASTM D-660 standard (ASTM 2013c) was used, that establishes an evaluation for the different kinds of deterioration that finishes face: irregular, long line, short parallels, mosaic and switch. In general, deterioration is evaluated on an even scale from 2 to 10, in which, as the number approaches 2 it means a greater deterioration of the finish. Y esta fue evaluado solamente al final de tiempo de exposición 365 dias en NW and 500 hours in AW.

Statistical analysis: A one-factor (one-way-Anova) analysis of variance per species was applied to finish color parameters. The model included the following sources of variation: finishing (f), pretreatment (*c*), the interactions between weathering and pretreatment (Equation 2). The difference among the averages was assessed through Dunnett's test with a level of significance of $P<0.05$, where the control treatment consists of wood samples without any finishing or pretreatment. Also, the influence of the change in color parameters (ΔL*, Δa* y Δb*) on total color change (AE *) was evaluated using multiple regression analysis (Equation

3) on the wooden surface with different finishes. Each parameter change in the regression was assessed using a significance level of 99%.

$$Y_{ij} = \mu + f_i + c_j + f * c_{ij} + e_{ij} \qquad (2)$$

$$\Delta E^* = \Delta L + \Delta a + \Delta b + e_{ij} \qquad (3)$$

where Y_{ij} is the single observation of each color parameter of the ij-wood sample, μ is the overall mean, *f* is the i_{th}-finishing type fixed effect, *c* is j_{th}-pretreatment fixed effect, $f*c_{ij}$ is the random interaction between the i_{th} finishing type and the j_{th} pretreatment, and e_{ij} is the residual random effect.

Regarding the quality of finishes with different coatings (with TiO_2) nanoparticles the quality index of degradation (SQI) was developed, that considers the 5 types of flaws evaluated under the ASTM D-660 standard (ASTM 2013c); namely, irregularities, long lines, short parallels, switch and mosaic. The weighting considered the importance of the appearance of flaws, the surface with long lines being the one with the highest weighting (50%), and then short lines (25%), switch surface (15%) and finally, irregular surface (10%). The mosaic flaw was not considered in this index because this flaw was not observed in any sample. Subsequently, SQI behavior was evaluated with exposure time in NW and AW using equation 4.

$$SQI = (IR * 0{,}10) + (LL * 0.50) + (SP * 0.25) + (SS * 0{,}15) \qquad (4)$$

Where: IR: Irregular flaw; LL: Long Line flaw; SP Short Parallel flaw; SS: Switch flaw.

Results and discussion

Coating characterization

TEM observations and XRD patters

TEM observations of TiO_2 nanoparticles showed that the TiO_2 powders in rutile phase consist of both spherical and rod shapes (Figure 1a-b). Furthermore, it can be estimated that the particle size of samples are microscale with the grain size about 30-70 nm. Entre tanto, XRD patterns de los nanopartículas de TiO_2, así como la presencia de estos en los acabados con mostrados en la Figura 1a. Las nanopartículas de TiO_2 exhibieron strong diffraction peak en 27,

36, 41, 43, 54, 56, 62, 68 and 69, correspondiente a la difraction de (110), (101), (200), (111), (210), (211), (220), (002), (310), (301) and (112) planes de rutille TiO_2 (JCPDS number 98-003-3842). El ritile fase, powder containing randomly crystals and both spherical and rod shapes (Kim et al., 2013, Tahir et al., 2006). El caso de las nanopartículas en el acabado en el patrón XRD es diferente, se presenta strong difraction peak en 27 en la pintura de las dos concentraciones (Figura 1c). En tanto, se señales débiles en 36, 41 and 43 de TiO_2 de los acabados con TiO_2 (Figura 1e y 1f), pero las señales en 54 y 56 de TiO_2 en XRD patrón se presentan débilmente en el acabado con concentración de 1.5% (Figura 1f). Este debilitamiento de las señales del TiO_2 en los acabados son atribuidos a que se está perdiendo cristalinidad y se están formando nuevas estructuras (Sun et al., 2013).

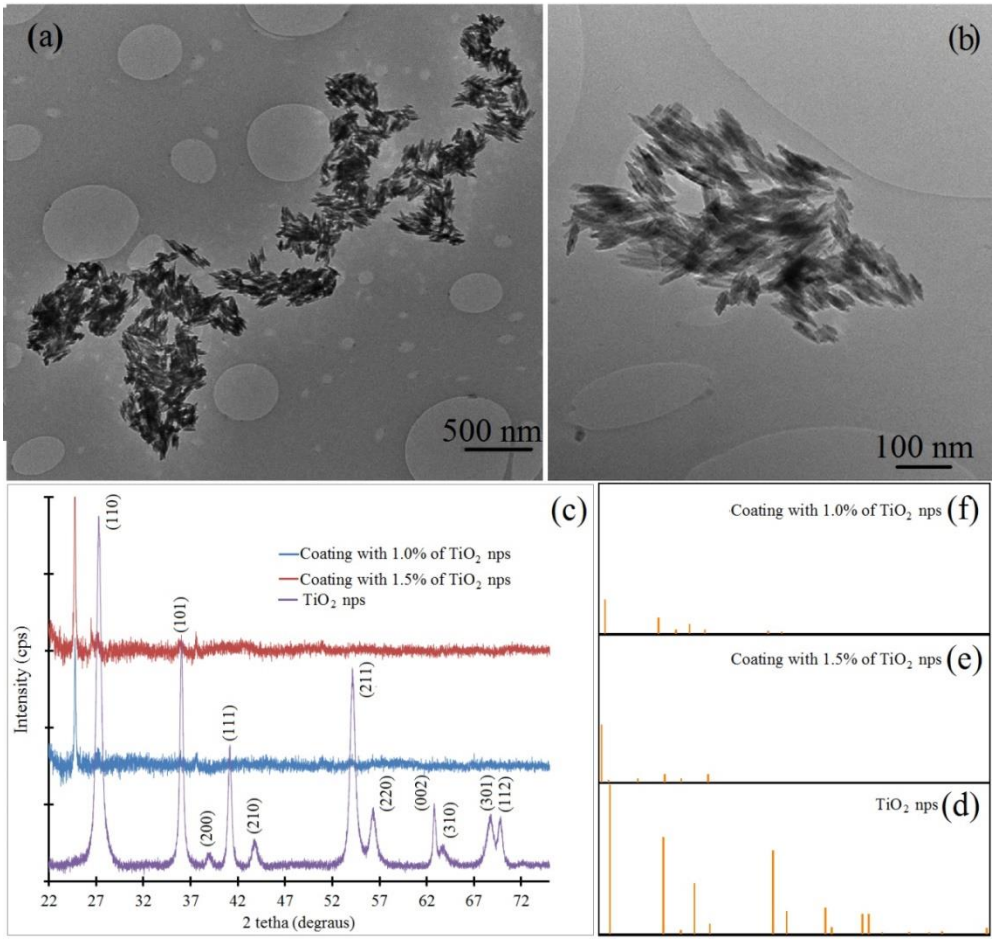

Figure 1. (a) and (b) Transmission electron microscopy-TEM showing shape of TiO2 nanoparticles. (c) XRD patterns of TiO_2 and coatings with 1.0% and 1.5% of TiO_2 nanoparticles and (d), (e) and (f) comparison of diffraction intensity between rutile TiO2 and coatings with 1.0% and 1.5% of TiO_2 nanoparticles and.

Viscosity

La viscosidad disminuye al aumentar the rotational speed en los 3 different coatings (Figura 2) comportamiento conocido como "shear-thinning", característico de los fluidos pseudoplásticos (Barnes et al., 1989). Los coatings que se le ha agregado las nanopartículas de TiO_2 no muestran una variación significativa en velocidades inferiores a las 5 rpm; pero luego de esta velocidad se observa una leve disminución en la viscosidad de los coatings modificados con respecto al coating without TiO_2 nanoparticles. Pero hay un comportamiento inestable con el incremento de la concentración de TiO_2. La viscosidad menor en el acabado con 1.5% de TiO2 en relación con el acabado con 1.0% (Figura 2).

Acorde con Santillán et al. (2008), al estudiar la viscosidad de soluciones de TiO2 de diferentes concentraciones indican que The shear-thinning flow en una solucción colloidal particles agglomerates son were broken with increased shear stress and rate, which resulted in the reduction of suspension viscosity, lo cual sería la explicación de la disminución de la viscosidad con la adición de las nanopartículas en el acabado. La menor viscosidad encontrada en el acabado con 1.0% de TiO2 en relación con el acabado con 1.5% puede ser debido a que en la concentración de 1.5% the start of sedimentation and the agglomeration of particles as a result of the Van der Waals attractive potential between neighbouring particles in the liquid medium (Tseng and Chen 2003).

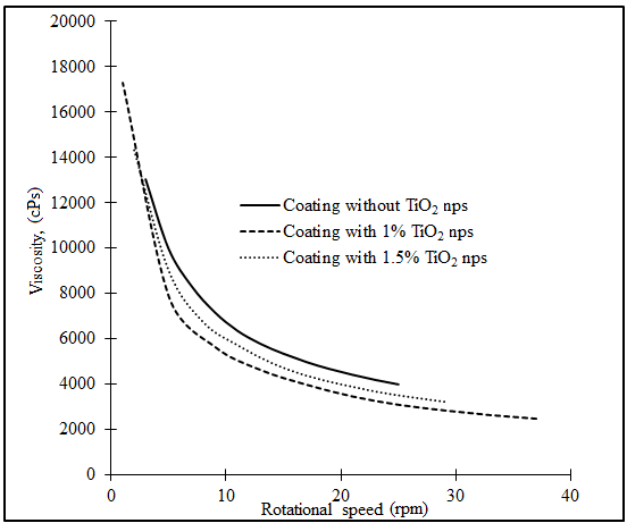

Figure 2. Absolute viscosity of tested coatings with different concentration of TiO_2 nanoparticles.

Film thickness and adhesion test measurements

The film thickness en los acabados con las dos concentraciones de TiO_2 no fueron afectados significativamente en la mayoría de las especies, a excepción de *G. arborea* y *T. grandis* que se presentaron diferencia estadísticas solamente entre el acabado con una concentración de 1.5% nanopartículas en el acabado sin estas nanopartículas (Tabla 1). Un aspecto importante de destacar en los resultados del film thickness de *O. pyramidale* es que valor fue varío de 58.0 a 60.5 μm, valores muy superiores al resto de las especies que varío de 30.5 a 35.1 μm.

La evaluación de adhesión test mostró que se presentaron diferencia en *G. arborea* y *T. grandis*. En las dos especies fue encontrado que la película de acabado fue evaluada con mayor adhesión cuando es aplicado acabado con nanopartículas de TiO_2 (Tabla 1). En el resto de las especies la adhesión no se presentó diferencias entre el acabado con la nanopartículas y el acabado sin estas nanopartículas.

La pueba de adhesión test valorá la resistencia entre la capaz de varniz sobre la superficie de madera, por un lado se mide la fuerza de adhesión entre el acabado y la superficie de madera, así como las fuerzas internas del acabado (cohesion) (Kaygin and Akgun, 2008). Entonces acorde con los resultados de adhesion test (en todos los casos mayor a 4B), el acabado al agregarle las nanoparticulas de TiO_2 mostró adecuado propiedades de adhesion y similares al acabado que no se le agrega ningun tipo de nanopartícula, por lo que las nanopartículas no afectan las fuerzas que intervienen en la adhesión de la pelicula de acabado y la superficie de madera. Sin embargo en *C. odorata* la adhesión de la película es debil, ya que se obtiene los valores más bajo en la prueba de adhesión, probablemente influenciado en la alta cantidad de extractivos no polares presente en este tipo de madera (Chan et al., 1967; Parra et al., 2015), dando como resultado las fuerzas que intervienen en la adhesión con el acabado y la superficie de madera no sean bajas (Kaygin and Akgun, 2008).

Table 1. Film thickness and percent area removed in coating test using different concentration of TiO_2 nanoparticles.

Species	TiO_2-nps (%)	Film Thickness (µm)	Area removed (%)
Acacia mangium	0.00	33.9 a	2 (4B)
	1.00	33.0 a	9 (4B)
	1.50	35.1 a	2 (4B)
Cedrela odorata	0.00	34.7 a	0 (3B)
	1.00	34.7 a	0 (3B)
	1.50	34.3 a	0 (3B)
Cordia alliodora	0.00	33.4 a	2 (4B)
	1.00	34.3 a	2 (4B)
	1.50	30.5 a	1 (4B)
Enterolobium cyclocarpum	0.00	34.7 a	0 (5B)
	1.00	35.1 a	0 (5B)
	1.50	34.3 a	1 (5B)
Gmelina arborea	0.00	36.4 a	1 (4B)
	1.00	33.9 ab	1 (5B)
	1.50	31.3 b	1 (5B)
Goethalsia meiantha	0.00	33.4 a	2 (5B)
	1.00	33.0 a	1 (5B)
	1.50	33.4 a	1 (5B)
Ochroma pyramidale	0.00	58.0 b	9 (4B)
	1.00	58.8 b	5 (4B)
	1.50	60.5 b	5 (4B)
Tectona grandis	0.00	33.0 b	2 (4B)
	1.00	34.3 ab	17 (5B)
	1.50	35.1 a	3 (5B)
Vochysia ferruginea	0.00	33.4 a	1 (4B)
	1.00	34.3 a	2 (4B)
	1.50	32.2 a	2 (4B)

Water permeability

Los resultados the water permeability test en los diferentes tiempos evaluados (24 h, 72 h y 168 h) mostró que el valor aumenta con el tiempo de inmersión agua de la madera con la película de acabado en los tres surface coatings (Figure 3). Además fue observado que para cada tiempo de absorción el valor de water permeability fue similar en las diferentes especies,

con la excepción de *C. odorata* y *G. arborea* (Figura 3b y 3e) que en los tiempos más prolongados los valores fueron ligeramente menores al resto de las especies. En los resultados de las diferentes especies se encontró que en *E. cyclocarpum* y *T. grandis* no se presentaron diferencia significativas en el valor de water permeability de los diferentes acabados de la superficie en los diferentes tiempos (Figura 3d y 3h). En tanto en *C. odorata* y *C. alliodora* no se presentaron diferencia significativas en el valor de water permeability en los tiempo de 24 y 72 horas, pero en el tiempo de 168 horas la superficie de la madera con acabado de nanopartículas de TiO_2 presentaron menor water permeability (Figura 3b y 3c). En el resto de las especies (*A. mangium*, *G. arborea*, *G. meiantha*, *O. pyramidale* y *V. ferruginea*) en 24 horas de inmersión en agua la superficie de la madera con el acabado de nanopartículas en cualquiera de las dos concentraciones no afecta water permeability, pero cuando el tiempo de inmersión aumenta a 72 o 168 horas, los dos acabados con TiO_2 disminuye los valores de water permeability en relación al acabado sin este tipo de nanopartículas (Figura 3a, 3e-g y 3i).

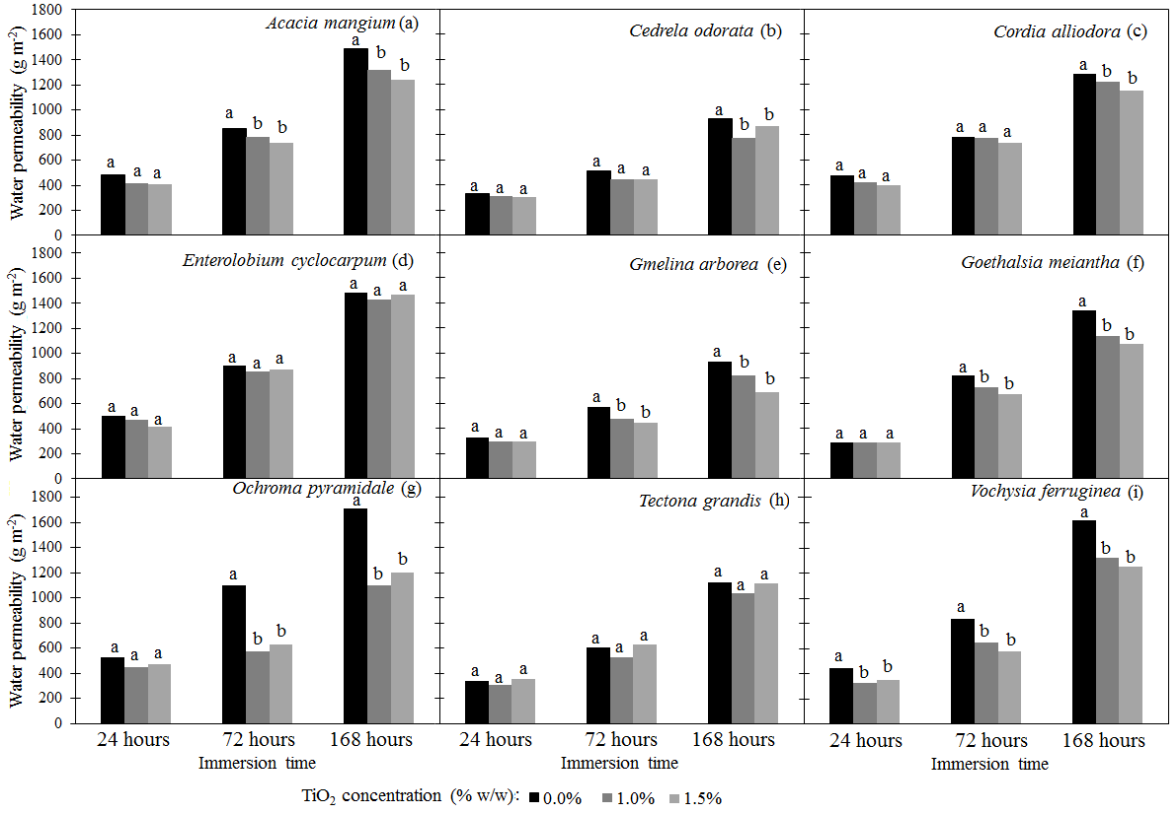

Figure 3. Water permeability for coatings with TiO_2 nanoparticles tested in nine tropical species.

El ingreso de la humedad en madera con acabados es determinada por la permeabilidad del acabado y es menos determinado por las propiedades de sustracto o madera (Ekstedt & Östberg 2001). Acorde con este afirmación es que se presentaron valores de water permeability similar entre las especie, comportamiento también encontrado por Ahola (1991) y Ekstedt & Östberg (2001) para varias especies de clima temperado. En el caso de los bajos valores de *C. odorata* y *G. arborea* puede ser explicado que estas especies tienen más altos valores de water permeability que las otras especies de madera (Eligon et al., 1992; Chauhan & Aggarwal, 2004), lo que hace que la poca cantidad de agua que absorbe el acabado sea poca afin con la maera de esas especies.

La permebilidad de los abacados esta influenciado en primer lugar por el tipo de solvente que se utiliza para disolver la resina, por lo general the water-borne coatings tending to be more permeable than the solvent-borne coatings (Ahola et al., 1999). Siendo este factor la principal causa que los valores de water permeability encontrado en el presente estudio sean altos (Figure 3) ya que el acabado usado es de tipo solvent-borne coatings Así mismo la permeabilidad del acabado es influenciado por la adición de binder and solvent types, and pigment volume concentration y sobre todo por componentes que contengan grupos de hydroxyl and etheric groups (Kowalczyk, 2014). Pero al agregar las nanopartículas de TiO2 estos grupos son menos disponibles al agua, reduciendo la absorción de agua en acabados modificado con estas nanopartículas en las diferentes especies que fueron analizadas en este estudio.

Cambio de color

El cambio de color (ΔE*) varío entre las especies, el tipo de weathering y la concentración de nanopartículas (Figura 4). Se encontró además un mayor ΔE* en las muestras que fueron expuestas al natural en relación a aquellas en condición acelerada. El acabado que no fue agregado las nanopartículas el cambio de color fue estadísticamente mayor que los dos acabados con las diferentes concentraciones nanopartículas de TiO_2 en la madera de *E. cyclocarpum* en la condición acelerada (Figura 4d), pero en *A. mangium* y *C. odorata* solamente se presentó diferencia en ΔE* en el acabado con 1.5% de nanopartículas de TiO_2 (Figura 4a-b). En tanto que *C. alliodora*, *G. arborea*, *G. meiantha*, *O. pyramidale* y *V. guatemalensis* en accelered weathering el acabado sin nanopartículas tuvo un valor de ΔE* estadísticamente menor de que los acabado con TiO_2 (Figura 4c, 4e-g, 4i). *T. grandis* fue la

única especies donde no se presentaron diferencias estadísticas entre los diferentes tipos de acabados (Figura 4h).

En relación con los diferentes tipos de acabados en la condición de accelered weathering se presentó valor estadísticamente menor en el acabado con 1.5% de nanopartículas de TiO_2 en *A. mangium*, *C. odorata*, y *V. ferruginea* (Figura 4a-b, 4i). No se presentaron diferencia estadísticas entre los acabados con TiO_2 en *C. alliodora*, *E. cylcocarpum* y *T. grandis*. La única especie donde la concentración de 1.0% fue mayor a la concentración de 1.5% fue en *G. arborea* y *G. meiantha* (Figura 4e-f).

En las condiciones de natural weathering fue observado que el acabado que no se le aplicó las TiO_2-nanoparticle en la condición de natural weathering a los 365 días de evaluación ya no estaba presente, por lo que ya estaba expuesta la superficie de madera y en ella condición fue medida el color. En la mayoría de las especies el acabado sin nanopartículas de TiO_2 el cambio de color (ΔE^*) fue estadísticamente mayor que en los acabados que presentaban nanopartículas, con la excepción de *E. Cyclocarpum* y *T. grandis* que no presentaron diferencia entre los tres tipos de acabados (Tabla 4d y 4h). Y al observar el comportamiento del ΔE^* con el tiempo en esta condición fue confirma nuevamente que, con excepción de *E. cyclocarpum* (Figura 5d), el cambio de color en la superficie de madera es menor en los acabados con TiO_2 nanoparticle (Figura 5). En relación con los acabados con las dos concentraciones (1.0 y 1.5%) solamente se observó un valor de ΔE^* estadísticamente menor en la concentración de 1.5% en la madera de *V. guatemalesis* (Figura 4i). El resto de las especies (*A. mangium*, *C. odorata*, *C. alliodora*, *G. arborea*, *G. meiantha* and *O. pyramidale*) los acabados con TiO_2-nanoparticulas fueron estadísticamente iguales (Figura 4). Pero en el comportamiento en el tiempo durante el tiempo de exposición en el tiempo se observa que en *C. odorata*, *C. alliodora* and *T. grandis* se el menor ΔE^* se presentó en el acabado con 1.0% de TiO_2-nanoparticule (Figure 5b-c, 5h), y en resto de las especies se presentan poca diferencia entre especies (Figura 5).

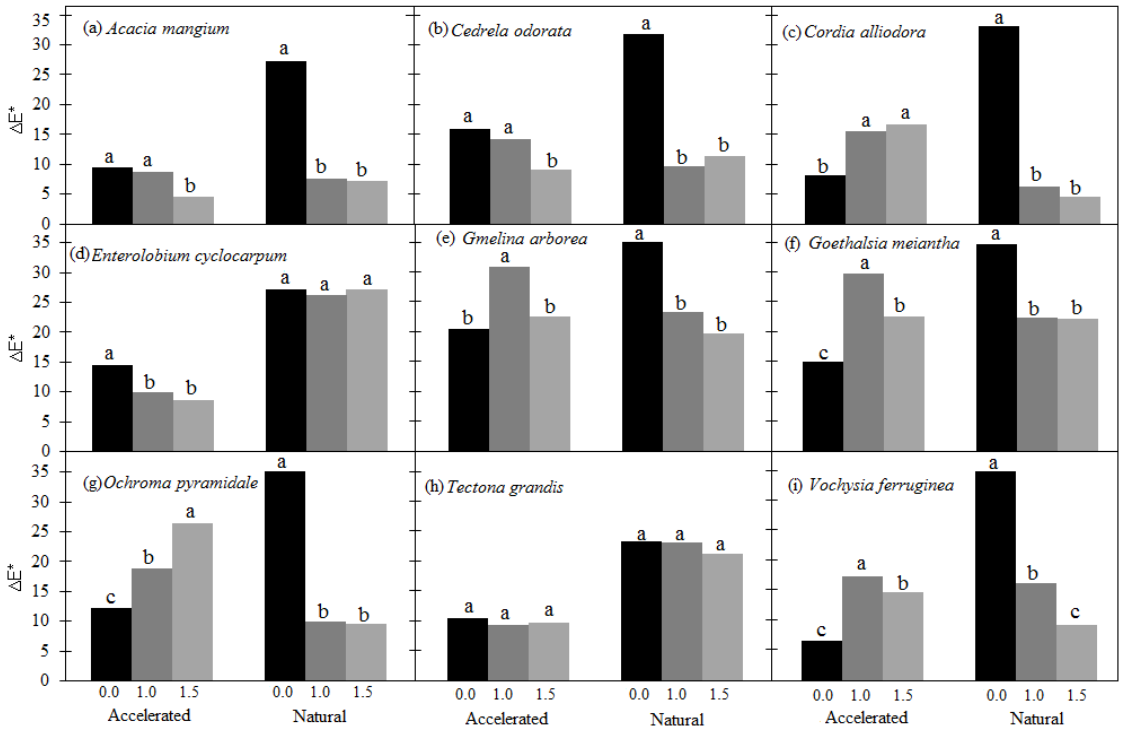

Figura 4. Color change (ΔE*) values of 3 types of coating with different TiO_2-nanoparticles exposed to natural and accelerated weathering in 9 tropical wood.

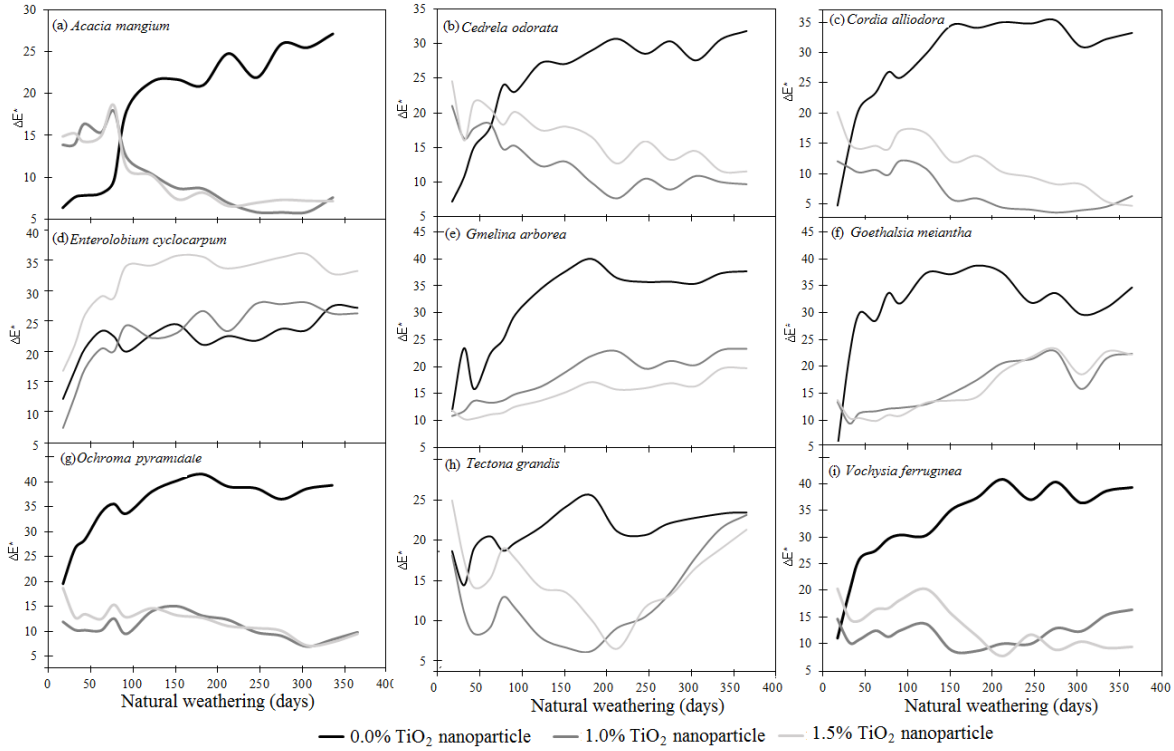

Figura 5. Variations in the time of ΔE * in of 3 types of coating with different TiO_2-nanoparticles exposed to natural weathering in 9 tropical wood.

Coating surface quality

According to the surface evaluation, white stains on the finish of three different coating appeared en madera expuesta en *C. alliodora*, *E. cyclocarpum*, *G. arborea* and *T. grandis*. Concerning fungi on the finished surface, it was not observed in the samples of the different species or finishes exposed to AW. But NW, fungi appeared in almost the entire surface of the finish of all the species. Además se observó que luego de un año, en la mayoría de las especies empieza a perderse la película de acabado (Figura 6), pero hay un desprendimiento den menor magnitud en film que fue aplicado con coating with TiO_2-nanoparticle.

Una de las limitaciones del AW es que por las condiciones de temperatura y alta intensidad de UV no permite el desarrollo de manchas y hongos (Ghost et al. 2009), lo que si se logra con la NW que se presenta las condiciones de temperatura y humedad relativa, en especial las condiciones tropicales, para el desarrollo de hongos o manchas (Valverde y Moya, 2013, Salas et al., 2015). Ello explica por qué los acabados en NW las manchas o hongos se observaron en la mayoría de las especies, pero que se ven ligeramente disminuidos cuando la superficie de madera es pintada con coating with TiO2-nanoparticle.

The evaluation of surface degradation showed that after accelerated weathering none of the species with any kind of coating presented crow foot, mosaic, shrinkage, short random or sigmoid defect. Pero fue observado que en *G. meiantha* and *T. grandis* en AW, la superficie pintada con el acabado sin TiO_2-nanaparticle si presentó el defecto de crow foot and mosaic, lo que no se presentó en los acabados con TiO_2-nanaparticle. Al evaluar la calidad de superfie por medio de the Surface Quality Index (SQI), in which irregular flaw, long and short line and switch flaw were evaluated together, showed, as expected, high values in the samples exposed to NW (Figure 6), for which the SQI was higher for NW than for AW.

Ya en la evaluación del SQI de las diferentes especies y acabados, fue encontrado que el acabado con una concentración de TiO_2-nanoparticules de 1.5%, a excepción de *A. mangium* y *V. guatemalensis* (Figura 6a y 6i), presentaron un valor estadísticamente más alto en SQI que cuando el acabado no se le agrega ningún tipo de TiO2-particule. En tanto que cuando la concentración 1% de TiO_2-nanoparticle, las especies que no presentaron diferencia estadísticas en el SQI con relación al acabado sin TiO_2-nanoparticle fueron *G. meiantha*, *T. grandis* and *V.*

ferruginea (Figura 6f, 6h-i). En las especies que se presentaron diferencia el SQI fue más alto en el acabado con TiO_2.

Al comparar las dos concentraciones de TiO_2-nanoparticle fue observado que en *C. adorata*, *C. alliodora*, *G. arborea*, *O. pyramidale* y *T. grandis* (Figura 6b-c, 6e, 6g-h) el SQI fue estadísticamente más alto cuando la concentración de TiO_2-nanoparticle es 1.5% en relación a la concentración de 1.0%. En el resto de las especies no se presentaron diferencias estadísticas entre las concentraciones (Figura 6ª, 6d,6f, 6i).

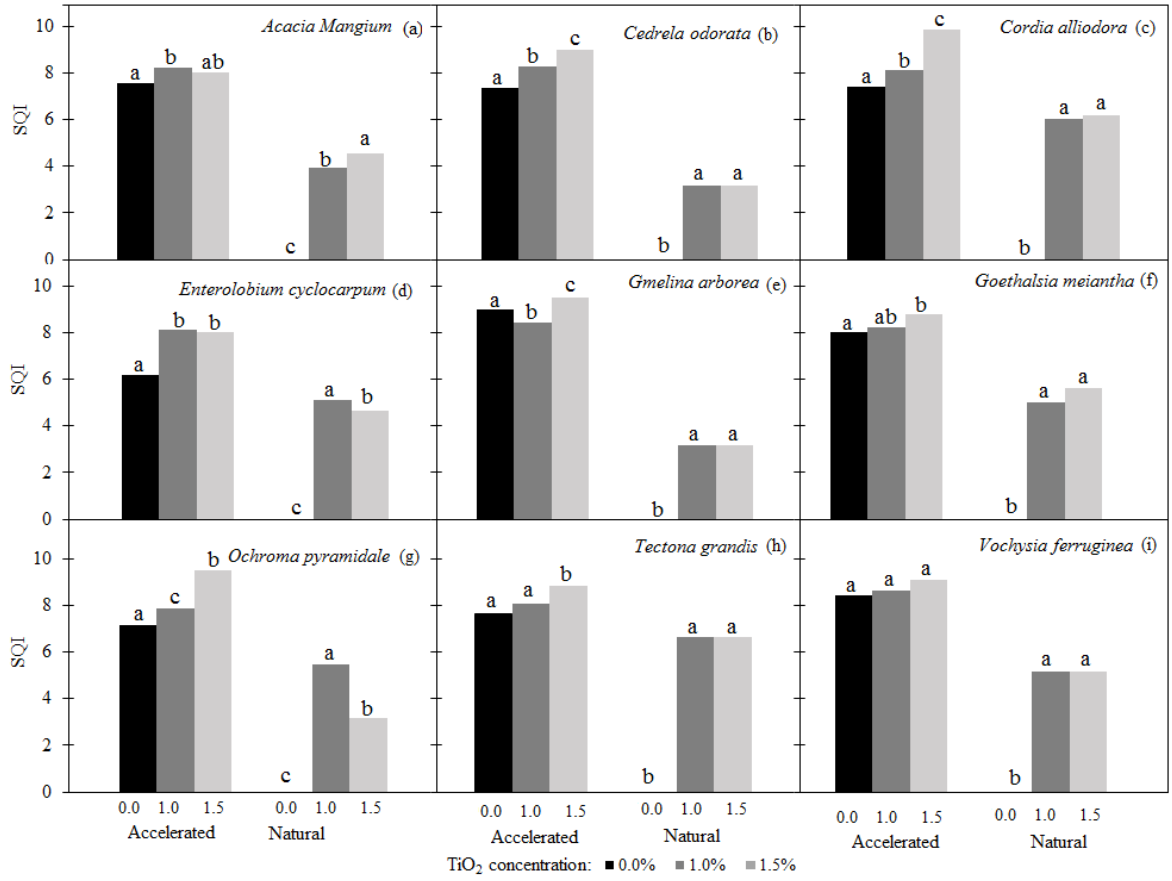

Figura 6. Surface Quality Index after to natural and accelerated weathering in of 3 types of coating with different TiO_2-nanoparticles in 9 tropical woods.

References

Ahola, P. (1991). Moisture transport in wood coated with joinery paints. *Holz als Roh-und Werkstoff*, *49*(11), 428-432.

Ahola, P., Derbyshire, H., Hora, G., & De Meijer, M. (1999). Water protection of wooden window joinery painted with low organic solvent content paints with known composition. Part 1. Results of inter-laboratory tests. *European Journal of Wood and Wood Products*, *57*(1), 45-50.

Ekstedt, J., & Östberg, G. (2001). Liquid water permeability of exterior wood coatings-testing according to a proposed european standard method. *Journal of Coatings Technology*, *73*(914), 53-59.

ASTM D3359. (2005). Standard Test Methods for Measuring Adhesion by Tape Test.

ASTM D6132. (2013). Nondestructive Measurement of Dry Film Thickness of Applied Organic Coatings Using an Ultrasonic Coating Thickness Gage.

ASTM D6132-13. (2013). Nondestructive Measurement of Dry Film Thickness of Applied rganic Coatings Using an Ultrasonic Coating Thickness Gage. 5p.

ASTM D3359-09. (2009). Standard Test Methods for Measuring Adhesion by Tape Test. 8p

Barnes, H. A., & Hutton, J. F. (1989). An introduction to rheology (Vol. 3). Elsevier.

Chauhan, S. S., & Aggarwal, P. (2004). Effect of moisture sorption state on transverse dimensional changes in wood. *Holz als Roh-und Werkstoff*, *62*(1), 50-55.

Chan, W. R., K. E. Magnus, and B. S. Mootoo. "Extractives from Cedrela odorata L. The structure of methyl angolensate." *Journal of the Chemical Society C: Organic* (1967): 171-177.

Diener, B. J., & Saklad, H. (1997). Portico, SA. Journal of Business Research, 38(1), 89-96.

Ekstedt, J., & Östberg, G. (2001). Liquid water permeability of exterior wood coatings-testing according to a proposed european standard method. Journal of Coatings Technology, 73(914), 53-59.

Eligon, A. M., Achong, A., & Saunders, R. (1992). Moisture adsorption and desorption properties of some tropical woods. *Journal of materials science*,*27*(13), 3442-3456.

Ghost, S. C., Militz, H. and Mai, C. (2009) Natural weathering of scoots pine (Pinus sylvestris L.) boards modified with functionalized

commercial silicone emulsions. Bioresources, 4, 659–673.

Kim, H. S., Lee, J. W., Yantara, N., Boix, P. P., Kulkarni, S. A., Mhaisalkar, S., Park, N. G. (2013). High efficiency solid-state sensitized solar cell-based on submicrometer rutile TiO2 nanorod and CH3NH3PbI3 perovskite sensitizer. Nano letters, 13(6), 2412-2417.

Kaygin, B., Akgun, E., 2008. Comparison of conventional varnishes with nanolacke UV varnish with respect to hardness and adhesion durability. International Journal of Molecular Sciences Int. J. Mol. Sci. 2008, 9, 476-485

Kowalczyk, K. (2014). Preparation and characterization of nanocomposite uralkyd varnishes for a wood substrate. Journal of Coatings Technology and Research, 11(3), 421-430.

Moya, R., Rodríguez-Zúñiga, A., Vega-Baudrit, J., 2015. Effects of adding nano-clay in polyvinyl acetate and urea-formaldehyde adhesives on tropical wood shear resistance. International Journal of Nanotechnology (Submitted)

Moya, R., Rodríguez-Zúñiga, A., Vega-Baudrit, J., 2015. Effects of adding Multiwall carbon-nanotubes (MWCNT) on performance of polyvinyl acetate (PVAc) and Urea-formaldhyde (UF) adhesive in Costarican *tropical timber species* . International Journal od adhesion and adhesive (Submitted)

Parra, A., J. G. Quiñones, H. Rodríguez, and E. Ybarra. "Natural weathering of eight important timber trade Mexican species." International Journal of Agricultural Policy and Research Vol.3 (1), pp. 29-38, (2015).

Salas, C., Moya, R., Vargas, L. 2015. Optical performance of finished and unfinished tropical timbers exposed to UV light in the field in Costa Rica. Wood Material Science and Engineering (Accept). 10.1080/17480272.2014.949855

Santillán, M. J., Membrives, F., Quaranta, N., & Boccaccini, A. R. (2008). Characterization of TiO2 nanoparticle suspensions for electrophoretic deposition. Journal of Nanoparticle Research, 10(5), 787-793.

Sun, Q., Lu, Y., Tu, J., Yang, D., Cao, J., & Li, J. (2013). Bulky Macroporous TiO 2 Photocatalyst with Cellular Structure via Facile Wood-Template Method.*International Journal of Photoenergy*, *2013*.

Tahir, M., Theato, P., Oberle, P., Melnyk, G., Faiss, S., Kolb, U., Janshoff, A., Stepputat, M., Tremel, W., 2006. Facile synthesis and characterization of functionalized, monocrystalline rutile TiO_2 nanorods. Langmuir 22: 5209-5212.

Tseng WJ, Lin KC (2003) Rheology and colloidal structure of aqueous TiO2 nanoparticle suspensions. Mater Sci Eng A355:186–192.

Valverde, J.C., Moya, R. 2014. Correlation and modeling between color variation and quality of the surface between accelerated and natural tropical weathering in *Acacia mangium*, *Cedrela odorata* and *Tectona grandis* wood with two coating. Color Research and Application 39(5) 519-529.

Ekstedt, J., & Östberg, G. (2001). Liquid water permeability of exterior wood coatings-testing according to a proposed european standard method. Journal of Coatings Technology, 73(914), 53-59.

Ahajji A, Diouf PN, Aloui F, Elbakali I, Perrin D, Merlin A, George B. Influence of heat treatment on antioxidant properties and colour stability of beech and spruce wood and their extractives. Wood Sci Technol 2009; 43: 69–83.

Cristea, M. V., Riedl, B., & Blanchet, P. (2010). Enhancing the performance of exterior waterborne coatings for wood by inorganic nanosized UV absorbers. *Progress in Organic Coatings*, 69(4), 432-441.

Corcione, C. E., & Frigione, M. (2012). UV-cured polymer-boehmite nanocomposite as protective coating for wood elements. *Progress in Organic Coatings*, 74(4), 781-787.

Deka M, Humar M, Kricej GB, Petric M. Effects of UV light irradiation on colour stability of thermally modified, copper ethanolamine treated and non-modified wood: EPR and DRIFT spectroscopic studies, Wood Sci Technol 2008; 42: 5-20

Fufa, S. M., Jelle, B. P., Hovde, P. J., & Rørvik, P. M. (2012). Coated wooden claddings and the influence of nanoparticles on the weathering performance. *Progress in Organic Coatings*, 75(1), 72-78.

Gornicka, B., & Sieradzka, K. (2009, January). Barrier properties of impregnating varnishes with nanosilica. *In Journal of Physics: Conference Series* (Vol. 146, No. 1, p. 012016). IOP Publishing.

Kaygin, B., & Akgun, E. (2008). Comparison of conventional varnishes with Nanolacke UV varnish with respect to hardness and adhesion durability. *International journal of molecular sciences*, 9(4), 476-485.

Moya, R., Muñoz, F. 2010. Physical and mechanical properties of eight species from fast-growth plantation in Costa Rica. Journal of Tropical Forest Science 22(3): 317-328

Nikolic, M., Lawther, J. M., & Sanadi, A. R. (2015). Use of nanofillers in wood coatings: a scientific review. *Journal of Coatings Technology and Research*,12(3), 445-461.

Oltean L, Teischinger A, Hansmann C. Wood surface discolouration due to simulated indoo sunlight exposure, Holz als Werkst 2008; 66: 51–56.

Peruzzo, P. J., Bonnefond, A., Reyes, Y., Fernández, M., Fare, J., Ronne, E., Leiza, J. R. (2014) 'Beneficial in-situ incorporation of nano-clay to waterborne PVAc/PVOH dispersion adhesives for wood applications'. *International Journal of Adhesion and Adhesives*, vol. 48, pp.295-302.

Petric M, Kricej B, Humar M, Pavlic M, Tomazic M.Patination of cherry wood and spruce wood with ethanolamine and surface finishes. Surf Coating Int B Coating Trans 2004; 87: 195-201.

Roussak, O.V. Gesser, H.D. (2013) Adhesives and Adhesion. In *Applied Chemistry: A Textbook for Engineers and Technologists*, Roussak, O.V. Gesser, H.D. Springer Science & Business Media, New York, pp. 219-232.

Salla, J., Pandey, K. K., & Srinivas, K. (2012). Improvement of UV resistance of wood surfaces by using ZnO nanoparticles. *Polymer Degradation and Stability*, 97(4), 592-596.

Schnabel, T; Zimmer, B; Petutschnigg, AJ. 2009. On the modelling of colour changes of wood surfaces. Journal of Wood Products. 67: 141-149.

Tolvaj L, Mitsui K. Light source dependence of the photodegradation of wood. Wood Sci Technol 2005; 51: 468–473.

Valverde, J.C., Moya, R. 2010. Efectos de la intemperie en el color de dos acabados aplicados en madera de *Cedrela odorata* y *Carapa guianensis*. Maderas: Ciencias y Tecnología 12(3): 171-180

Veigel, S., Grüll, G., Pinkl, S., Obersriebnig, M., Müller, U., & Gindl-Altmutter, W. (2014). Improving the mechanical resistance of waterborne wood coatings by adding cellulose nanofibres. *Reactive and Functional Polymers*, 85, 214-220.

Vlad-Cristea, M., Riedl, B., Blanchet, P., & Jimenez-Pique, E. (2012). Nanocharacterization techniques for investigating the durability of wood coatings. *European Polymer Journal*, 48(3), 441-453.